A STUDY COMPARING CHANGES IN LOADING CONDITIONS OF AN EXTENDED SERVICE LIFE AIRCRAFT USING 17-7PH STAINLESS STEEL

by

Tony Clayton Hyer

A thesis submitted to the faculty of
The University of Utah
in partial fulfillment of the requirements for the degree of

Master of Science

Department of Mechanical Engineering

The University of Utah

August 2014

The University of Utah Graduate School

STATEMENT OF THESIS APPROVAL

The thesis of Tony Clayton Hyer.

Has been approved by the following supervisory committee members:

Ken J. Monson, Chair	4/25/2014 Date Approved
Mark L. Thomsen, Member	4/25/2014 Date Approved
K. Larry DeVries, Member	4/25/2014 Date Approved

and by Timothy A. Ameel, Chair/Dean of

the Department/College/School of Mechanical Engineering

and by David B. Kieda, Dean of The Graduate School.

ABSTRACT

Industry and the military are always looking for ways to stretch their dollar. One way to do this is to make the equipment they currently own last longer in lieu of buying new. For example, many of the aircraft in the USAF have gone beyond their expected service life and over that time have experienced changes in usage. In order for the USAF, or others in the aviation industry, to make their aircraft last longer, they must understand how the changes in usage affect their aircraft.

The purpose of this study was to determine the sensitivity of a representative stainless steel specimen to two different load spectra, spectrum A and spectrum B. This was accomplished by conducting fatigue experiments, baselines for each spectrum and three different combinations of the two spectra, performing fractographic examinations of the fracture surfaces and developing computer simulations, using AFGROW, to represent test data. The results showed that crack growth under spectrum B type loading conditions was significantly slower than under spectrum A. The fractography showed clear distinctions between the spectra fracture surfaces. Also, AFGROW simulations were successful in replicating test data. These results emphasize the need for continual monitoring of fatigue critical locations to better maintain aircraft.

I would like to dedicate this work to my wife Joni, our children Thomas, Lucy and Logan and to our future.

TABLE OF CONTENTS

LIST OF TABLES

Tables Page

ACKNOWLEDGEMENTS

I feel a distinct need to give thanks to the many people who made this work possible. The first thanks need to go to Dr. Mark Thomsen, Robert Pilarczyk, Scott Carlson and Dallen Andrew who were the main players in procuring the specimens, arranging lab time and giving continued guidance during this project. I very much appreciate their willingness to work with me and give me this opportunity to get some real, hands-on, experience in running a fatigue experiment. I also need to thank Dr. Ken Monson and Dr. K. Larry DeVries who were also willing to work with me during this project and help with its completion. Thanks need to go to Tom Slowick in the machine shop at the University of Utah for allowing me to use the equipment there for a portion of this project.

I need to thank those in the Engineering and Science Lab on Hill AFB, namely, Wayne Patterson, Wes Finneran, Cody Hone and Scot Frew. These gentlemen went the extra mile in working with me so that I could use the facilities and equipment in their lab during a significant portion of this project. Without their assistance, this project would have been extremely more difficult to complete.

I would like to thank Luciano "Lucky" Smith and Jim Feiger from Southwest Research Institute. When the fatigue machine on Hill AFB went out of commission for a time, these gentlemen made it possible to complete the fatigue testing of several test

specimens. I greatly appreciate their patience with the routine phone calls and answering all the questions that I had.

I also have a deep appreciation for all the help and assistance offered to me by my fellow student, Roger Beal. He and I spent many long hours figuring out what was going to be necessary for every step of this project. He was very willing to counsel me and help me find answers to most of the questions that arose during this process.

I need to thank my supervisors, Ronald Montgomery, Chad Hogan and Brad Martin in the Landing Gear Office at Hill AFB. These gentlemen were very willing and supportive during my whole graduate school experience. They were constantly willing to work with my schedule and accommodate my needs. A special thanks also goes to Dan Christensen, Douglas Ball, Jared Butterfield and Jim Yerke, who were instrumental in helping me to be admitted to the Palace Acquire program.

Lastly but most importantly, I need to thank my wife and children for the many years of support and love they have given to me. They were my motivation during all my years of schooling. They are the reason I've accomplished as much as I have over these past several years that they have been a part of my life.

CHAPTER 1

INTRODUCTION

1.1 Extended Service Life Aircraft

Few players have as critical of a role in the defense strategy of the United States, and many other countries for that matter, and world transportation as the aerospace industry. Having said that, it is extremely expensive to buy and maintain aircraft. According to Boeing's website, a new 737 MAX 9 will cost a buyer upwards of $109.9 million in 2013 dollars. [1] A new 777-300ER will cost a buyer a staggering $320.2 million in 2013 dollars. [1] On the military side, the unit cost for just one F-16C/D model is $18.8 million in 1998 dollars. [2] Those figures don't even reflect the cost of maintaining each of those aircraft. Due to the large amounts of money involved, industry and the military look for ways to reduce cost.

When faced with the decision to buy expensive new aircraft or maintain what they have, industry and the government often resort to the latter. Some examples of extended service life aircraft can be seen in the United States military. The Air Force has extended the service life of the A-10 Thunderbolt II and the B-52 Stratofortress, as just a couple of examples. The A-10 had an initial service life of 6,000 hours and was due to retire in Fiscal Year (FY) 2005. [3] The Air Force, after several upgrades, has now extended the

service life of the A-10 to FY 2028. [3] The B-52 is slated to be in service beyond 2040, equating to approximately 90 years of military service. [4]

From an engineering standpoint, several obstacles are encountered when attempting to extend an aircraft's life beyond that for which it was originally designed. Some of these obstacles include corrosion, wear and fatigue. Fatigue is a particular concern to the aviation industry due to the fatigue-prone conditions. According to ASTM E1823, which is the standard for terminology relating to fatigue and fracture testing, fatigue is:

> The process of progressive localized permanent structural change occurring in a material subjected to conditions that produce fluctuating stresses and strains at some point or points and that may culminate in cracks or complete fracture after a sufficient number of fluctuations. [5, p. 8]

An added obstacle develops when the usage of the aircraft changes over time. In order to protect against the effects of fatigue on aircraft, designers and maintainers develop philosophies of how to maintain their integrity over time. The current philosophy being used today by several aircraft industries is the Damage Tolerant Design Philosophy.

1.2 Damage Tolerant Design Philosophy

Several design philosophies, used to protect against fatigue, have been developed over the years, but the one currently used today by many in the aviation industry is the Damage Tolerant Design philosophy. Starting in the late 70s, the USAF began to use the Damage Tolerant Design Philosophy to sustain their fleet of aircraft. [6] According to MIL-STD-1530, the specification for standard practice of aircraft structural integrity programs, damage tolerance is:

> the attribute of a structure that permits it to retain its required residual strength for a period of unrepaired usage after structure has sustained specific levels of fatigue, corrosion, accidental, and/or discrete source damage. [7, p. 5]

Damage tolerance relies heavily on fracture mechanics concepts, namely, fatigue crack growth, residual strength as well as nondestructive inspections (NDI), to help manage the remaining life in an aircraft's structure.

Damage Tolerant Designs assume that initially, there is some discontinuity in a given material, new or old, used in the aircraft's structure. [6] Often these discontinuities become origination sites for crack development. [6] It is the objective of the Damage Tolerant Design concept to not allow these discontinuities to develop into cracks, by means of fatigue, that reach a critical length resulting in unstable crack growth and failure. [7] The following sections explain in greater detail the role of fatigue crack growth, residual strength and NDI techniques in the Damage Tolerant Design philosophy.

1.2.1 Fatigue Crack Growth

As was mentioned previously, the Damage Tolerant Philosophy begins with assuming that there exists some discontinuity in the material from which a crack may developed when subjected to some type of loading. Records collected by the USAF have shown that the primary reasons that cracks grow in their aircraft are due to fatigue, stress corrosion and corrosion-fatigue mechanisms. [6] According to the USAF Damage Tolerance Design Handbook, when referring to flaws in the aircraft structure:

> The safety of the aircraft is dependent on their initial sizes, the rates of growth with service usage, the critical flaw sizes, the inspectability of the structure, and the fracture containment capabilities of the basic structural design. [6, p. 1.2.1]

This reference also states that:

> it is essential that safety of flight be provided through the consideration of an "initial flaw" model in which some size of initial damage is assumed to exist consistent with the inspection capability either in the field or during manufacture. [6, p. 1.2.1]

Those models, to which the Damage Tolerant Handbook is referring, are developed through a process of fatigue testing and developing crack growth simulations that replicate the results of the tests.

Today, the aviation industry and the military develop fatigue life models using crack growth modeling programs. An example of a crack growth modeling program that the USAF uses is AFGROW. These programs can be used for a wide variety of structures as they are typically not system, or aircraft, specific. The results from the tests and analyses allow users to approximate crack growth rates and critical flaw sizes. These data are then used to determine appropriate inspection intervals and the resulting component life expectancy. Fig. 1 is an example of a plot displaying a typical crack growth curve. In order to develop a model that can accurately predict what is actually occurring on the aircraft, one must understand the loading conditions that are occurring on the aircraft.

1.2.1.1 Load History

There are primarily two types of loading conditions used for fatigue tests. One type of loading is known as constant amplitude loading. According to ASTM E1823, constant amplitude loading is, "a loading (straining) in which all of the peak forces (strains) are equal and all of the valley forces (strains) are equal." [5, p. 4] This type of loading is used often for developing material properties, but it is not appropriate for characterizing how a material will behave on an aircraft due to the fact that the loading

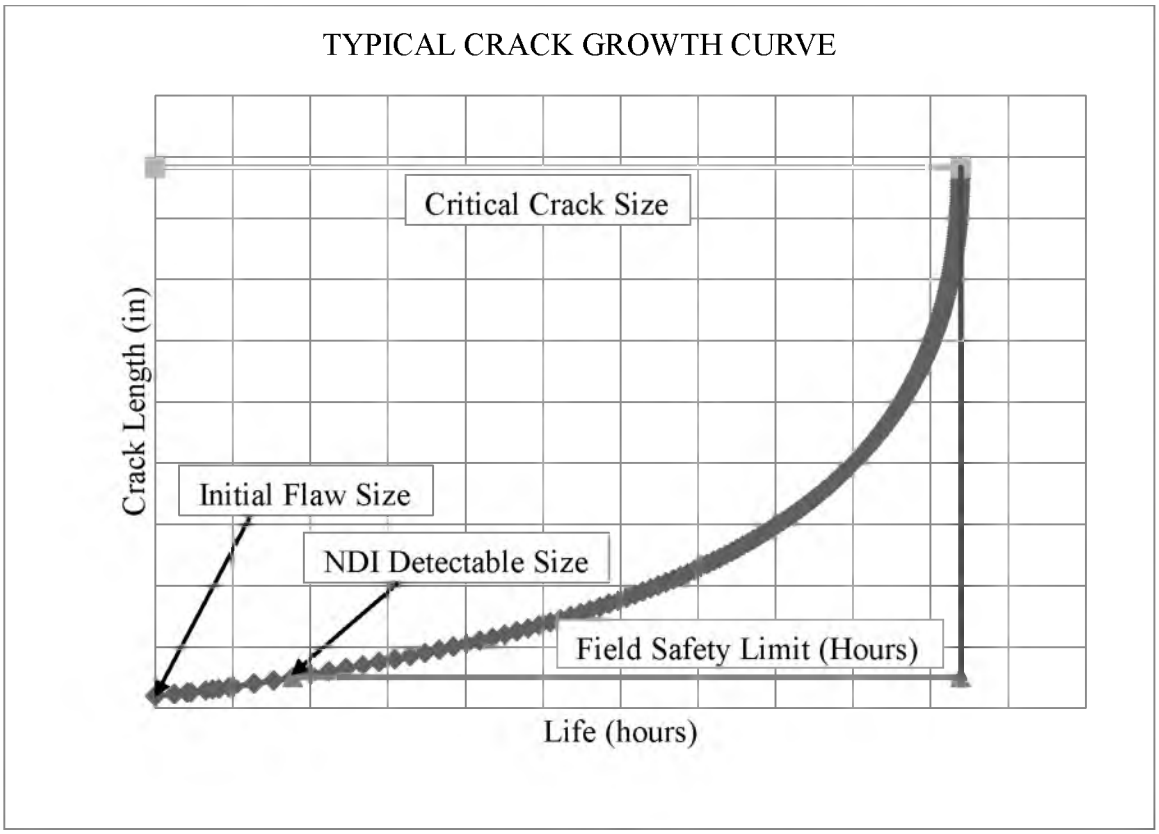

Figure 1 Typical Fatigue Crack Growth Curve used for Damage Tolerance Analysis

conditions are not constant.

The other type of loading used in fatigue experiments is known as spectrum loading, variable amplitude loading or irregular loading. [5] The ASTM E1823 definition for spectrum loading simply states that it is, "a force-time program consisting of some (or all) unequal peak and valley forces." [5, p. 16] If one can obtain the load history of a location on an aircraft, a loading spectrum can be developed. These data are then entered into a fatigue machine program and used to run an accelerated fatigue test. The results of these tests, if done correctly, will give a more accurate representation than the constant amplitude test of how a material will perform on an aircraft, or any other product for that matter.

1.2.1.2 Aircraft Spectrum Development

Different methodologies can be used to obtain loading data for different locations on an aircraft. The type of measurement method used will be determined by the loading conditions. The fatigue testing conducted for this study used measurements from the Individual Aircraft Tracking Program (IATP) for military aircraft. [8] This program recorded acceleration changes while the aircraft were in flight using a counting accelerometer. [9] Those changes in acceleration can be used to derive loading conditions at various points in the aircraft. The point chosen for this study was picked due to the severity of the loading conditions and the fact that the material in that location is 17-7PH stainless steel, about which little data has been gathered for this particular aircraft. One of the desired outcomes of this study was to determine how the stainless steel material would behave under the two spectra. A similar study, performed in conjunction with this one, was also conducted using 2024-T351 aluminum. [10]

The data obtained from the IATP system were converted into loads compiled, using a methodology called cycle counting in such a manner that showed the number of times load levels were exceeded during a given period of time. An example of an exceedance curve, which is a graphical representation of loads and occurrences, is shown in Fig. 2. Once its known how many times different loads should be represented in the spectrum, a randomized base-peak-base sequence of loads is developed.

Over the years that the IATP system had been in use, it was noticed that the usage of the aircraft had changed significantly. With this new information, it was determined that several spectra would need to be developed to represent the different usage periods. For the purposes of this study, two different spectra were compared and were given the

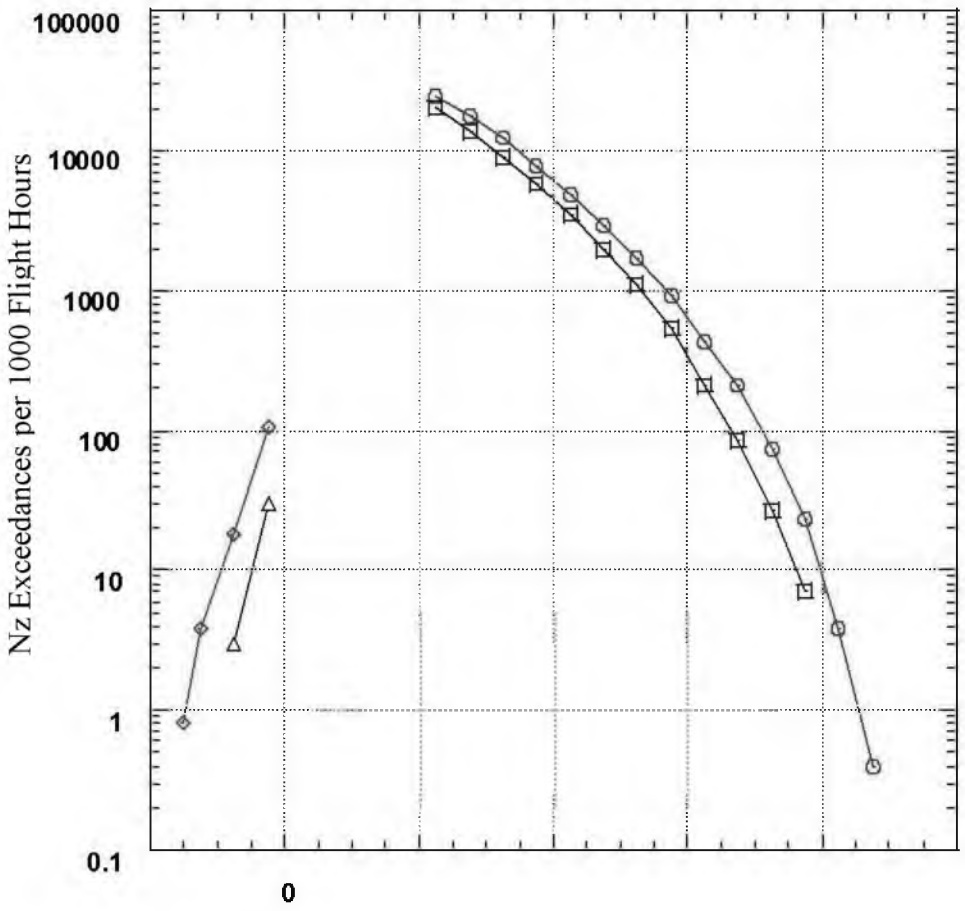

Figure 2 Example of an Exceedance Curve [11]

simple designations of A and B. Spectrum A represents usage observed during most of the 90s while Spectrum B represents usage observed from the early 2000s to the present day. The spectra were then compiled into data files that could be used in a fatigue machine and crack growth analysis program.

1.2.2 Residual Strength

Residual strength is, "the maximum value of the gross stress, neglecting the area of the crack, that a cracked specimen is capable of sustaining." [5, p. 15] Hence, as the

crack increases in length, the residual strength of the specimen decreases. The residual strength of the specimen can be determined using Linear Elastic Fracture Mechanics (LEFM).

Beginning in the 19th century, with the advent of the Industrial Revolution, a dramatic increase in the use of metals for structural purposes occurred. [12] With the dramatic increase in metal usage, there came an increase in the number of failures due to fracture. In 1920, a researcher by the name of Alan Arnold Giffith came up with a successful method to analyze crack propagation in brittle structures, i.e., glass. [12] His research involved relating the elastic strain energy with the surface energy of a system. In other words, he determined that crack extension occurs when the elastic strain energy available is larger than the available surface energy. [12] This research, which Griffith developed, became the foundation for future Fracture Mechanics studies. In the late 1940s, Irwin suggested that, "the Griffith theory for ideally brittle materials could be modified and applied to both brittle materials and metals that exhibit plastic deformation." [12, p. 12] Similar to Griffiths approach, Irwin recognized that, "a material's resistance to crack extension is determined by the sum of the surface energy and the plastic strain work." [12, p. 12] Irwin's approach is now known as stress intensity and is given by the following equation. [12]

$$K = \sigma\sqrt{\pi a}\beta$$

K is the stress intensity factor, σ is the far field stress, a is the crack length and β is the geometry correction factor. This equation suggests that crack extension will occur when K is at a critical value. [12] In order to use the stress intensity approach, one must know

if a crack is present and its size in the structure. Today, NDI methods are used to help make those determinations.

1.2.3 Nondestructive Inspections

As was mentioned previously, it is assumed that all materials have some discontinuity in them that can eventually produce a crack by means of fatigue. Thus, those in the aviation industry on a routine basis inspect aircraft on a predetermined interval to assess if any damage is detectable and to what extent. In order to save money, these inspection methods need to leave the component intact so that it can be reused or repaired, if the damage is not too severe. Some typical types of inspections that are used today are liquid penetrants, eddy current, x-ray and ultrasonic. If damage is detected using one of these NDI methods, the remaining life can be determined from fatigue crack growth data generated for that specific component.

1.3 Previous Research

As was explained earlier, the beginnings of fracture mechanics began in the 1920s. In the time since then, it has been observed that crack growth behavior is dependent on several factors, such as material properties, type of structure, environmental conditions and loading conditions. [13] The one factor of particular interest in this study is the effect of loading conditions. Many tests over the years have been conducted to better understand how overloads and underloads affect the fatigue life of a component.

1.3.1 Overload and Underload Affects

In constant amplitude loading, the max and min loads remain constant over the duration of the test. The simplest form of an overload event occurs when at least one cycle exceeds the typical max value of a constant amplitude test. One would probably at first conclude that such an event would decrease the fatigue life of the item when in reality, the opposite is usually true. This phenomenon is referred to as retardation of the crack growth rate.

In an article written by P.J. Bernard, T. C. Lindley and C.E. Richards, they reported on experiments of two types of steel, Ducol W30B and FV520B. [14] The main differences between the two materials were yield strength and strain hardening. [14] Ducol has a yield strength of 366 MNm^{-2} (53.1 ksi) and a percent elongation of 38 while FV520B has a yield strength of 940 MNm^{-2} (136.3 ksi) and a percent elongation of 20. [14] The results of the tests showed that FV520B experienced a sharp decrease in the crack growth rate immediately following the overload. [14] Ducol also experienced a decrease in the crack growth rate following the overload event with the difference being that the transition to the slower rate was more gradual. [14] In both cases, the crack continued to grow at the slower rate for a period of time then reverted back to the original crack growth rates. [14] It was also observed that in order for the overload to have any effect on the fatigue life, it had to exceed a limit, which the authors determined to be in the range of a 40 to 60 percent load increase. [14]

Another article by W.X. Alzos, A.C. Skat, Jr. and B.M. Hillberry reported on the effects of overloads preceded and followed by underloads. [15] The material used in these experiments was 2024-T3 aluminum. [15] The tests were conducted such that the underload followed the overload at varying stress ratios of overload and underload

events. These tests showed that the more negative the stress ratio, the greater the reduction of the retardation effect. [15] This same study also showed that when the underload preceded the overload, the result was the same as a test conducted with only overloads. [15] Similar results were seen in a study conducted by R.I Stephens, D.K. Chen and B.W. Hom. [16] Over the years, it has been observed that in order to more accurately determine how a material will behave under real life conditions, methods had to be developed to study more complex loading conditions.

1.3.2 Variable Amplitude Load Affects

With the aid of computer-controlled fatigue testing, researchers have been able to test materials using complex loading scenarios that represent actual operational conditions. In a study by J.A. Reiman, M.A. Landy and M.P. Kaplan, they conducted tests using several different types of loading to determine the effect on fatigue life. [17] The results of the study showed that spectrum or flight-by-flight type loading conditions were more accurate in representing field data than previous methods relying on constant amplitude data. [17]. Similar results were also seen in a study by W. Zhuang, S. Barter and L. Molent where they assessed the effects of flight-by-flight fatigue conditions. [18] They studied a variety of metals used on the F/A-18 using a spectrum developed for that aircraft. [18]

Various explanations have been given over the years as to why the differences in crack growth rates occur under variable amplitude loading. The crack growth rate has been shown to be a function of the amount of cracking, crack front orientation, crack tip blunting, crack closure, strain hardening, environment, frequency and magnitude of the loads on a given material. [13] All of these interaction effects make modeling crack

growth behavior extremely difficult. Thus, most often experimental results are used to validate analytical predictions.

1.3.3 Crack Growth Prediction Methods

Numerous interaction effects make predicting how a crack will behave under variable amplitude loading a difficult venture. In spite of the many difficulties present, many have worked extensively to develop representative models of crack growth behavior. In a report by S.U. Khan, R.C. Alderliesten, J. Schijve and R. Benedictus, they explain the differences between several prediction methods and how they are categorized. [19] One of the categories explained in the report is labeled as Interaction Effects.

1.3.3.1 Interaction Effect Models

A long history of experiments has shown that interaction effects occur when a material is subjected to variable amplitude loading. [19] Variable amplitude testing alters the conditions at the crack tip, which in turn alters the crack growth rate. Many experiments have been conducted to determine what the interaction effects are and how to model them. Studies indicated that Yield Zone and Crack Closure models were typically used to characterize crack growth in materials similar to that used in this study. AFGROW was used in this study to determine which retardation model, if any, would best represent test data.

1.3.3.1.1 Yield Zone Models

In fracture mechanics, it is known that the material in front of the crack tip experiences stresses beyond the yield point and creates a plastically deformed zone. It is

thought that large loads produce a large "yield zone" that when followed by smaller loads retards crack growth. Wheeler and Willenborg were the first researchers to model crack growth behavior using this type of interaction effect. [19] In a study conducted by S. Kalnaus, F. Fan, Y. Jiang and A.K. Vasudevan, they investigated fatigue crack growth of 304L Stainless Steel. [20] In their experiments, they used 304L round compact tension specimens under various Mode I loading conditions. [20] In the analysis portion of the experiment, they used a modified Wheeler's model to simulate the test data. [20] Another study conducted by Southwest Research Institute (SwRI) evaluated several materials, including 17-7PH, and modeled the results using the Willenborg Retardation Model to derive differences in SOLR values. [21] In a paper written by J. Willenborg, R. M. Engle and H. A. Wood, they describe how the retardation model, which would later be named after Willenborg, compared well with experimental data for D6AC steel. [22]

1.3.3.1.2 Crack Closure Models

Crack closure is a phenomenon that, like the Yield Zone models, involves the plastic zone created from the crack, but in a different light. It is thought that the large plastic zone contains compressive residual stresses that resists opening of the crack when a tensile load is applied. [19] Thus, it has been observed that a crack will not open as soon as a load is applied, but only when the load is sufficiently high to overcome the residual compressive stresses. [19] Elber was the first to observe and attempt to model this phenomenon. [19] In the study mentioned earlier, by W. Zhuang and his colleagues, they mention using crack closure models to simulate the data they gathered from their tests. [18]

1.4 Scope of This Research

This study differed from others in that it compared the effects of two different usage periods of a type of aircraft over time. To conduct this experiment, simplified test specimens, known as corner crack at a hole specimens, were fabricated out of the same material used in the location of concern. The tests were conducted such that each spectrum would be run individually to develop spectrum baselines. Running in conjunction with the baseline tests, three combinations of the spectra were then applied by running the first spectrum until the crack grew to certain lengths, at which point the second spectrum was then applied. The three different combinations, explained in greater detail in Chapter 2, were conducted to give the user a representative range of aircraft usage and to see how the different crack lengths might affect the results.

After the testing was completed, the specimens were subject to a fractographic examination. The purpose of this inspection was to verify initial flaw sizes, when the transitions of spectra occurred and to note any distinct features the spectra create on the fracture surface. [8]

The last critical portion of this research was to use the crack growth modeling program, AFGROW, to make analytical predictions of the crack growth under the different spectra. This was done using a standard center hole model with a corner crack, which was representative of the test specimens.

1.5 Goals of This Research

The main objective of this study was to better understand the sensitivity of 17-7PH to the different, consecutive, spectra. The crack growth curves, fractographic

examinations and AFGROW models provide critical information to the engineers supporting the aircraft. Knowing the differences between the two spectra allows engineers to know what changes to maintenance practices, repair procedures and inspection intervals may be available to them in order to optimize overall lifecycle management. These changes in return will reduce costs over the life of the aircraft in the form of potentially reducing maintenance and preserving the integrity of the aircraft.

CHAPTER 2

TESTING SETUP AND PROCEDURES

2.1 Test Specimen Specifications

2.1.1 Specimen Material

The specimens used in this experiment were meant to be representative of longeron straps on a military aircraft. These straps are made from 17-7PH stainless steel per specification AMS 5528 heat treated to the TH1100 condition. The material composition for 17-7PH stainless steel can be seen in Table 1. Material properties for this material were verified by Northrop Grumman and the results of that testing can be seen in Table 2. 17-7PH stainless steel is a semi-austenitic stainless steel used where high strength and corrosion resistance are needed, characteristics required for aerospace applications. [23]

Table 1 Composition of 17-7PH Stainless Steel. Data from [24]

Element	min	max
Carbon	--	0.09
Manganese	--	1.00
Silicon	--	1.00
Phosphorus	--	0.040
Sulfur	--	0.030
Chromium	16.00	18.00
Nickel	6.50	7.75
Aluminum	0.75	1.50

Table 2 Material Properties of 17-7PH TH1100 Stainless Steel. Data from [25]

Properties	Tensile Strength (ksi)	Yield Strength (ksi)	% Elongation
Avg.	168.9	156.8	12.5

2.1.2 Test Specimen Fabrication

These particular test specimens were simplified for ease of testing and to meet several of the recommendations of ASTM E 647, a standard for testing methods to determine fatigue crack growth rates. The test specimens, on average, measured 16 inches in length, 4 inches wide and 0.125 inches thick with a 0.157 inch center hole. Located along the centerline of the hole and 90 degrees to the load path was a notch that served as a crack starter. GT270KB003 is the drawing for the test specimens and is shown in Fig. 3. The certification sheets detailing the manufacturing and testing of the specimen material can be seen in Appendix A. The specimens were provided by Northrop Grumman.

The specimens were all manufactured from sheets of the same heat treatment lot with the grains running in the longitudinal direction of the specimens. Making all the specimens in this manner reduces variability in the testing. After the test specimens were heat treated and fabricated, they were shot peened on both ends to reduce the risk of fatigue cracks growing near the fatigue machine grips. The final step in fabricating the test specimens was to machine a notch in the bore perpendicular to the load path. This was done using an electrical discharge machining (EDM) process. See Fig. 4 for a cross-sectional view of the machined notch. In total, 33 test specimens were delivered, 15 for the test and 6 spares with the remaining 12 to be used for another program.

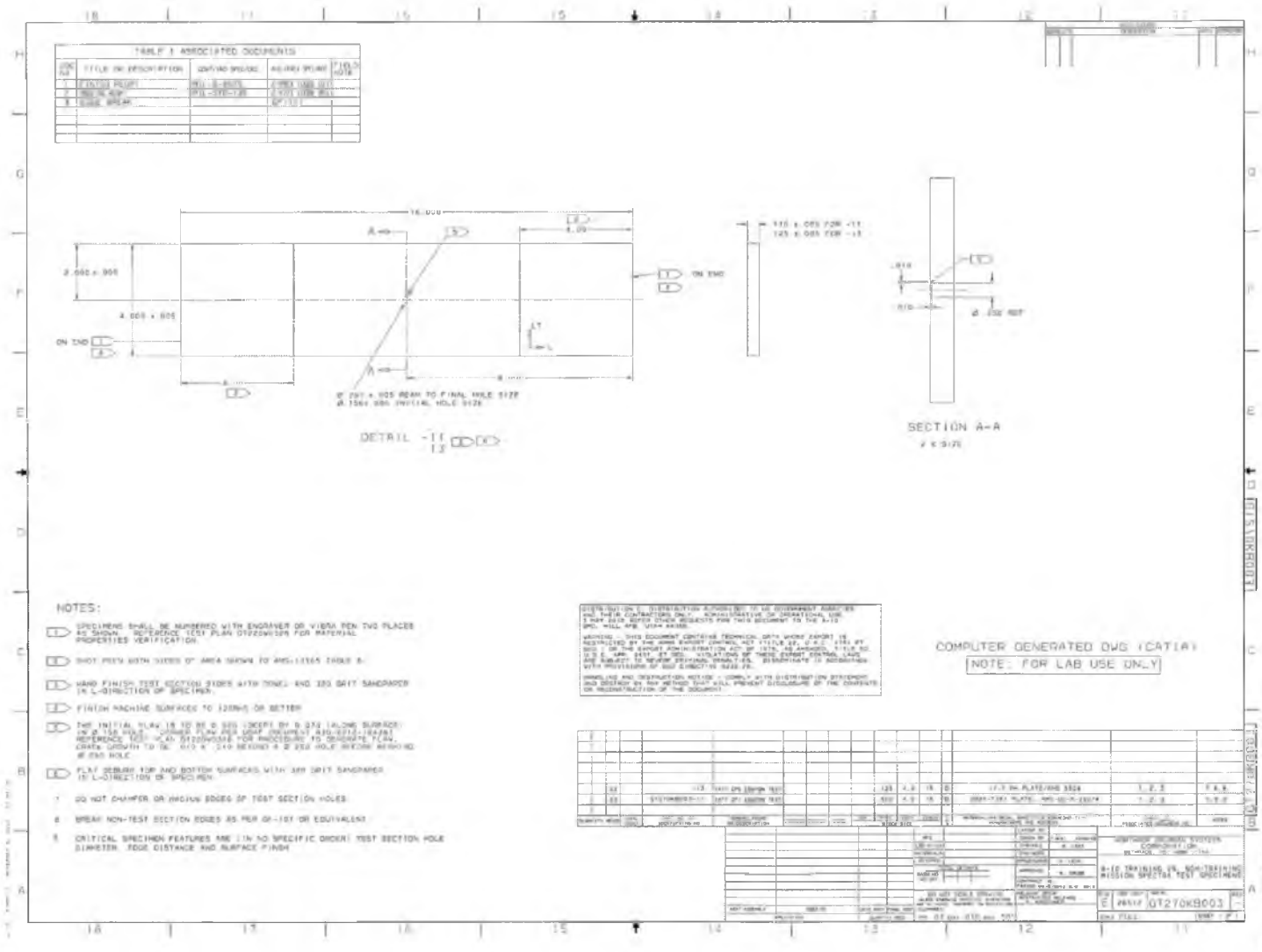

Figure 3 Test Specimen Drawing GT270KB003 [8]

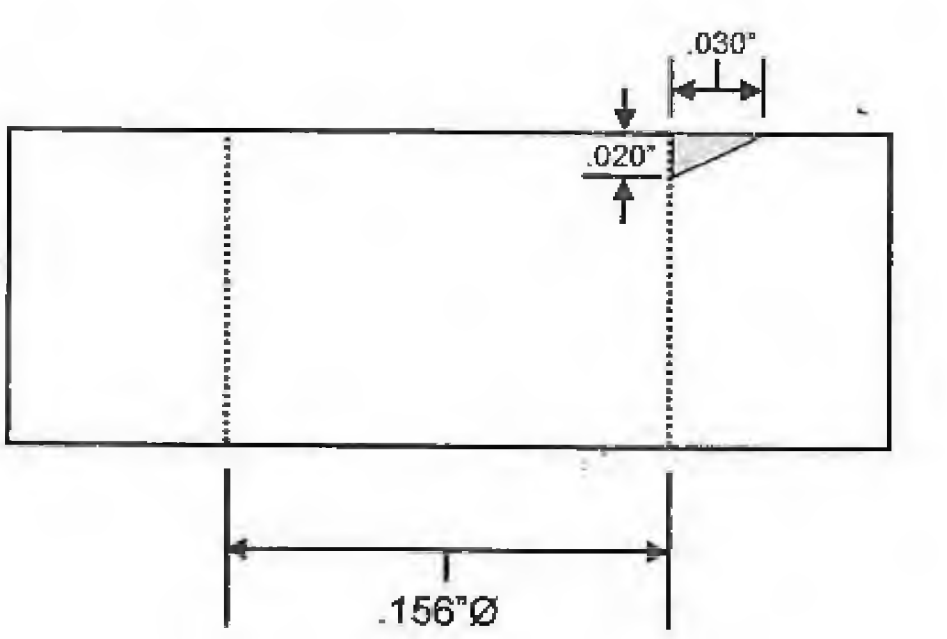

Figure 4 Cross-Sectional View of the EDM Notch in the Center Hole

2.2 Test Specimen Polishing

The specimens were delivered in an as-machined surface finish state. This finish made seeing and measuring the crack difficult. It was known, from previous experiments, that polishing the area along the cracking plane would facilitate crack measurements. [26] The procedures used for polishing the surface of the test specimens can be seen in Appendix B. Pre- and postpolished specimens can be seen in Figs. 5 and 6, respectively.

Following these steps produced a near mirror finish, making the crack much easier to see and measure as expected. Pre- and postspecimen measurements of the polished areas were taken using calipers, model number CD-6" CXWW, with a tolerance of ±0.0005. These measurements resulted in a difference in thickness below the tolerance limit of the calipers.

Figure 5 As-received Test Specimen

Figure 6 Polished Test Specimen

2.3 Test Equipment

During the fatigue testing for this study, the primary test system experienced a malfunction. The result was that two different laboratories were used to conduct the testing. One of the labs used to perform the testing is located at Hill AFB, UT in the Science and Engineering Laboratory. The other lab used to conduct the testing is located at SwRI in San Antonio, TX. The following sections give information about the equipment used at Hill AFB lab to give the reader an idea of what was used during testing. Details of the equipment used at SwRI can be seen in Appendix C. All tests were conducted in lab air conditions.

2.3.1 Fatigue Machine and Equipment Specifications

2.3.1.1 Interlaken Series 3300 55 kip Fatigue Machine

Interlaken was the original manufacturer of the load frame used to conduct the testing. The actuator on this machine has a 55 kip capacity and can be seen in Fig. 7. The actuator is located below the specimen, has a ± 3 inch range and is equipped with a positioning sensor. Above the specimen is the crosshead to which the Interface 50 kip load cell, model 1032AF-50K-B, is attached. The load cell provides the feedback to the controller indicating how much load is being applied to the specimen. Every year, the fatigue machine and load cell must be calibrated to ensure the accuracy of the experiments performed. The calibration for these items was performed by Instron Corporation on 4/15/13 for the fatigue machine and 4/16/13 for the load cell in accordance with ASTM E4. The calibration certifications can be seen in Appendix D. The testing done for this experiment was done within the year calibration timeframe. The

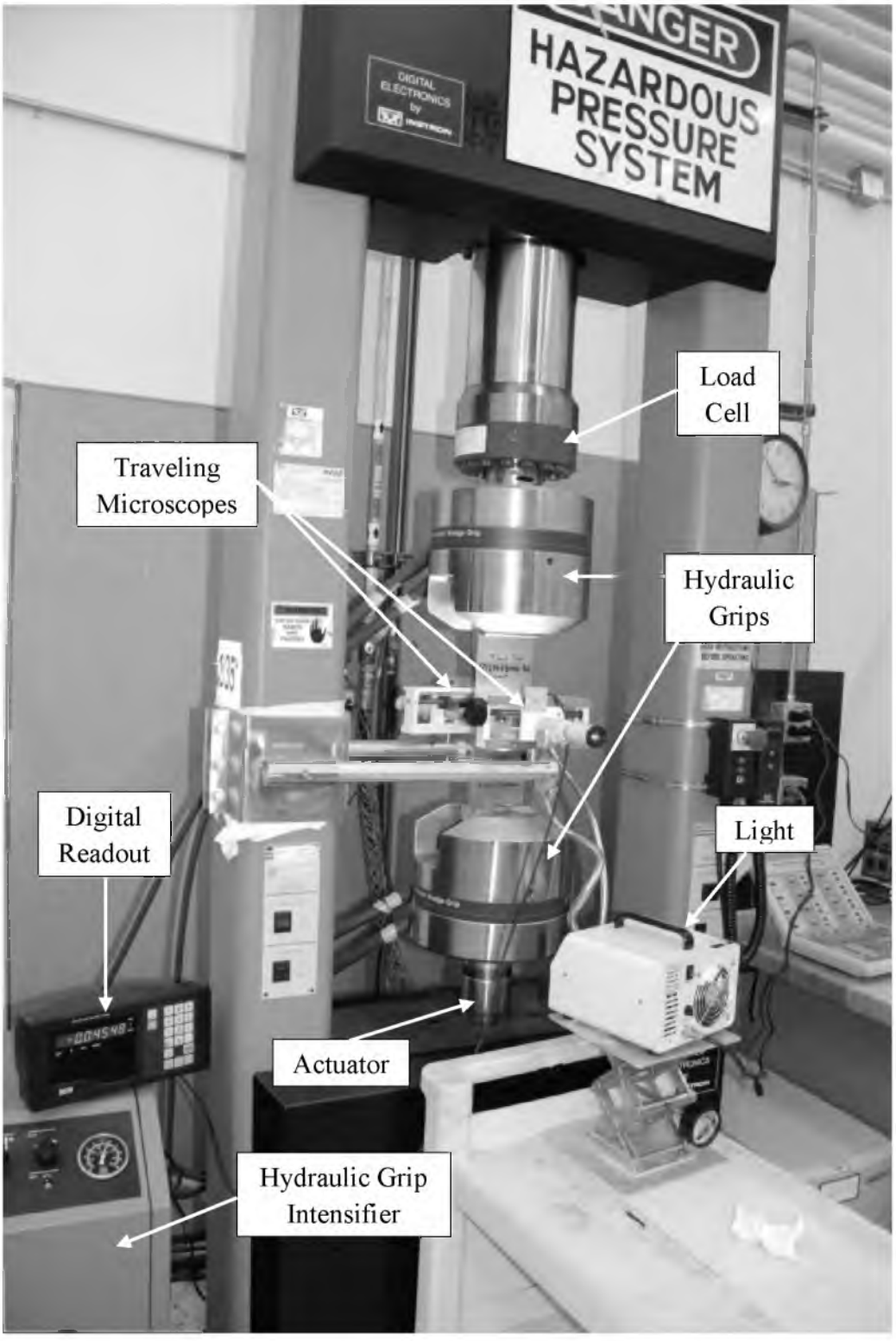

Figure 7 Interlaken 55 kip Fatigue Machine

alignment of the grips, which is necessary to prevent unexpected loading, met specification ASTM E1012 requirements.

2.3.1.2 MTS Hydraulic Wedge Grips

Hydraulic wedge grips, model 647, were used during this experiment in lieu of other gripping techniques. Using hydraulic grips simplifies the specimen installation process and reduces variability with mechanical grips. This is due to the fact that techniques require bolts to clamp onto the specimen, which require holes to be drilled creating stress concentration areas. These specific grips have a 55 kip capacity with a grip area that is 2.5 inches long by 4 inches wide. The MTS hydraulic wedge grips can be seen in the middle of Fig. 7.

2.3.1.3 MTS Hydraulic Over Hydraulic Intensifier

This particular model of hydraulic grips requires a hydraulic intensifier to increase line pressure from 3,000 psi to a maximum of 10,000 psi depending on the maximum load to be applied, static or fatigue. Based on this testing, the pressure was set at 5,400 psi in order to maintain consistent gripping throughout the tests while not providing too much clamp pressure, thus reducing the chance of a grip failure.

2.3.1.4 Instron 8800 Fast Track Controller and Software

An Instron 8800 series controller was used with different Instron software packages. The Bluehill 2 software was used for tuning, balancing and constant amplitude

loading. Tuning and balancing of the fatigue machine was necessary for every sample to ensure the accuracy of the data being collected.

As part of the Bluehill 2 software package, the constant amplitude model, called WaveMatrix, was used during the precracking phase of this experiment. This program allows one to select the wave shape, frequency and amplitude at which the test will be conducted. The only other piece of information needed to conduct the test is the mean stress, which is the value established by the user in the setpoint window of the Bluehill 2 module. The details of how the precracking was performed will be explained later.

A third software package, called RandomModule, was used to perform the variable amplitude portion of this experiment. This software allows for a load history file, in this case, the spectrum files, to be loaded into the program and used to run the machine. This program also allows for the user to select how long the test will run and if the load is to be applied at a certain frequency or load rate. For error checking, RandomModule will record any error above a value established by the user. The user interface for this program is shown in Fig. 8.

2.3.2 Measurement Equipment

2.3.2.1 Mitutoyo Calipers

To take measurements of each of the specimens width and thickness, Mitutoyo calipers, model CD-6" CXWW, were used. The calipers have a tolerance range of ±0.0005 and were calibrated on 1/23/2013, which is due on 7/23/2015.

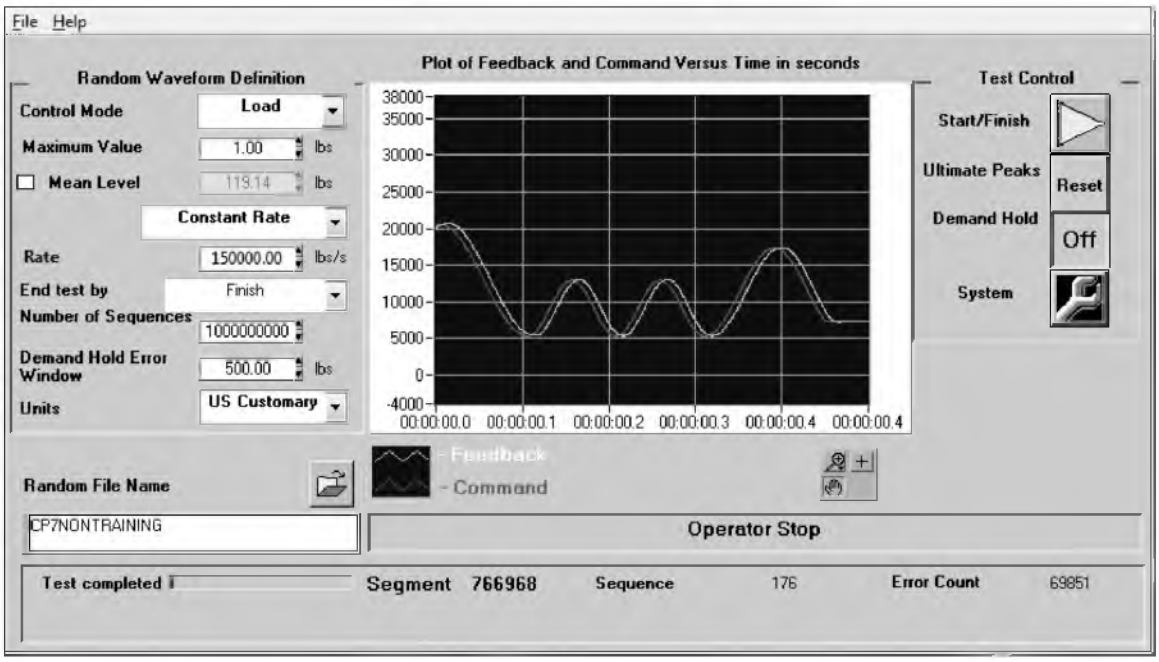

Figure 8 Random Module Interface

2.3.2.2 Gaertner Taveling Microscopes

Two Gaertner traveling microscopes, model M101A, mounted on custom-made frames were used to measure hole diameter and to track crack growth in the bore and front and back surfaces during testing. These microscopes can be seen mounted on the load frame in Fig. 9. The microscopes provided a 32x magnification with crosshairs, which were necessary to accurately track crack growth. [27] These microscopes had a variety of different eyepieces that could be used depending on the application. For this experiment, the eyepiece with a 60 millimeter focal length was used for tracking the surface cracks while the 80 millimeter focal length eyepiece was used for tracking the bore crack.

In order to measure the bore crack, the back microscope was focused on the bore wall at an angle. A diagram of the setup can be seen in Fig. 10. In order to measure what

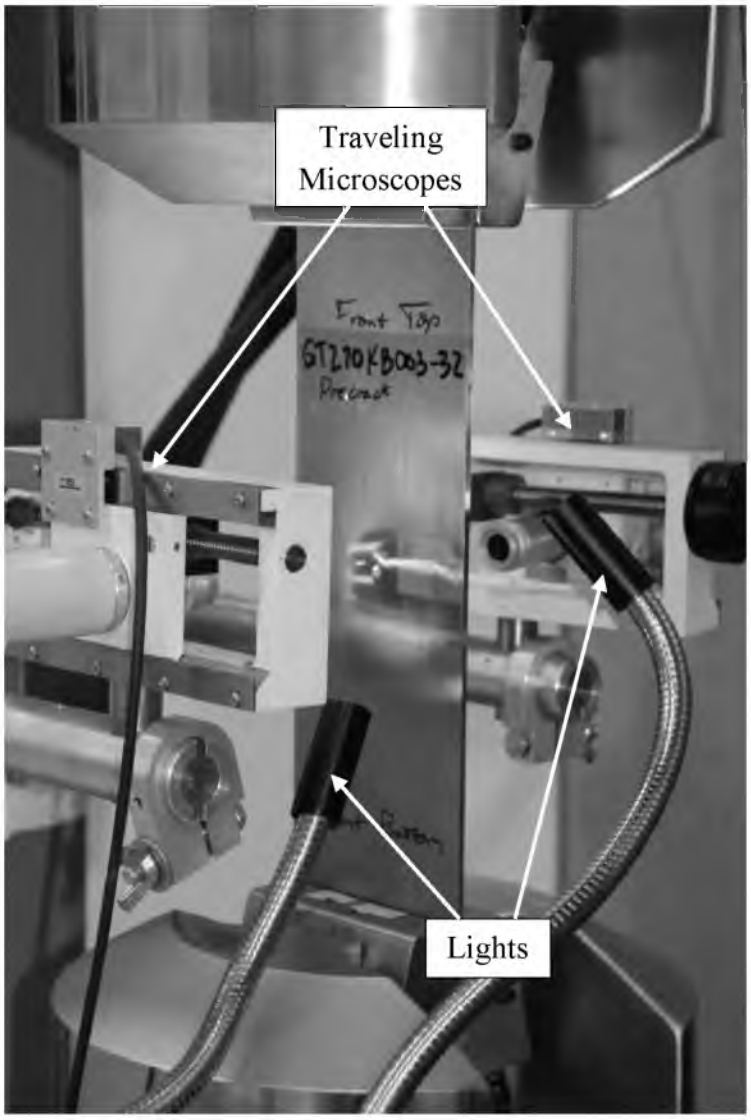

Figure 9 Gaertner Microscopes, Front and Back, Used to Take Measurements

the crack length was in the bore, the angle at which the traveling microscope was placed needed to be known. Calculating the angle was accomplished by using simple trigonometric concepts of right triangles. If the thickness of the specimen is known and the apparent thickness of the specimen, through the microscope, can be measured, then one can calculate the angle of the microscope using the following formula.

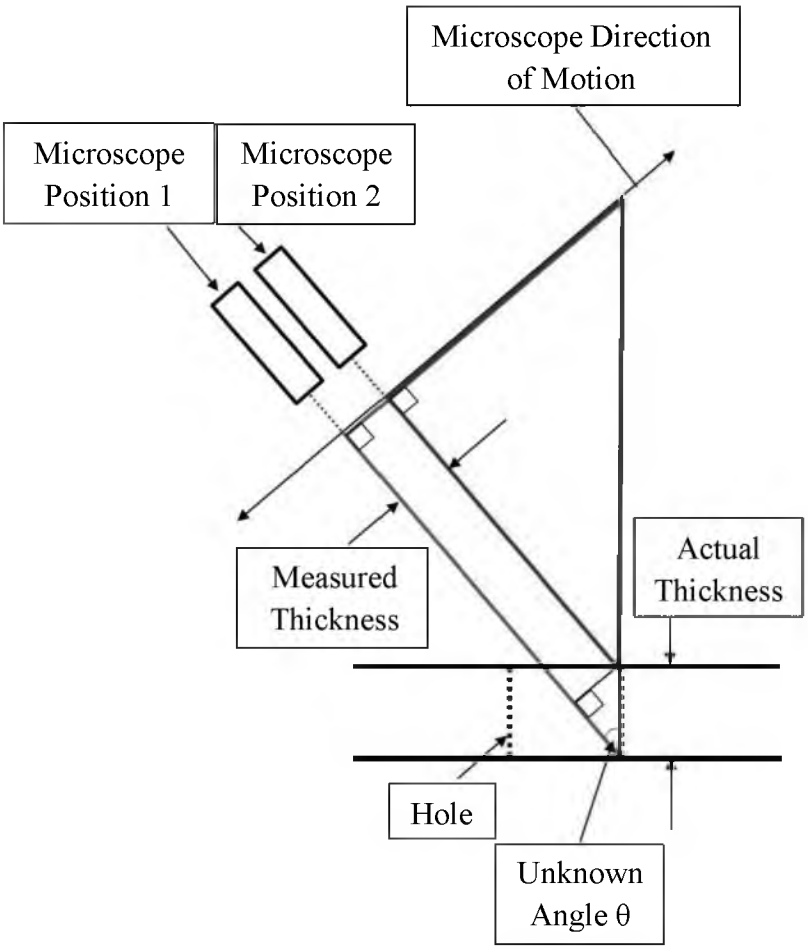

Figure 10 Illustration of Microscope Setup for Bore Measurements [26]

$$\theta = \sin^{-1}\left(\frac{Measured\ thickness}{Actual\ thickness}\right)$$

Once the angle of the microscope is determined, the crack length in the bore can be calculated by simply rearranging the same formula. The only difference at this point is that the measured crack length is now the variable for crack length as shown in the following formula.

$$Crack\ Length = \frac{Measured\ crack\ length}{\sin(\theta)}$$

The measurements from the microscopes were displayed on Fagor Automation digital readouts. The tolerance range on the Fagor readouts is ±0.00002, which exceeds the requirements of ±0.004 required by ASTM E647. One of the readouts can be seen mounted on the hydraulic intensifier in Fig. 7.

2.3.2.3 AmScope Lamp

To increase the visibility of the crack, an AmScope lamp, model HL150-AY, was used to illuminate the specimen. This lamp incorporates two snake lights, which could be put in any position necessary to illuminate the crack. Images of the lamp can be seen in Figs. 7 and 9.

2.4 Reaming and Bore Polishing

2.4.1 Reaming

After the precracking was performed on each of the specimens, the center hole was reamed from a 0.157" hole to a 0.250" hole, which is representative of a fastener hole. The procedure used for reaming the bore can be seen in Appendix B. The reaming operation was performed on a Supermax Mill, model YC-1.5VS-1 and seen in Fig. 11, is manufactured by the Jih Fong Machinery Co. LTD. The dial indicator used to find the center of the bore is accurate to within 0.001 of an inch.

2.4.2 Bore Polishing

After the reaming was performed, the bore surface had machining marks, which made it difficult to view the crack. To obtain better visibility of the crack in the bore, it

Figure 11 Supermax Mill Model YC-1.5VS-1

was necessary to polish the bore. A Dremel, model number 3000, was used to polish the bore. The procedures used to polish the bore can be seen in Appendix B. This polishing process provided a near mirror finish that made tracking the crack growth much easier. The difference in diameter, measured using the Gaertner microscopes mentioned previously, from this polishing process was on average 0.005 of an inch on the diameter.

2.5 Fractographic Equipment

After the fatigue testing was concluded, a fractographic examination of the test specimen fracture surfaces was conducted using a Hitachi Scanning Electron Microscope

(SEM), model S-2600N, see Fig. 12. Due to the limitations of the space within the vacuum chamber, the specimen had to be placed in the holder on an angle. A view of how the tests specimens had to be placed in the machine can be seen in Fig. 13.

2.6 Testing Procedures

2.6.1 Precracking

The test plan for this experiment required that the test specimens be precracked before the actual testing takes place. [8] This serves the purpose as stated in ASTM E647:

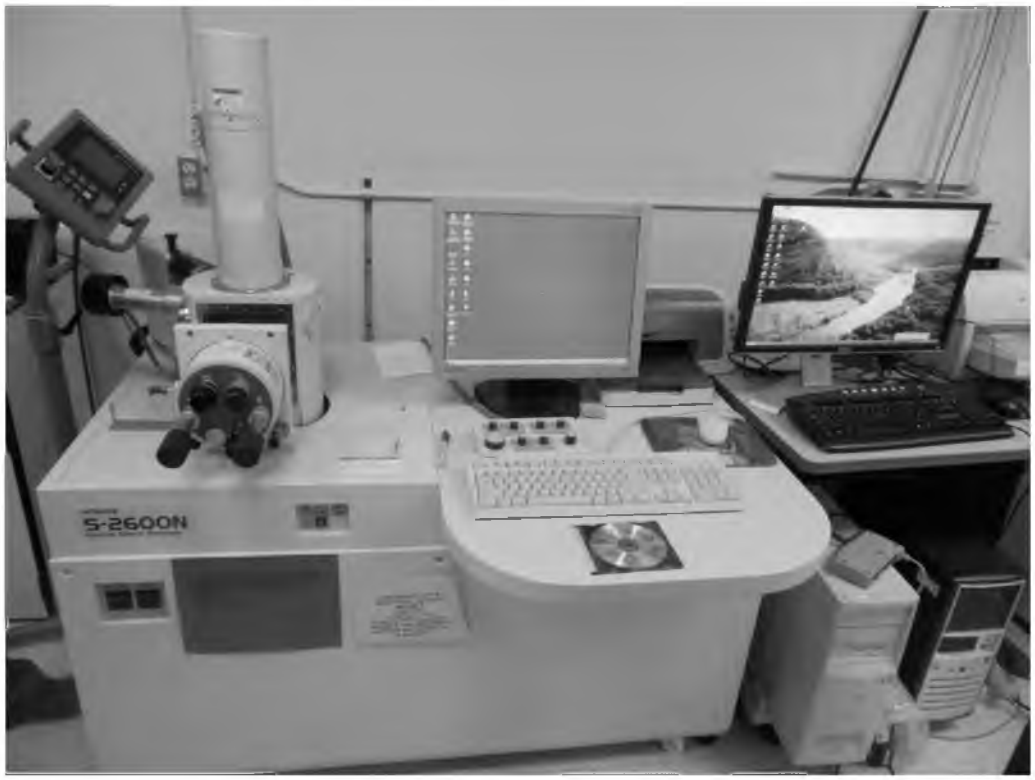

Figure 12 Hitachi SEM Model S-2600N

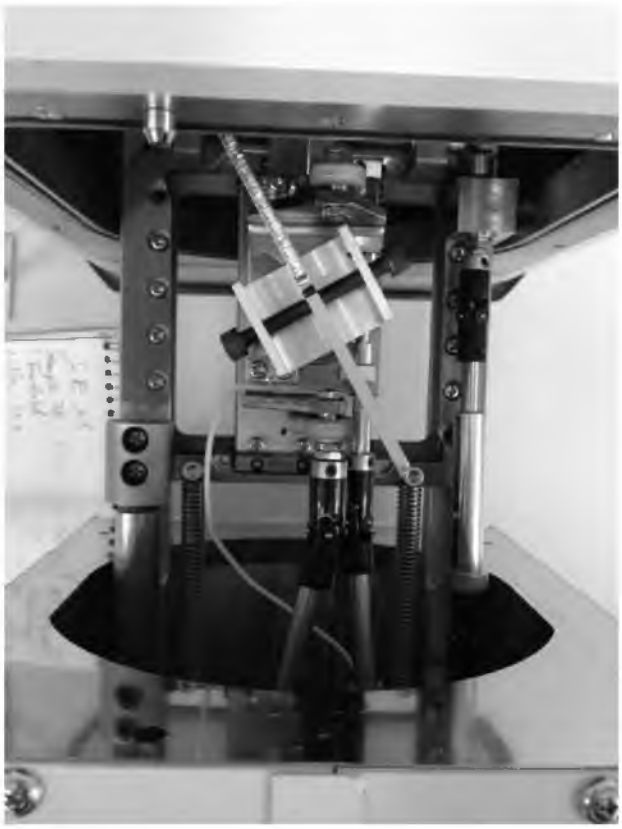

Figure 13 Position of Fatigue Specimen Once Inside the SEM

> to provide a sharpened fatigue crack of adequate size and straightness which ensures that 1) the effect of the machined starter notch is removed from the specimen K-calibration, and 2) the effects on subsequent crack growth rate data caused by changing crack front shape or pre-crack load history are eliminated. [28, p. 6]

As mentioned previously, each specimen started off with a 0.157" hole with a 0.020" by 0.030" triangular-shaped EDM corner notch placed perpendicular to the load path. The EDM notch serves as a stress concentrator to get the crack started.

The test plan also specified that a constant amplitude cyclic load be applied to the specimens that would result in precracks 0.030 to 0.050 of an inch in length beyond the final ream sized hole. [8] These precracks were representative of flaws in the material that are assumed to be present according to the Damage Tolerant philosophy. [6] The

size of the precrack was chosen because 0.030" to 0.050" is the NDI detectable limit. [6] The Constant amplitude loading was applied at 15.4 ksi and a stress ratio of 0.05. [8] The 15.4 ksi stress, which is 70% of the max stress in the test, was chosen because ASTM E647 requires that any precracking performed end with a max stress intensity that is lower than the initial stress intensity of the test. [28] A complication that arises from this ASTM E647 requirement is that it was intended for constant amplitude loading and mentions nothing for variable amplitude loading, which is what was used during actual testing. It was determined that as long as the final precracking stress intensity was less than the initial max stress intensity created by the highest load in the spectrum, the intent of E647 requirement would be met.

2.6.1.1 Load Shedding

Soon after the precracking on the first sample was initiated, it became apparent that something needed to be done to speed up the process. Initially, the precracking ran for several hours at the 15.4 ksi stress level with no detectable crack progression. ASTM E647 specifies a load shedding technique that can be used to speed up the precracking process. Load shedding is a process where one runs the sample at a high load to get the crack started from the notch. The load is then progressively decreased over a number of steps until the final step is at the desired stress level. A graph that illustrates the load shedding concept is shown in Fig. 14.

One of the load shedding requirements from ASTM E647 is that each step must be run long enough to get through the plastic zone of the previous load shedding step. [28] Another requirement is that there can be no more than a 20% drop difference

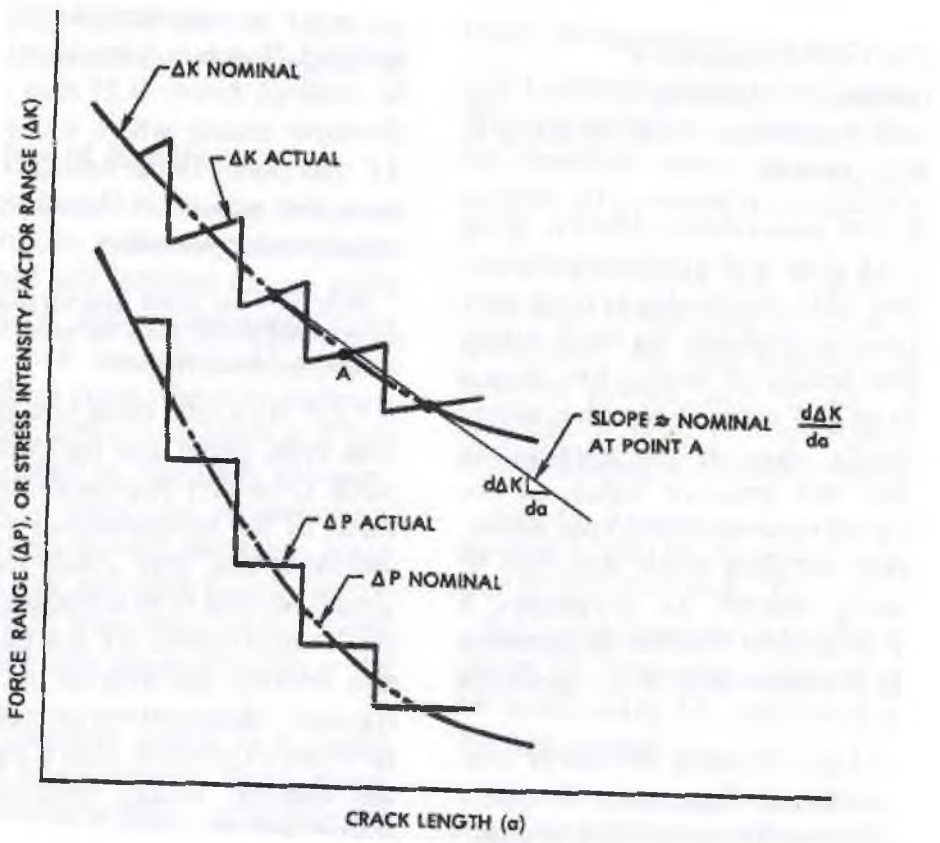

Figure 14 Plot Demonstrating the Load Shedding Concept [28]

between the final load max of one step and the beginning load max of the next step. The requirements are to reduce, as much as possible, any transient effects that occur from the plastic zones from one step to the next. [28] To determine the crack size increments for each step, E647 suggested using the following formula, which is the formula for calculating plastic zone sizes. [28]

$$\Delta a = \left(\frac{3}{\pi}\right)\left(\frac{K'_{max}}{\sigma_{YS}}\right)^2$$

Here, Δa is the crack size increment, K'_{max} is the terminal value of K_{max} from the previous step. The difficulty that arises from using this formula is determining the correct K'_{max} value. This is due to the fact that geometry of the specimens used in the experiment, particularly the EDM notches, differs from that typically used in the E647 test. The middle tension specimens in E647 have a hole in the center, just like this experiment, but with two, through thickness notches on opposite sides of the hole perpendicular to the load path. The specimens used in this experiment had only one corner notch, which requires a different formula to determine the K'_{max} value.

The formulas used to determine the K'_{max} value were obtained from the Handbook of Stress Intensity Factors. [29] The primary function is the following equation, which was derived from finite element results. [29] A step-by-step process of how this function is used is shown in Appendix E. [29]

$$K = S_t \sqrt{\pi \frac{a}{Q}} F_{ch}\left(\frac{a}{c}, \frac{a}{t}, \frac{r}{t}, \frac{r}{b}, \frac{c}{b}, \phi\right)$$

K is the stress intensity at a point along the curve at angle ϕ, which is in radians. [29] S_t is the tension stress, a is the crack length in the bore, c is the crack length on the surface, t is the specimen thickness, b is the width of the specimen and r is the hole radius. [29] Q is expressed in the following equation. [29]

$$Q = 1 + 1.464\left(\frac{a}{c}\right)^{1.65}$$

where a and c are the same as the previous function. It was assumed that the aspect ratio, a/c, remained a constant 0.667.

Once it was known how to calculate the stress intensity values, the number of load shedding steps now needed to be determined. ASTM E647 recommends:

> The rate of force shedding with increasing crack size shall be gradual enough to 1) preclude anomalous data resulting from reductions in the stress-intensity factor and concomitant transient growth rate, and 2) allow the establishment of about five da/dN, ΔK data points of approximately equal spacing per decade of crack growth rate. [28, p. 7]

It was known that the crack needed to grow approximately 0.047 to 0.067 of an inch beyond the EDM notch to achieve the 0.03 to 0.05 inch fatigue crack beyond the 0.250 inch reamed hole. To start off, the 0.047 was divided up into 5 segments of about 0.010 inch crack growth capacity. The methodology used to determine the load per step was to start off with a load that when decreased by 20% per step would result in a final load that corresponded to the 15.4 ksi stress level desired. The loads could then be used to calculate the stress levels, which in turn were used, with the respective final crack length for each step, to determine the max stress intensity value along the crack front. Once the max stress intensity was determined, the plastic zone sizes could be determined, which showed what was required for the crack growth increments between steps. The results of the final calculations are shown in Table 3.

Table 3 Load Shedding Calculation Results for Each Step

Step	Crack Length (in)		Stress (ksi)	Stress Intensity (ksi$\sqrt{in}$)	Plastic Zone (in)
	Dim. a	Dim. c			
1	0.030	0.045	37.5	20.4	0.0180
2	0.040	0.060	30.0	18.0	0.0145
3	0.050	0.075	24.0	15.5	0.0110
4	0.056	0.084	19.2	13.1	0.0075
5	0.061	0.091	15.4	11.4	0.0050

2.6.2 Fatigue Testing

To compare the two spectra developed for this research, five different combinations of the spectra were tested. These different combinations were given the following nomenclature: A baseline, A plus B_1, A plus B_2, A plus B_3 and B baseline tests. For each combination, three specimens were used to establish a level of confidence in the results. The baseline tests, A and B showed how each spectrum performed individually. The mixed spectra tests were set up to run the A spectrum first then transition to the B spectrum when the bore crack length reached a predetermined range. The differences between the mixed spectra tests were that the transitions from A to B occurred at different crack lengths. This was done because no two aircraft have experienced the exact same usage; hence, a range of crack size applicability had to be considered in the testing. Thus, the B_1 to B_3 tests were meant to show a progression of effective flight hours (EFH) spent under A loading condition. B_1 tests represent the least amount of time an aircraft spent under A loading conditions while B_3 tests represented the most. The attributes for each spectrum are shown in Table 4.

Before actual testing began, the test run order was randomized. This was done to reduce any abnormalities that may occur while testing from skewing the test data. For instance if all of the A baseline tests were done sequentially while some error had occurred in the machine, then all of the data for those specimens would be affected. But

Table 4 Test Spectra Attributes. Data from [8]

Spectrum	σ_{max} (psi)	$Load_{max}$ (lb)	σ_{min} (psi)	$Load_{min}$ (lb)	Blocksize (Hours)	Endpoints per Block
A	21,953	10,977	197	99	240	16,731
B	21,953	10,977	266	133	1,000	4,371

if the run order is randomized, only a portion of the data would be affected and not the whole set. The test order for this study is shown in Table 5.

To determine the load rate at which the tests could be run, a spare specimen was subjected to the different loading spectra at varying rates. While these tests were running, the Random Module program was used to record the error and log the information into a file. This information, which contained the command load and the feedback load, was used to calculate the average error during the testing. Due to the limitations of the equipment used, it was determined that an average error of 2% or below, at the load rate used, would be acceptable. The loading rate used on most of the testing at Hill AFB was 150 to 200 kip/s for the A spectrum and 100 to 150 kip/s for the B spectrum. These loading rates produced errors of greater than 2% on individual load points mostly on loads 20% or less of the peak load, but some were as high as 60%. The

Table 5 Specimen Test Order

Test Type	Test Specimen ID Number	Test Order
A Baseline	7	1
	2	14
	5	6
A + B_1	6	9
	1	10
	8	28
A + B_2	9	12
	10	7
	11	29
A + B_3	12	2
	13	30
	14	8
B Baseline	28	5
	29	11
	30	13

max load variation producing the error was 135 lb. The equipment used at Hill AFB made managing the error any better than what was observed difficult. SwRI was able to keep all points below 2% error while running at 100 kip/s. Therefore, it is recommended that the load rate be reduced to better manage the error.

2.7 AFGROW Procedures

As has been stated, AFGROW is a program used to model crack growth behavior subject to fatigue. Essentially, how this program works is it uses the inputs provided by the user, i.e., geometry of the sample, material used, loading conditions etc., and calculates how much the crack will grow on each load cycle. [30] Starting with an initial flaw size, the program calculates the stress intensity on the crack front and uses that information to determine how much the crack will grow on that cycle. This process is repeated cycle per cycle until certain failure or termination criteria are met. The analysis for this study was conducted using procedures, seen in Appendix F, which were based on a set of guidelines prepared by the USAF. [31] Fig. 15 is an image of the AFGROW interface.

As was mentioned earlier, past research showed that Yield Zone and Crack Closure crack growth retardation models provided good fits to steel type materials tested under similar conditions. However, soon after starting the modeling process, it was discovered that better fits to the data could be obtained when no retardation models were utilized. Further discussion on this topic can be seen in section 4.3.

Figure 15 AFGROW Interface

2.8 Data Collection and Test Matrix

Excel spreadsheets were used to collect the data during fatigue testing. These data sheets identified the specimen and what type of test was performed. Concerning the specimens themselves, the following measurements were recorded: specimen thickness, specimen width, EDM notch length, pre- and postream center bore diameter and postream corner crack surface and bore lengths. Other items of interest that were recorded on the data sheets were testing dates, load conditions, load rates and comments. An example of a crack growth data sheet can be seen in Fig. 16.

Concerning the frequency on which measurements should be recorded during the test, the researchers took into consideration a guideline in ASTM E647. This specification recommends that measurements be recorded on a minimum of 0.004 of an inch crack growth. [28] Having said that, the same specification also states that the, 0.004 of an inch, measurement could be adjusted depending on the circumstances. [28]

GT270KB003-13-5 Fatigue Crack Growth Data Sheet

Width: 4.004 in. Thick: 0.125 in. Area: 0.501 in^2

Pre-crack Information

Pre-crack Date: 6/4/13 Loading Condition: Constant Amplitude R=0.05

Hole Dia.: 0.157 in. Surface EDM: 0.0298 in.

Pre-crack Tuning Data

Tuning Step	Frequency (Hz)	Tuning Cycles	Max Stress (ksi)
1	13	1977	37.5
2	15	1923	24
3	18	2940	15.4

Pre-crack Run Data

Cycles	Stress (ksi)	Frequency (Hz)	Crack Length (in.)
0	0	0	0.1083
32759	37.5	13	0.1233
54099	30	13	0.1397
92092	24	15	0.1529
128284	19.2	15	0.1620
173327	15.4	18	0.1687

Experiment Information

Exp. Date: 2/11/14 Loading Condition: Variable Amplitude

Exp. Type: Spec. A Loading Rate: 400 to 500 kip/s Hole Dia.: 0.253 in.

Max Stress (Sp. A): 21.953 ksi Surface Crack: 0.046 in. Bore Crack: 0.082 in.

Experiment Run Data

Spectrum	EFH	Crack Length (in.)			Comments
		Front	Bore	Back	
A	0	0.046	0.082		500 kip/s
	4497.77	0.048	0.082		
	25347.35	0.069	0.098		
	45425.05	0.090	0.116		Reduced to 400 kip/s due to limit trip
	66581.12	0.120	0.125	0.073	
	84059.44	0.153		0.109	
	107210.63	0.193		0.163	
	129839.13	0.244		0.221	
	152402.17	0.305		0.284	

Figure 16 Example of a Crack Growth Data Sheet

Thus, it was anticipated that measurements would be recorded in these small increments during the initial stages of the test, then increase to larger increments as the tests proceeded. The test matrix used for this research is shown in Table 6.

Table 6 Fatigue Testing Matrix

No. of Specimens Tested	Identification	Spectrum and Sequence	Test Sequence
3	Baseline A	A only	Baseline, testing from initial crack to at least 100,000 EFH with this spectrum
3	A + B_1	A + B	Spectrum A testing until initial crack grows to a = 0.090 to 0.095", then switch to spectrum B
3	A + B_2	A + B	Spectrum A testing until initial crack grows to a = 0.105 to 0.110", then switch to spectrum B
3	A + B_3	A + B	Spectrum A testing until initial crack grows through thickness, then switch to spectrum B
3	Baseline B	B only	Baseline, testing from initial crack to at least 100,000 EFH with this spectrum

CHAPTER 3

RESULTS

3.1 Accelerated Fatigue Tests

The results shown in this chapter are based on data gathered from testing conducted at both Hill AFB and SwRI. It is important to note that both Hill AFB and SwRI conducted at least one of each type of test. It was not originally planned to perform fatigue tests at two locations, but it helped to determine if any error occurred due to the equipment being used. Each of the five variations of tests used three test specimens. The data sheets for all of the fatigue testing conducted can be seen in Appendix G. Additionally, curves not displayed in the section can be seen in Appendix H

3.1.1 Spectrum A Baseline

Baseline data for spectrum A were developed for comparison purposes with spectrum B and analytical data. Whenever possible, it is a good idea to validate analytical data with testing results. Specimens designated as GT270-2, -5 and -7 were used to conduct these tests. The average bore and front surface cracks for these specimens were 0.074 and 0.044 of an inch, respectively. Fig. 17 plots the crack lengths vs. EFH of the fatigue testing conducted to establish the baseline for spectrum A. The plot shows that all three tests agree very well until about 200,000 EFH, at which point

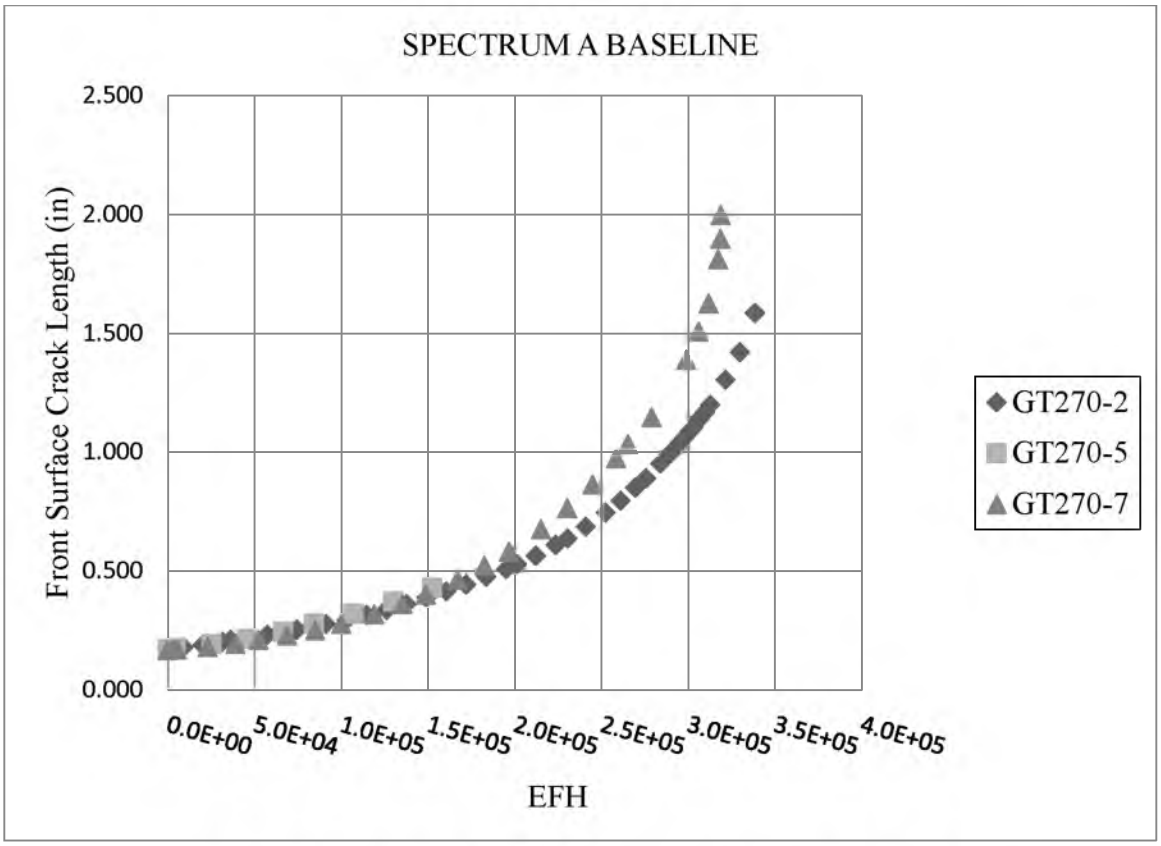

Figure 17 Front Surface Crack Spectrum A Baseline Results

tests GT270-2 and -7 begin to diverge. Even though the two tests began to differ from each other, the difference equates to only 6 % of total fatigue life. Two of the tests used for this baseline data were run until failure occurred. Running these tests until failure showed that the life of the specimen was about 330,000 EFH. The third test was run for only 150,000 EFH because that time exceeded the minimum requirement of 100,000 EFH. At 100,000 EFH, all three tests show that the front surface crack grew on average about 0.127 of an inch to a total of 0.297 of an inch.

For a plot showing how the bore and the back surface crack grew on specimen GT270-2, see Fig. 18. This plot shows that the bore crack grew to through thickness in about 50,000EFH under this spectrum. The plot also shows that the crack on the back

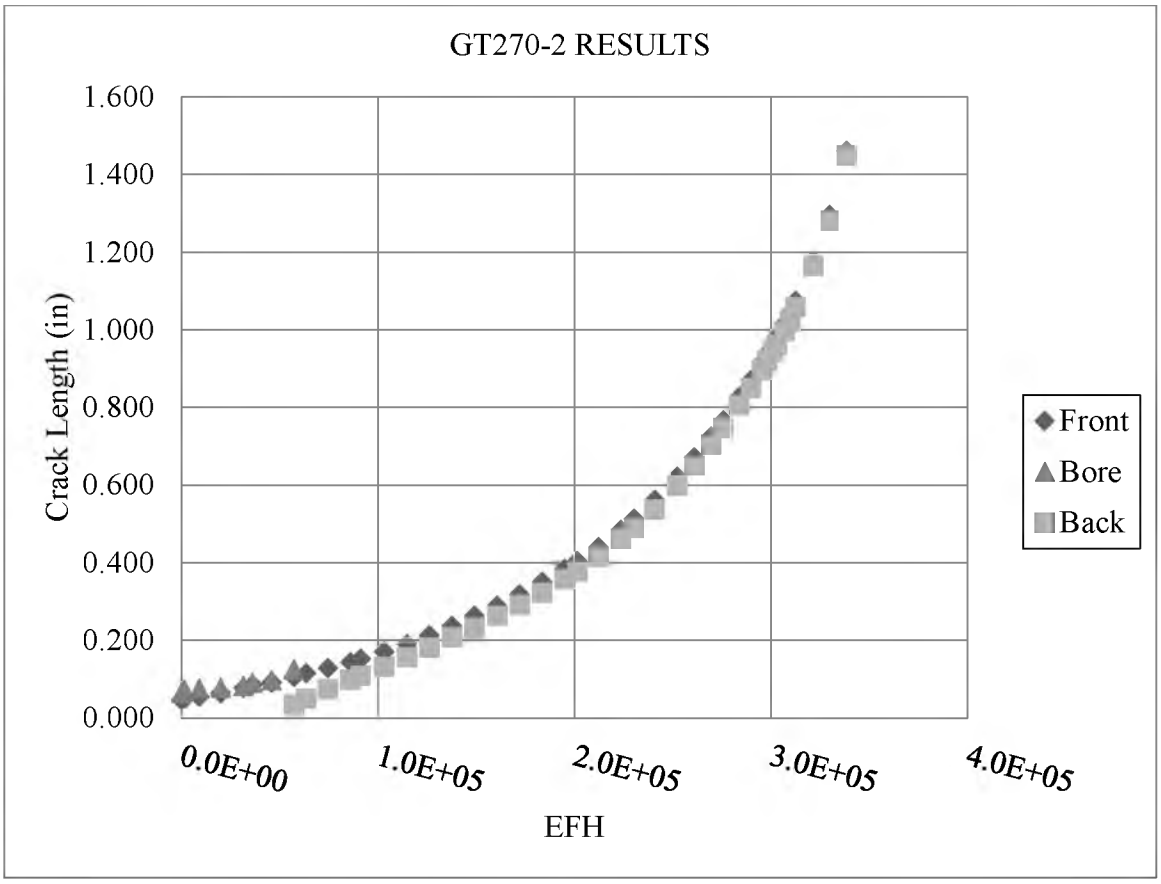

Figure 18 Front Surface, Bore and Back Surface Crack Growth Data for GT270-2

surface of the specimen initially grew at a slightly faster rate than the front crack. This is expected due to the higher Beta value that exists initially on a surface when a crack has just gone through thickness. The back surface crack continued to grow at a faster rate than the front surface crack until both were at a length of about 0.600 of an inch. At this point, the two crack measurements remained within about 0.020 of an inch of each other for the remainder of the test. This type of crack growth behavior validates that no irregular loading was occurring. The data for the other two specimens showed similar results.

3.1.2 Spectrum B Baseline

Specimens designated as GT270-28, -29 and -30 were used to conduct the spectrum B tests. The average bore and front surface cracks for these specimens were 0.081 and 0.171 of an inch, respectively. Fig. 19 plots the crack lengths vs. EFH of the fatigue testing conducted to establish the baseline for spectrum B. The plot shows that all three tests agree very well for the first 500,000 EFH, at which point GT270-28 begins to diverge from the other two tests. All three tests were terminated before the complete failure of the specimens occurred. Even without running to complete failure, all three tests were run for at least 900,000 EFH, which provided ample data. Fig. 19 shows that

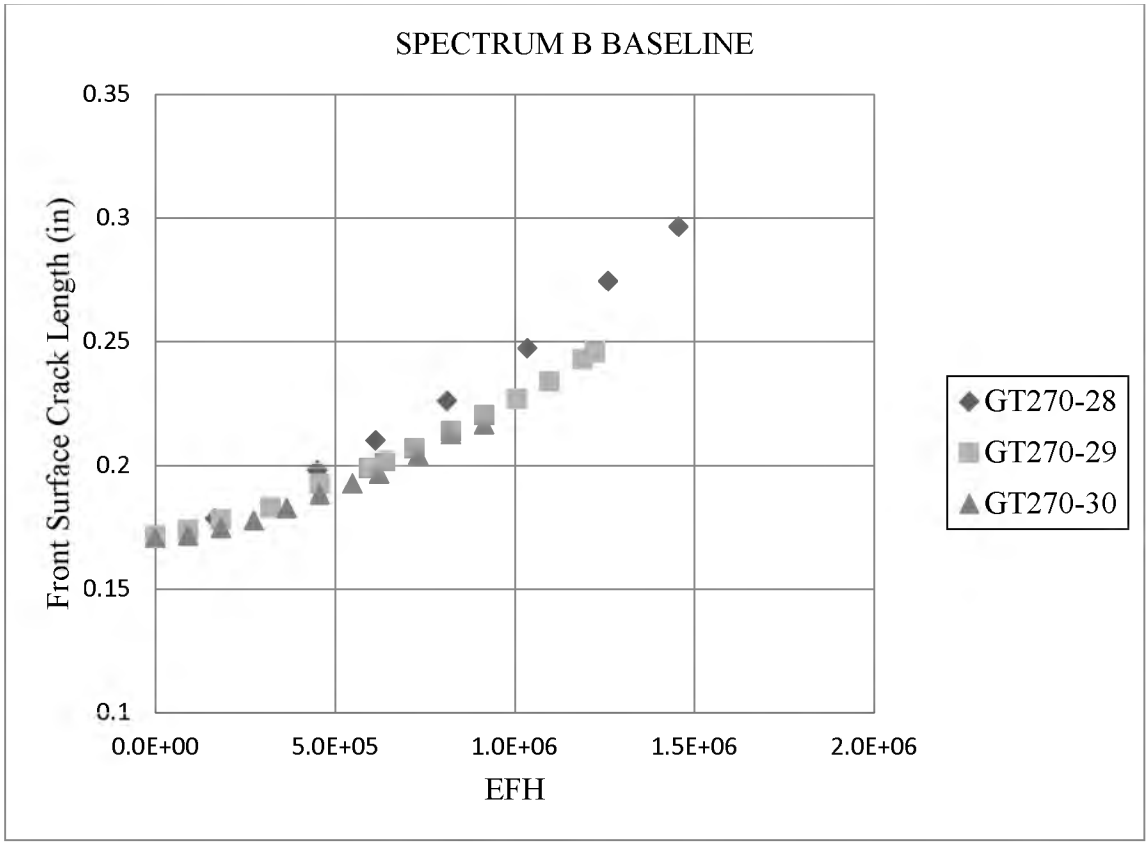

Figure 19 Front Surface Crack Spectrum B Baseline Results

even when the testing had ran for 450,000 EFH, the front surface crack had only grown on average 0.021 of an inch to a total of 0.192 of an inch.

For a plot showing how the bore crack and the crack on the back surface grew on specimen GT270-28, see Fig. 20. This plot shows that the bore crack grew to through thickness in about 500,000 EFH under this spectrum. The plot also shows that the crack on the back surface of the specimen initially grew at a slightly faster rate than the front surface crack. The back surface crack continued to grow at a faster rate than the front surface crack until they both grew to a length of about 0.300 of an inch. At this point, the back surface crack surpasses the front surface crack, but remains to within about 0.020 of an inch of the front surface crack for the remainder of the test. The data for the other two

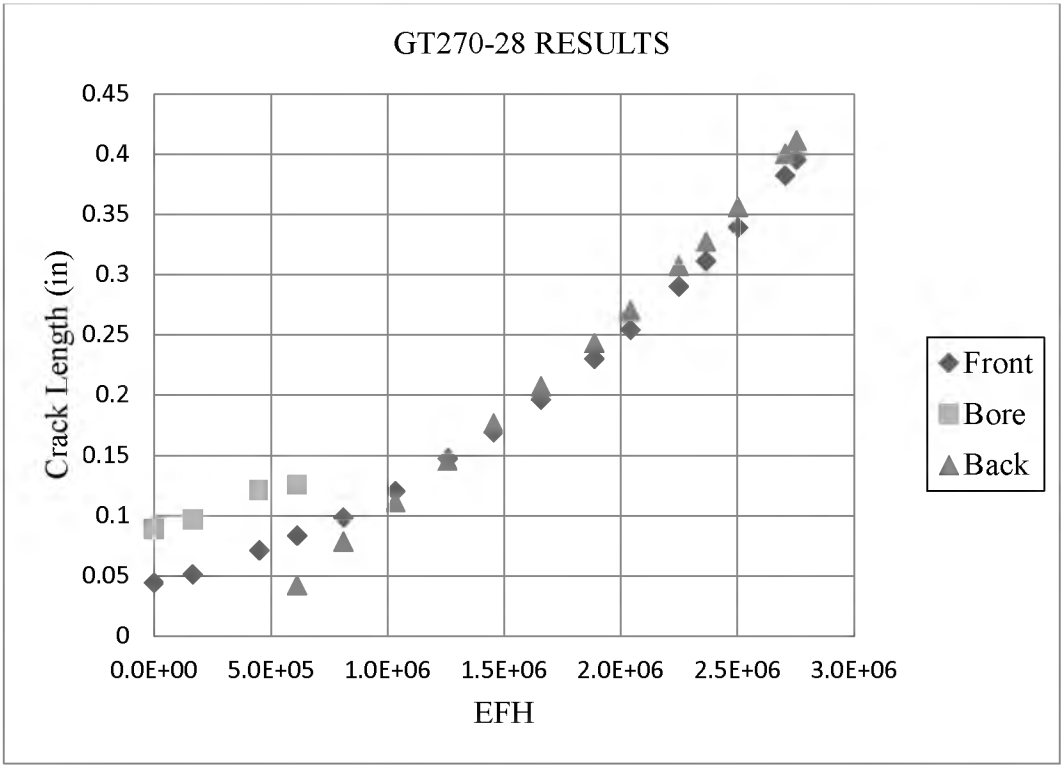

Figure 20 Front Surface, Bore and Back Surface Crack Growth Data for GT270-28

specimens showed similar results except that the back surface cracks never exceed the length measurements of the front surface cracks. The other difference on this specimen was that the bore to back surface crack transition took place at about 614,000 EFH while the others took on average about 686,000 EFH to make the same transition.

3.1.3 Combinations of Spectra A and B

Combination tests using both spectra were developed to directly determine how 17-7PH would behave during the transition from spectrum A to B. As was stated earlier, the bore cracks were allowed to grow to three different ranges of length under spectrum A before transitioning to spectrum B. This was done to represent the range in life of the actual fleet of aircraft under spectrum A before the transition occurred to spectrum B. It also allows investigators to determine if the crack growth behavior changes significantly between the different transition points. Note that since these tests were conducted for varying amounts of EFH, some of the plots were created with shortened data sets for visualization purposes.

3.1.3.1 Spectrum A + Spectrum B_1

The first type of combination spectrum tests conducted were the spectrum A + spectrum B_1 tests. These tests were run under spectrum A until the bore crack reached a length in the range of 0.090 to 0.095 of an inch. Specimens GT270-1, -6 and -8 were used to conduct these tests and the results of the front surface and bore cracks are shown respectively in Figs. 21 and 22. The average initial front surface and bore crack lengths for these specimens were 0.038 and 0.081 of an inch, respectively. Specimen GT270-1

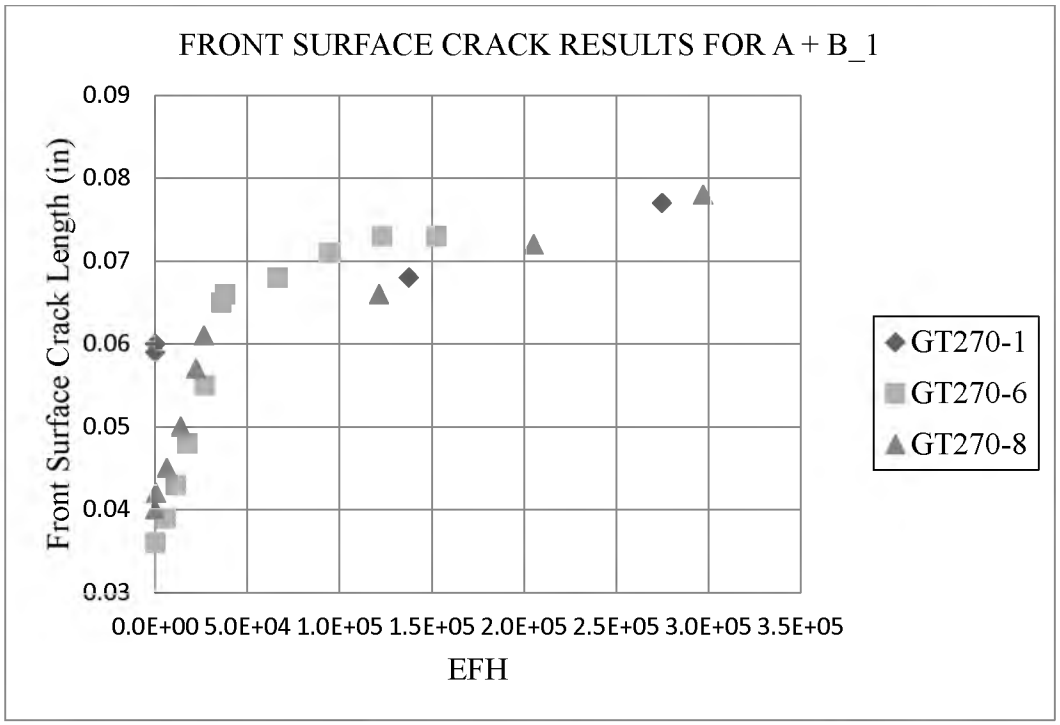

Figure 21 Front Surface Crack A + B_1 Combination Results

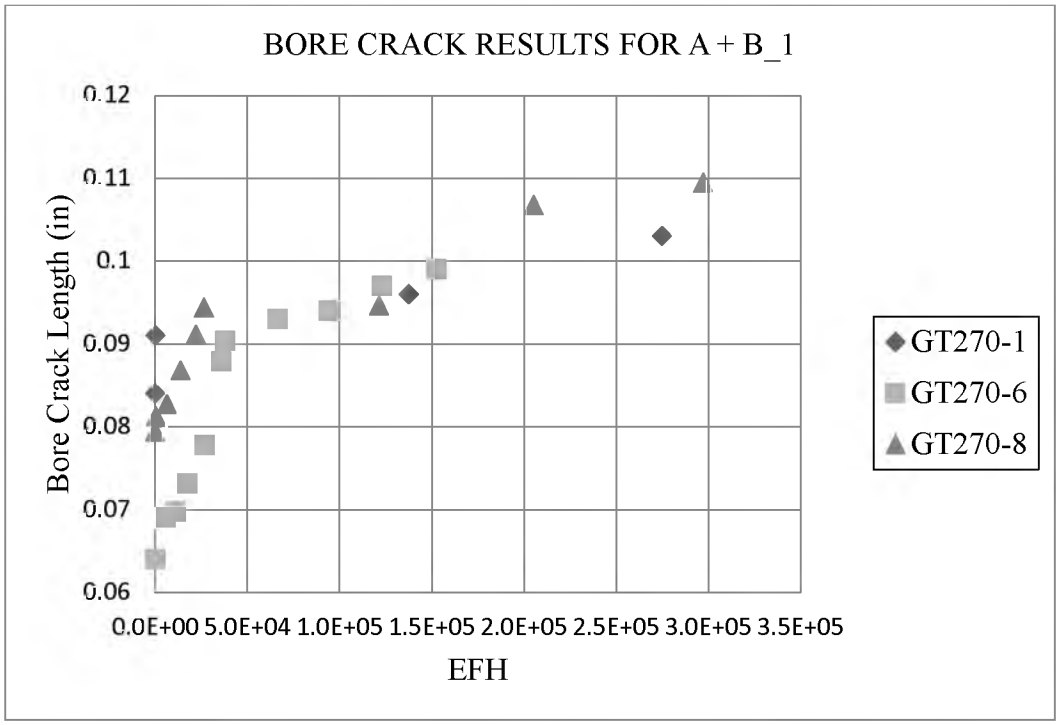

Figure 22 Bore Crack A + B_1 Combination Results

actually had larger initial crack sizes due to reasons that will be explained in section 4.1.2.1. The plots are the crack lengths vs. EFH of the fatigue testing conducted for the spectrum A to spectrum B_1 transition. These plots show that all three tests agreed very well as far as crack growth is concerned, with the exception of the initial measurements of GT270-1. All three tests were terminated prior to specimen failure but only after the minimum 100,000 EFH requirement had been met. For specimens GT270-6 and -8, the transition to spectrum B occurred at about 37,000 and 26,000 EFH, respectively. Once the transition to spectrum B was made, the crack growth essentially stalled for the remainder of the test. All three tests showed that during the spectrum B portion, the crack grew only 0.006 of an inch on average for 100,000 EFH.

For a plot showing how the bore and the surface crack grew for specimen GT270-6, see Fig. 23. This plot shows a clear distinction in crack growth between the two

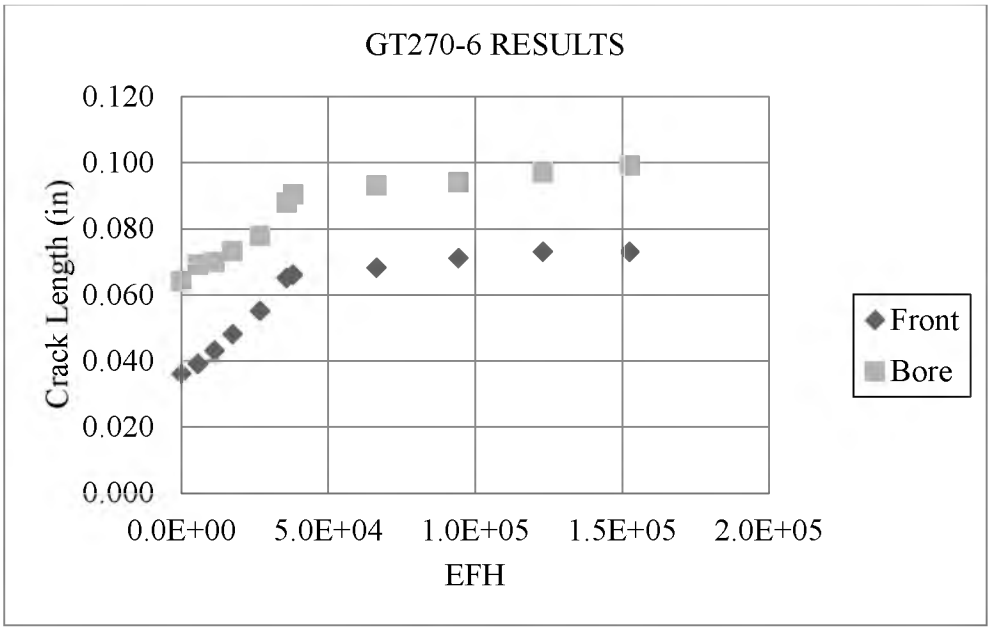

Figure 23 Front Surface and Bore Crack Growth Data for GT270-6

different spectra. One can see from the plot of either crack that they grew under spectrum A for about 0.025 of an inch in the 37,000 EFH period before transitioning to spectrum B. After the transition to spectrum B was made, the front surface and bore cracks grew approximately 0.007 and 0.009 of an inch, respectively, for 100,000 EFH.

3.1.3.2 Spectrum A + Spectrum B_2

The next type of combination spectrum tests conducted were the spectrum A + spectrum B_2 tests. These tests were run under spectrum A until the bore crack reached a length of 0.105 to 0.110 of an inch. Specimens GT270-9, -10 and -11 were used to conduct these tests. The average initial front surface and bore crack lengths for these specimens were 0.041 and 0.076 of an inch, respectively. Figs. 24 and 25 plot the crack

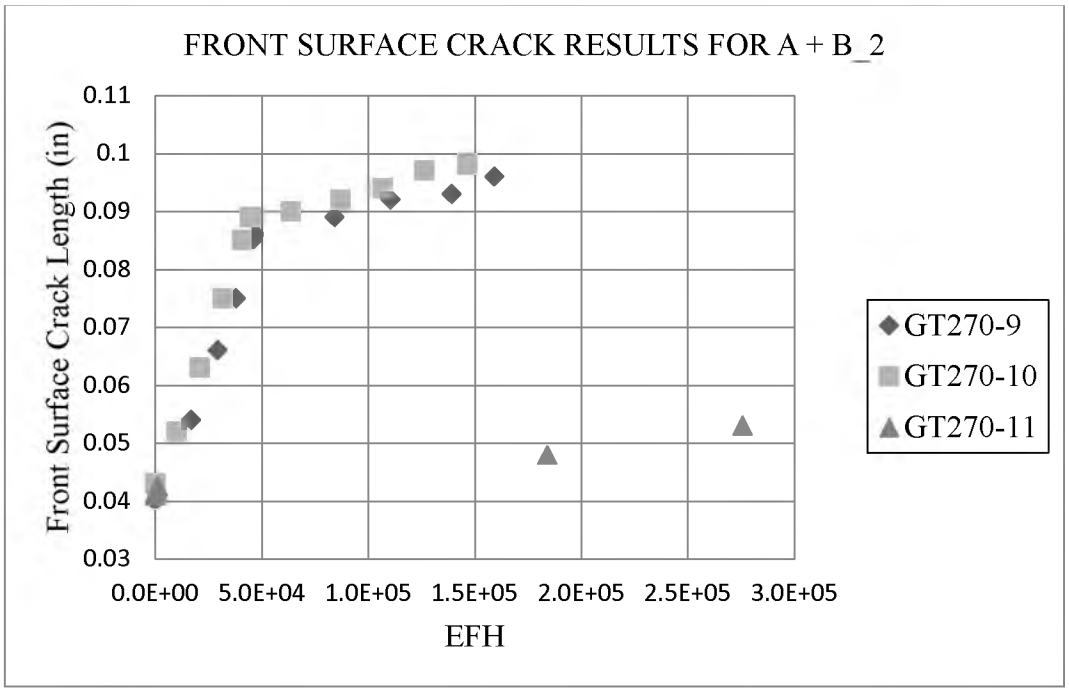

Figure 24 Front Surface Crack A + B_2 Combination Results

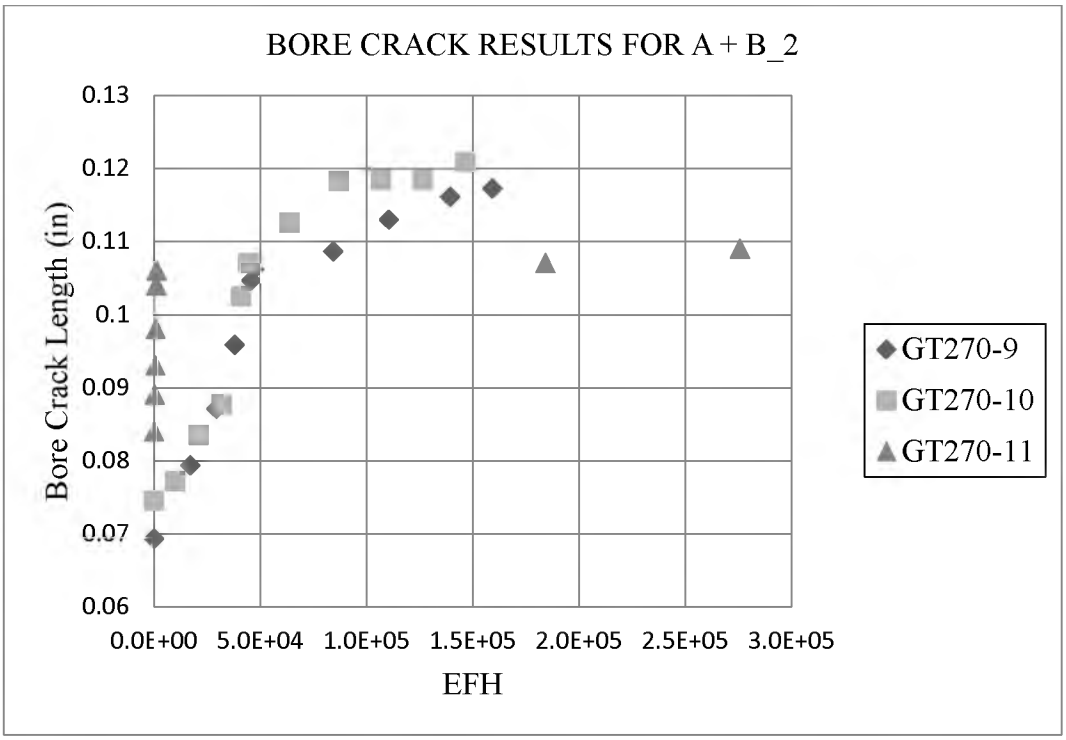

Figure 25 Bore Crack A + B_2 Combination Results

lengths vs. EFH of the fatigue testing conducted for the spectrum A to spectrum B_2 transition. These plots show that the results agree well with each other except for the results from specimen GT270-11. See section 4.1.2.1 for more details on specimen GT270-11. All three tests were terminated prior to specimen failure after meeting the minimum EFH requirement. For specimens GT270-9 and -10, the transition to spectrum B occurred at about 47,000 and 44,000 EFH, respectively. As was seen in the spectrum A + spectrum B_1 tests, the transition to spectrum B also caused the crack growth to stall. All three tests showed that during the spectrum B portion of the test the crack grew only 0.008 of an inch on average for 100,000 EFH.

A plot showing how the bore and the surface crack grew for specimen GT270-9 see Fig. 26. This plot also shows the clear distinction in crack growth between the two

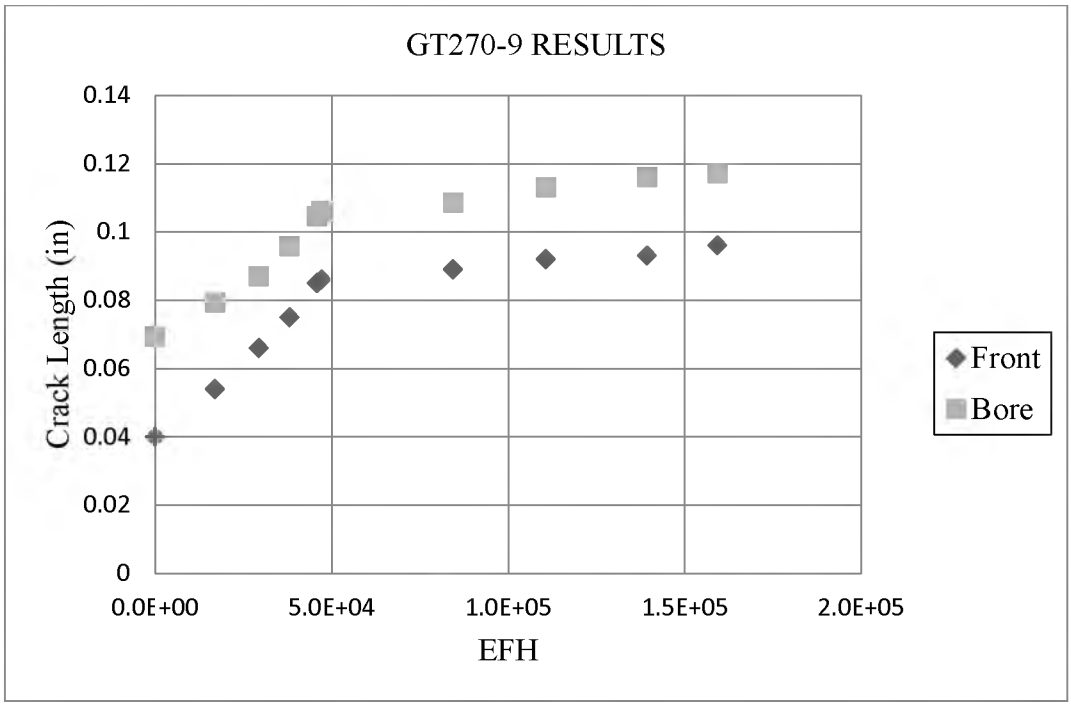

Figure 26 Front Surface and Bore Crack Growth Data for GT270-9

different spectra. The plot also shows that the crack grew under spectrum A for about 0.040 of an inch in the 47,000 EFH period before the transition to spectrum B. After the transition to spectrum B was made, the front surface and bore cracks grew approximately 0.010 and 0.011 of an inch, respectively, for the 100,000 EFH period.

3.1.3.3 Spectrum A + Spectrum B_3

The third type of mixed spectrum tests conducted were the spectrum A + spectrum B_3 tests. These tests were run under spectrum A until the bore crack grew through thickness. Specimens GT270-12, 13- and -14 were used to conduct these tests and the results are shown in Figs. 27 and 28. The average initial front surface and bore crack lengths for these specimens were 0.043 and 0.076 of an inch, respectively. The

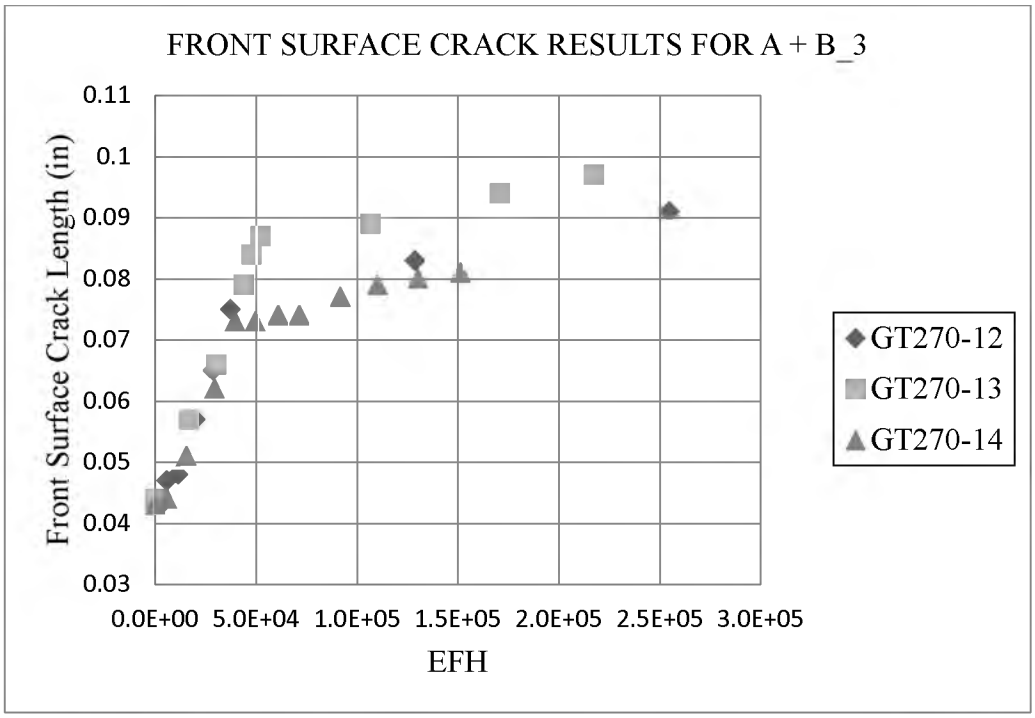

Figure 27 Front Surface Crack A + B_3 Combination Results

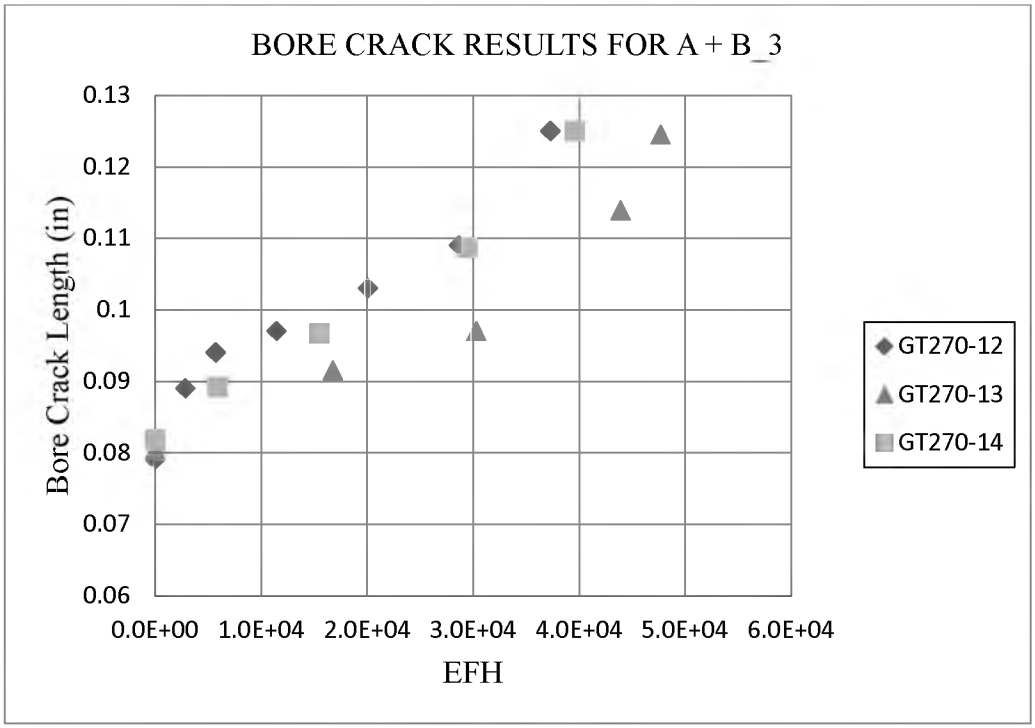

Figure 28 Bore Crack A + B_3 Combination Results

plot shows that all three tests agreed very well with respect to crack growth throughout both spectra. These tests were also terminated prior to specimen failure after meeting the minimum EFH requirement. The transition to spectrum B was made when GT270-12, -13 and -14 reached approximately 37,000, 48,000 and 40,000 EFH, respectively. As was seen in the other two types of combination spectra tests, the transition to spectrum B also caused the crack growth to stall. All three tests showed that during the spectrum B portion of the test the crack grew about 0.008 of an inch on average for 100,000 EFH.

A plot showing how the bore and the surface cracks grew for specimen GT270-13 see Fig. 29. This plot shows that the cracks grew under spectrum A for about 0.040 inches in the 47,000 EFH period before the transition to spectrum B. After the transition to spectrum B was made, the front surface and back surface cracks grew approximately 0.010 and 0.040 of an inch, respectively, for the 100,000 EFH period.

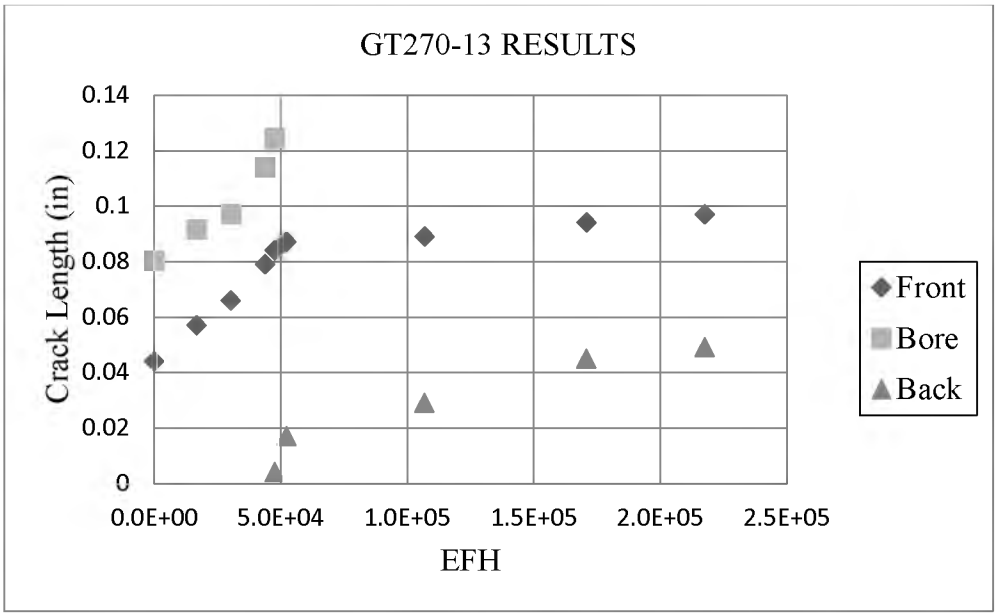

Figure 29 Front Surface, Bore and Back Surface Crack Growth Data for GT270-13

3.2 Fractography Examinations

As was mentioned previously, in Chapter 1, the purpose of the fractographic examination was to verify initial flaw sizes and transition crack lengths, but primarily to make note of any distinct features the spectra created on the crack surfaces. This was accomplished using the Hitachi SEM at the University of Utah. This section will go over general observations of the images for each type of test combination performed. A more detailed discussion of fracture surface features will be given in Chapter 4. It is important to remember that each test specimen was precracked to a predetermined length before the spectra were applied. Note that the specimens are angled in the images due to the limitations of space in the SEM used. For additional images of fracture surfaces see Appendix I. The process followed for using the SEM can be reviewed in Appendix B.

3.2.1 Spectrum A Baseline Fractography

For the spectrum A baseline tests, the specimens first precracked then tested to completion under spectrum A. Fig. 30 shows the widest view that could be obtained for the fracture surface of specimen GT270-7. The precrack surface can be seen propagating from the upper right corner on the fracture surface. Also notice how each of the precrack load shedding steps can be seen in the precrack area. The figure also confirms the testing data of the precrack front surface crack length to be approximately 0.040 of an inch.

The next figure, Fig. 31, is a close up of the transition from the constant amplitude precrack fracture surface to the variable amplitude Spectrum A surface. There appear to be no real distinct fracture surface features between the precrack and Spectrum A other

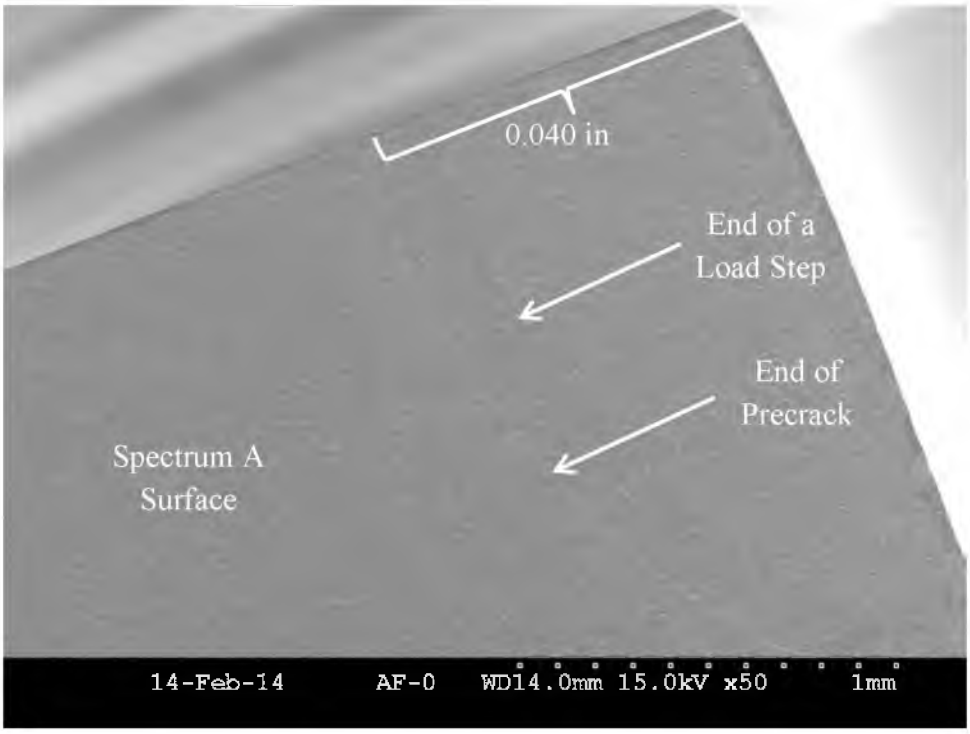

Figure 30 Wide View of GT270-7 Fracture Surface

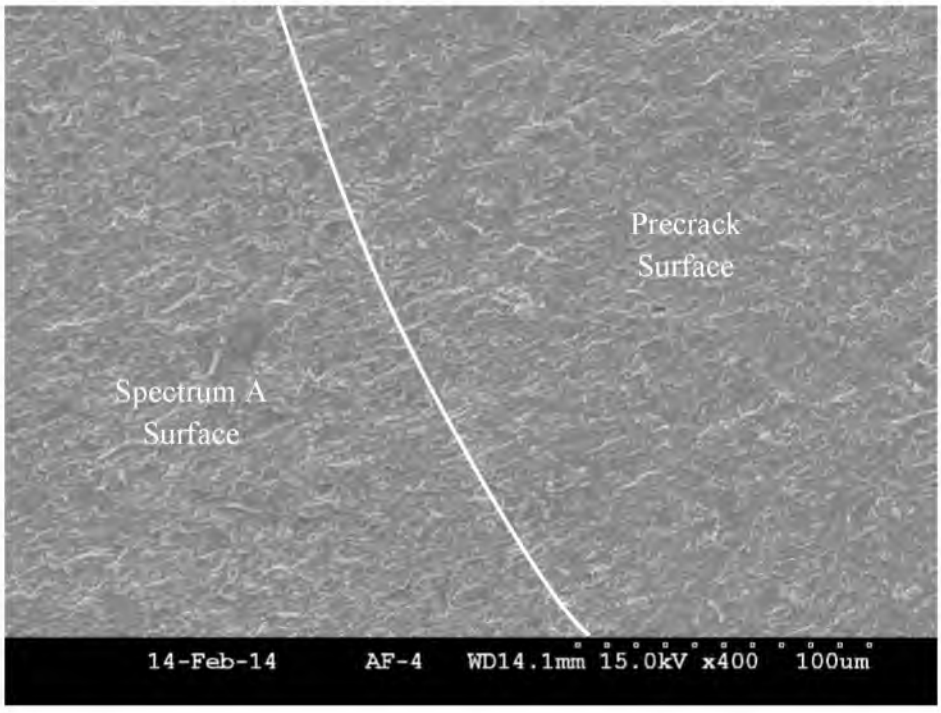

Figure 31 400x View of the Precrack to Spectrum A Transition on GT270-7

than the fact that the end of the precrack surface is slightly smoother. Fig. 32 shows the striations on the spectrum A fracture surface, which are indicative of fatigue.

3.2.2 Spectrum B Baseline Fractography

For the spectrum B baseline tests, the specimens were also precracked first, then switched to spectrum B for the duration of the test. Fig. 33 shows the widest view that could be obtained for the fracture surface of specimen GT270-28. The precrack surface in this case in more difficult to distinguished from the spectrum B surface, but it is present. Notice that the spectrum B fracture surface is much smoother in its appearance than the spectrum A fracture surface seen in previous figures. The figure also confirms test data of the approximate precrack front surface crack length of 0.045 of an inch. Fig. 34 shows what appear to be striations on a plateau in the spectrum B surface area.

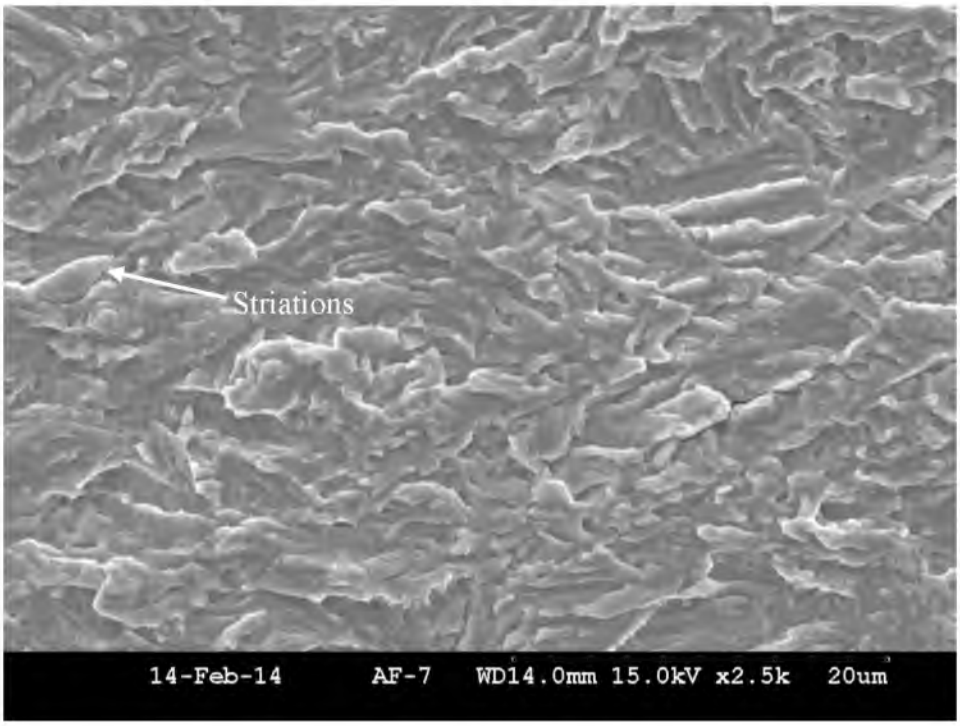

Figure 32 Spectrum A Striations on GT270-7

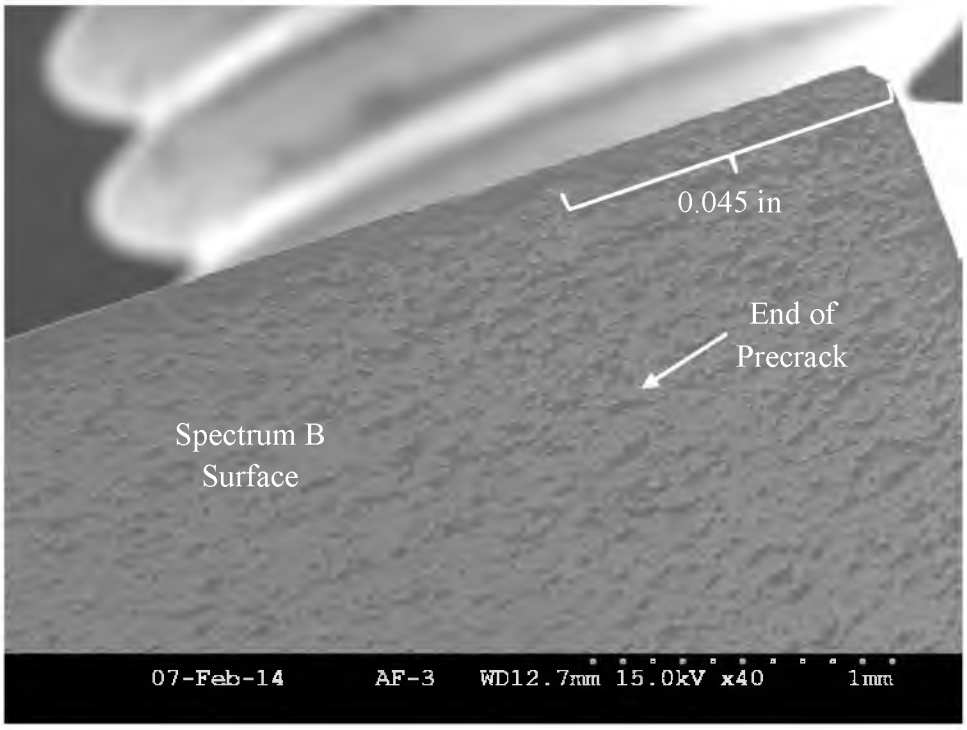

Figure 33 Wide View of GT270-28 Fracture Surface

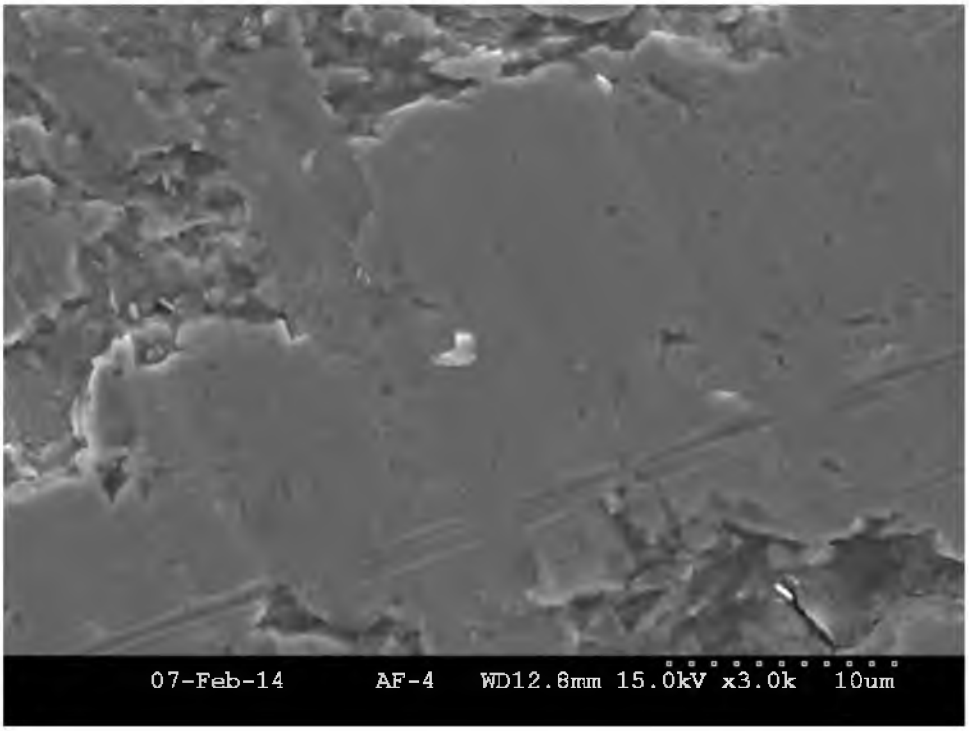

Figure 34 Spectrum B Striations on GT270-28

3.2.3 Combinations of Spectrum A and B Fractography

This section will cover the three types of combination spectrum tests that were done for this study. The combination spectrum tests were done by first, precracking, then applying spectrum A until the bore crack reach a predetermined length, followed by applying spectrum B for a minimum 100,000 EFH.

3.2.3.1 Spectrum A + Spectrum B 1 Fractography

After the precracking was accomplished on these tests, spectrum A was applied until the bore crack reached a length of 0.090 to 0.095 of an inch. As was seen in the baseline fractography images, the precrack area is distinguishable from the rest of the surface. Fig. 35 shows the widest view obtained of test specimen GT270-6. This figure

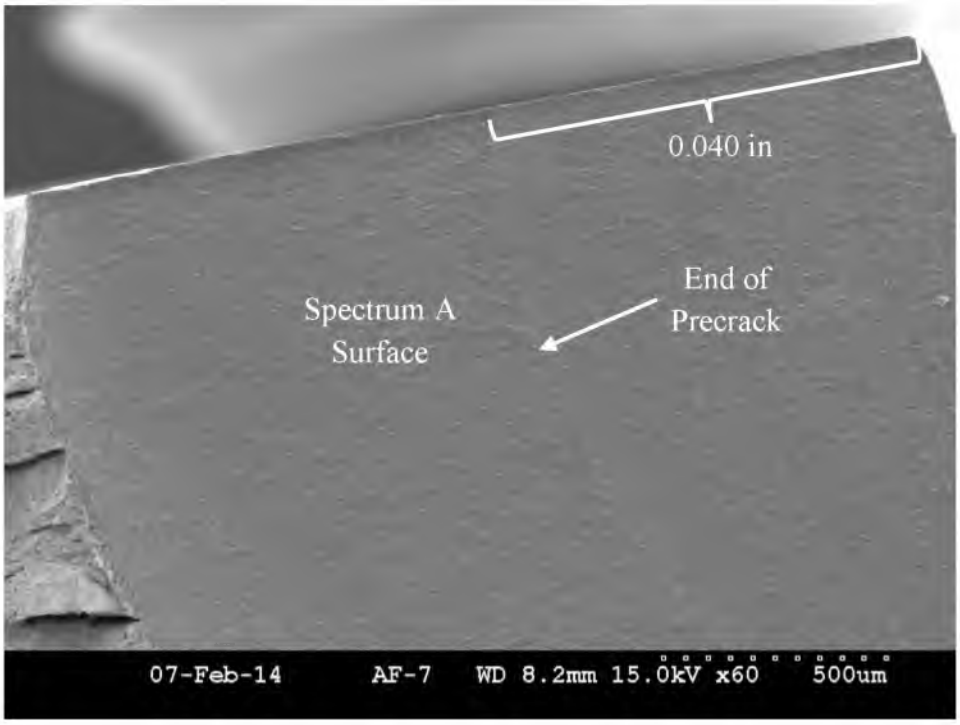

Figure 35 Wide View of GT270-6 Fracture Surface

confirmed test data that the front surface crack length was 0.040 of an inch. The bore crack length, confirmed in another image, was approximately 0.064 of an inch.

The spectrum B portion of the fracture surface is difficult to see in Fig. 35. For a better view of the effects of spectrum B on the fracture surface and the transition length from spectrum A to B, see Fig. 36. The smoother surface is the actual test fracture surface while the rest is overstress produced from pulling the specimen apart. The figure shows that the transition to spectrum B occurred when the bore length was approximately 0.100 of an inch. Fig. 37 is a closer view of the transition from spectrum A to B. One can clearly see the spectrum A has a much smoother appearance to it compared to spectrum B.

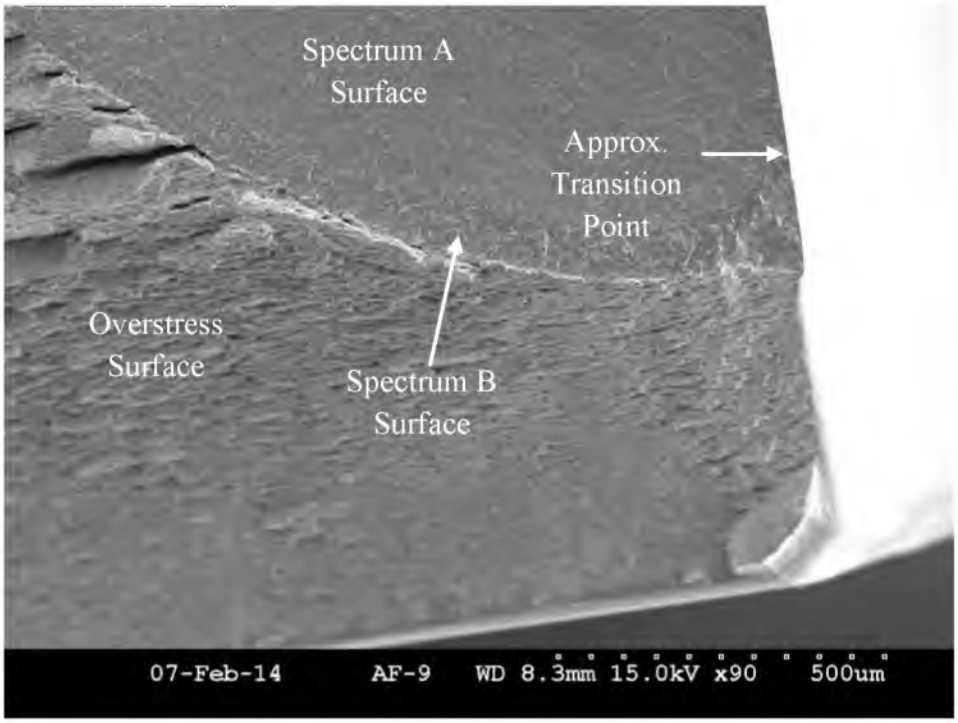

Figure 36 Wide View of the GT270-6 Transition Point from Spectrum A to B

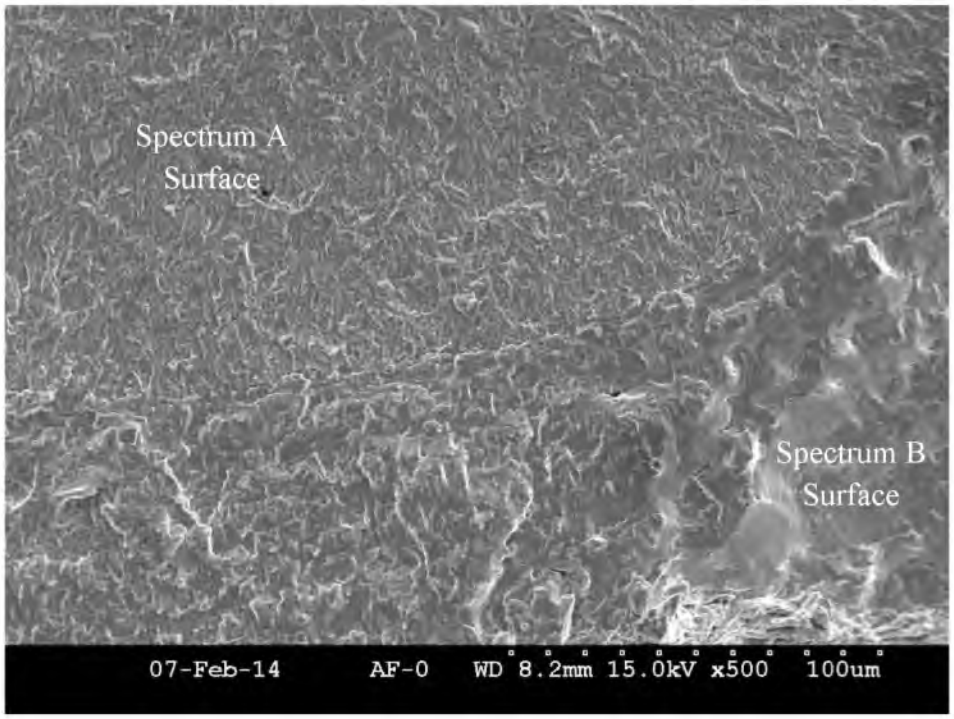

Figure 37 Transition from Spectrum A to B for GT270-6

3.2.3.2 Spectrum A + Spectrum B 2 Fractography

Like the previous test type, this second type of tests started with a precrack followed by spectrum A, which transitioned to spectrum B. The transition from spectrum A to B was supposed to occur when the bore crack reached a length of 0.105 to 0.110 inches. Fig. 38 shows the widest view obtained of test specimen GT270-9. Clear distinctions between the precrack region and spectra regions are visible. This figure also validates that the front surface precrack length was approximately 0.042 of an inch. The bore precrack length was approximated from this same image and was determined to be about 0.090 of an inch, about 0.020 of an inch longer than test data.

Fig. 39 shows a better view of the transition from spectrum A to B. This figure

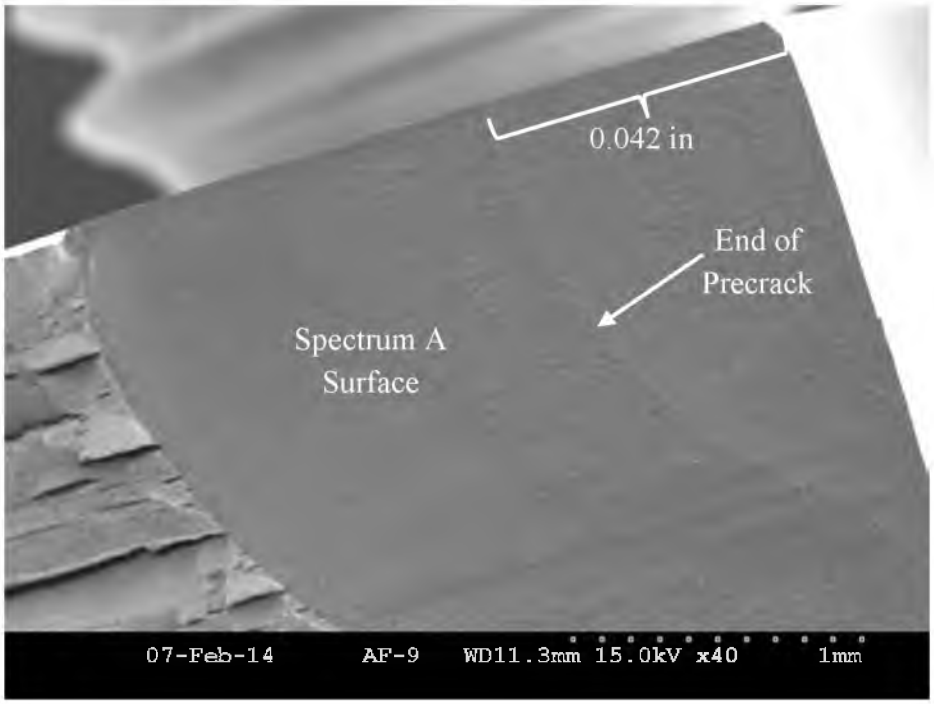

Figure 38 Wide View of GT270-9 Fracture Surface

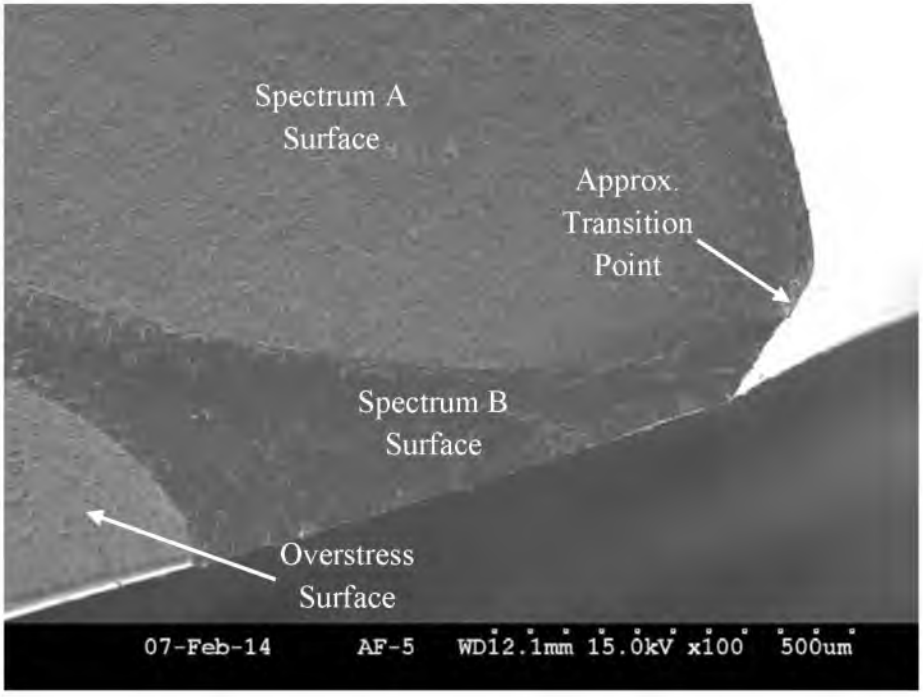

Figure 39 Wide View of the GT270-9 Transition from Spectrum A to B

shows that the transition point actually occurred at a longer crack length than what was recorded in the test data. The figure shows that the transition point occurred at approximately 0.120 of an inch, which is about 0.014 of an inch longer than test data. Once again, spectrum A creates a significantly rougher surface than spectrum B. The figure also shows that the crack grew through thickness, which was not recorded in the test data. Fig. 40 shows a closer view of the spectrum A to B transition.

3.2.3.3 Spectrum A + Spectrum B_3 Fractography

Like the previous two test types, this type of test started with a precrack followed by spectrum A with a transition to spectrum B. The transition from spectrum A to B was supposed to occur when the bore crack went through thickness. Fig. 41 shows the widest

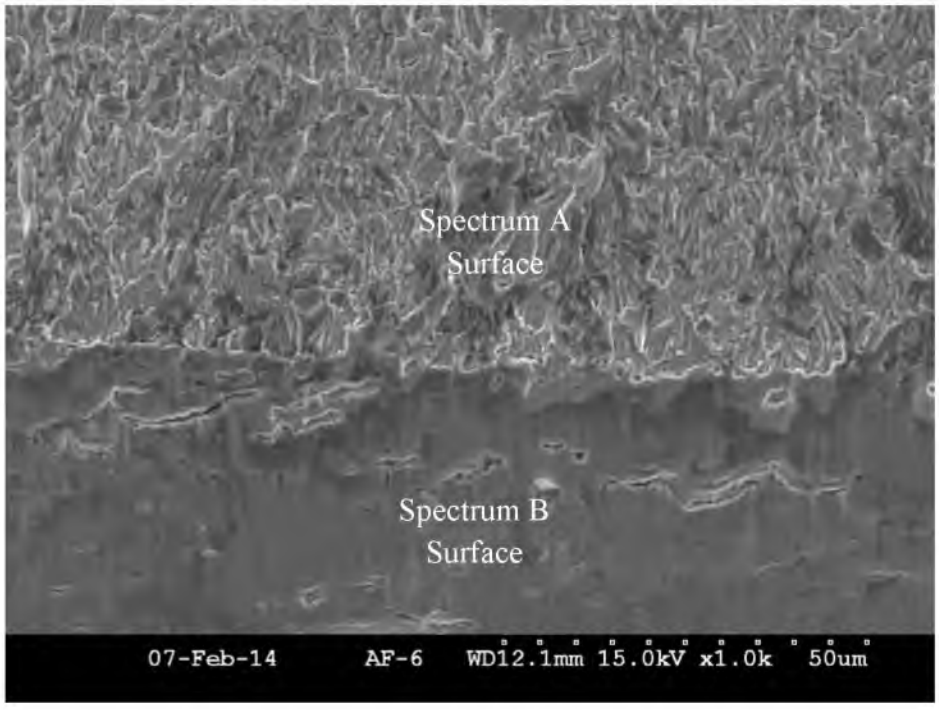

Figure 40 1,000x View of the GT270-9 Transition From Spectrum A to B

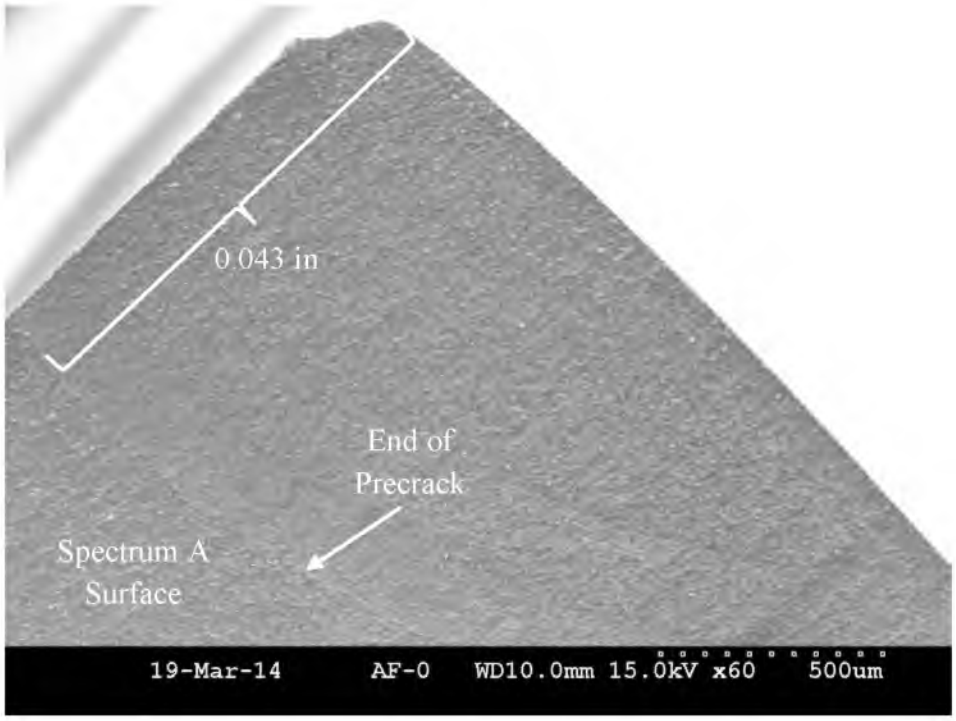

Figure 41 Wide View of GT270-14 Fracture Surface

view obtained of test specimen GT270-14. For this specimen, it was difficult to obtain an image that clearly showed the precrack region, but it can be distinguished. The front surface precrack length occurred at approximately 0.043 of an inch, validating the test data. The bore precrack length, verified in another image, was determined to be approximately 0.090 of an inch in length, about 0.010 of an inch longer than test data. Once again, the spectrum B fracture surface is difficult to see due to the fact that the region is so small in the image. For a better view of the spectrum A to B transition, see Fig. 42.

Fig. 42 shows that the transition point occurred after the bore crack under spectrum A had gone through thickness. The figure shows that the transition point occurred at approximately 0.039 of an inch on the back surface, which is about 0.020 of an inch longer than test data.

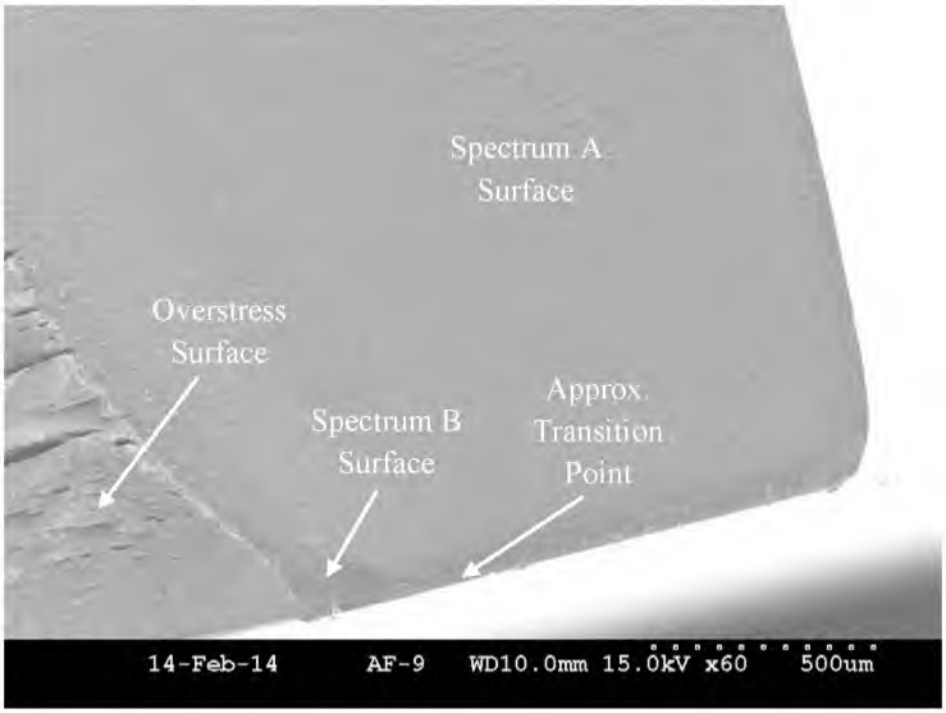

Figure 42 Wide View of the GT270-14 Transition from Spectrum A to B

3.3 AFGROW Simulations

This section shows the results of the AFGROW models developed to simulate the test data gathered for each type of test. The 17-7PH data in the NASGRO material database were used for most of these simulations. The TH1050 heat treatment condition was used for the simulations because the specific heat treatment condition of the test specimens was not available in the NASGRO database. No retardation models were used in the development of these models. Note that all the simulations were done in such a manner as to make them agree well with the test data and produce conservative results. All initial crack lengths used in the simulations were approximations to the actual initial crack lengths of the respective tests.

3.3.1 Spectrum A Baseline Simulations

This simulation was done using the 17-7PH data in the NASGRO model database. The initial front surface and bore crack lengths were 0.040 and 0.070 of an inch, respectively. One of the equation parameters, the slope parameter *n*, had to be slightly adjusted from 3.4 to 3.45 to make the data correlate better. Fig. 43 displays the results of the simulation along with spectrum A baseline test results. As one can see, the simulation correlates well with the test data and ends conservatively. The difference in life equates to less than 4.5 % in the overall life of the item.

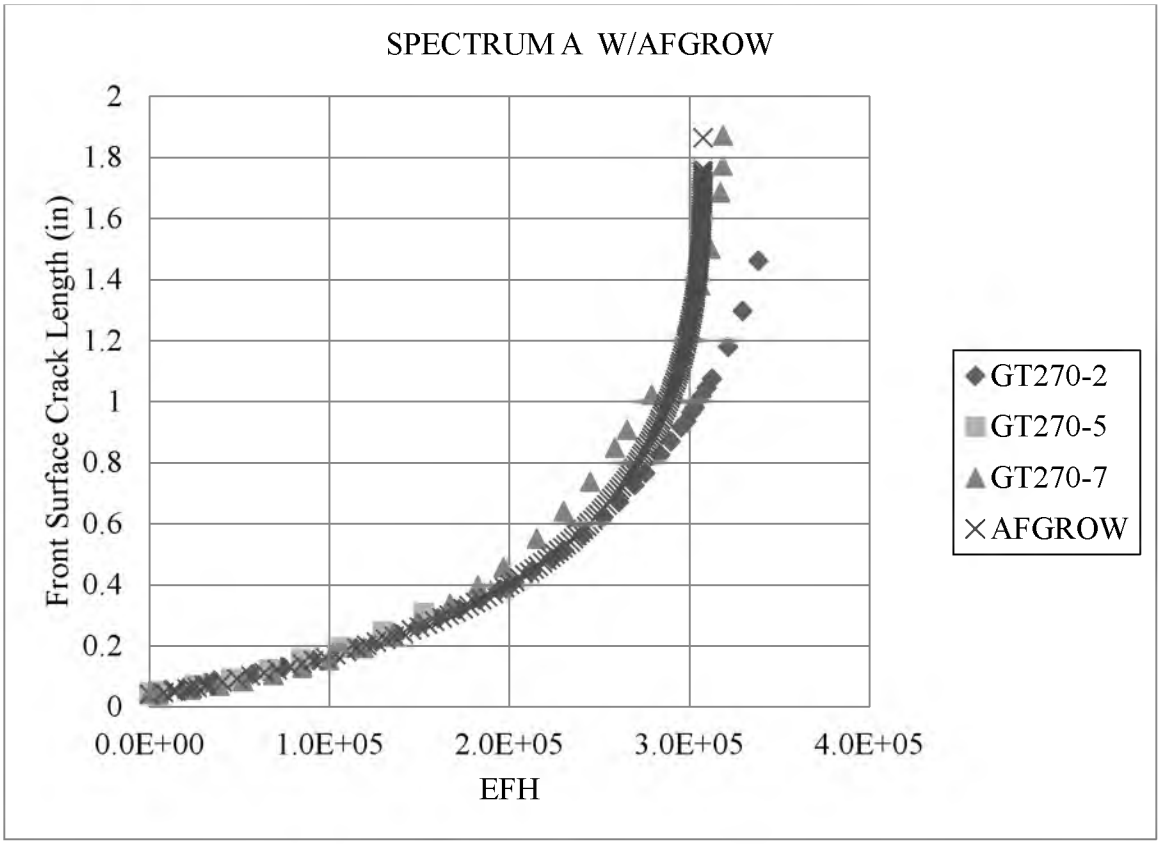

Figure 43 Front Surface Crack AFGROW Simulation Results for Spectrum A

3.3.2 Spectrum B Baseline Simulations

This simulation was also done using the 17-7PH data in the NASGRO model database. The initial front surface and bore crack lengths were also 0.040 and 0.070 of an inch, respectively. None of the equation parameters had to be changed for this simulation. Fig. 44 displays the results of the simulation along with spectrum B baseline test results. The figure shows that this simulation also correlates well with the test data. At a crack length of approximately 0.400 of an inch, the difference in life equates to less than 6.2 %.

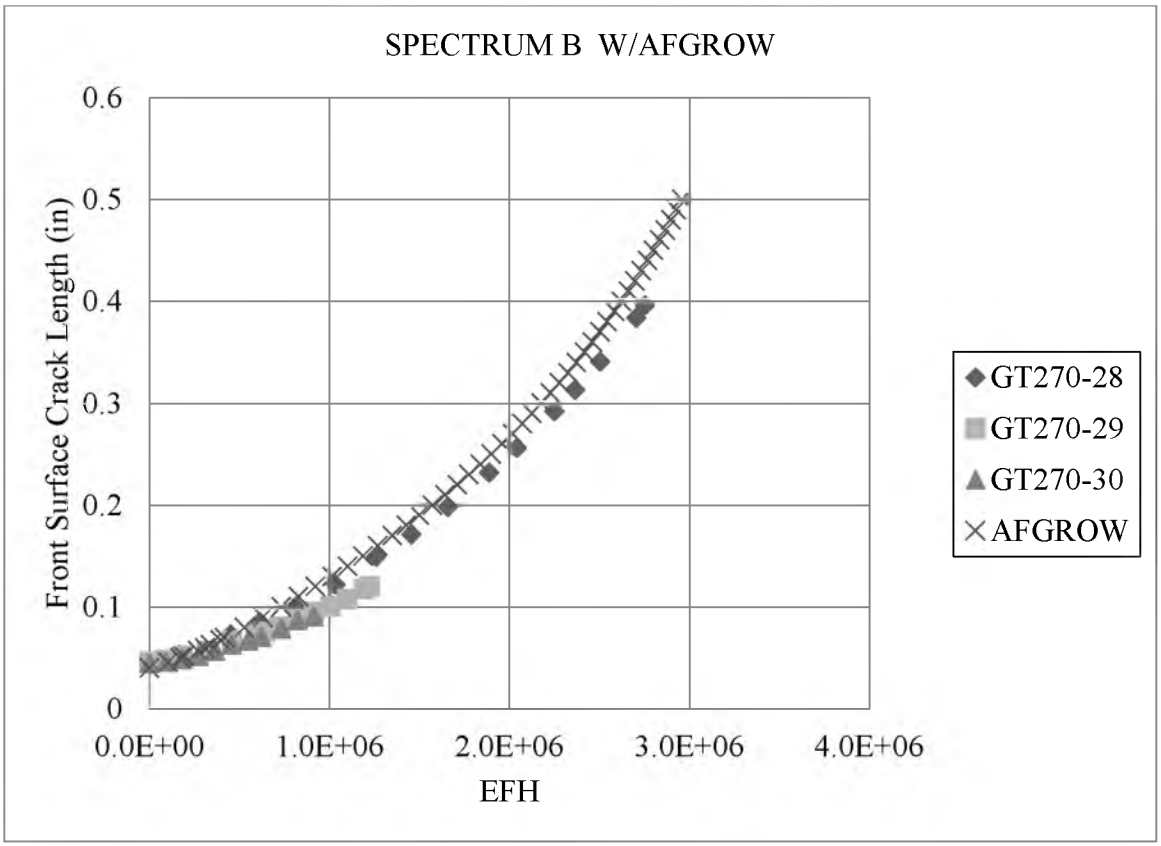

Figure 44 Front Surface Crack AFGROW Simulation Results for Spectrum B

3.3.3 Spectrum Combination Simulations

In this section, simulations for the front surface crack were developed. To match the data for each type of combination, test two simulations were developed, one for the spectrum A portion of the curve and the other for the spectrum B portion. Both the spectrum A and B portions of the crack used the NASGRO database. In these simulations, it was not necessary to change any of the NASGRO equation parameters. For greater detail on how these simulations were developed, see section 4.3.1.

3.3.3.1 Spectrum A + Spectrum B_1 Simulation

The initial front surface and bore crack lengths used for this simulation were 0.040 and 0.070 of an inch, respectively. The transition to spectrum B occurred when the front surface and bore crack lengths reached approximately 0.064 and 0.090 of an inch, respectively. Fig. 45 displays the results of the simulation along with spectrum A + B_1 test results. This figure shows that the simulation correlated well with the test data.

3.3.3.2 Spectrum A + Spectrum B_2 Simulation

The initial front surface and bore crack lengths used for this simulation were 0.050 and 0.070 inches, respectively. The initial front surface crack length slightly differs from that recorded for these specimens, but it was changed to better match the test data. The transition to spectrum B occurred when the spectrum A portion of the simulation reached a front surface and bore crack lengths of 0.088 and 0.110 of an inch, respectively. Fig. 46 displays the results of the simulation along with spectrum A + B_2 test results. This figure also shows that the simulation correlated well with the test data.

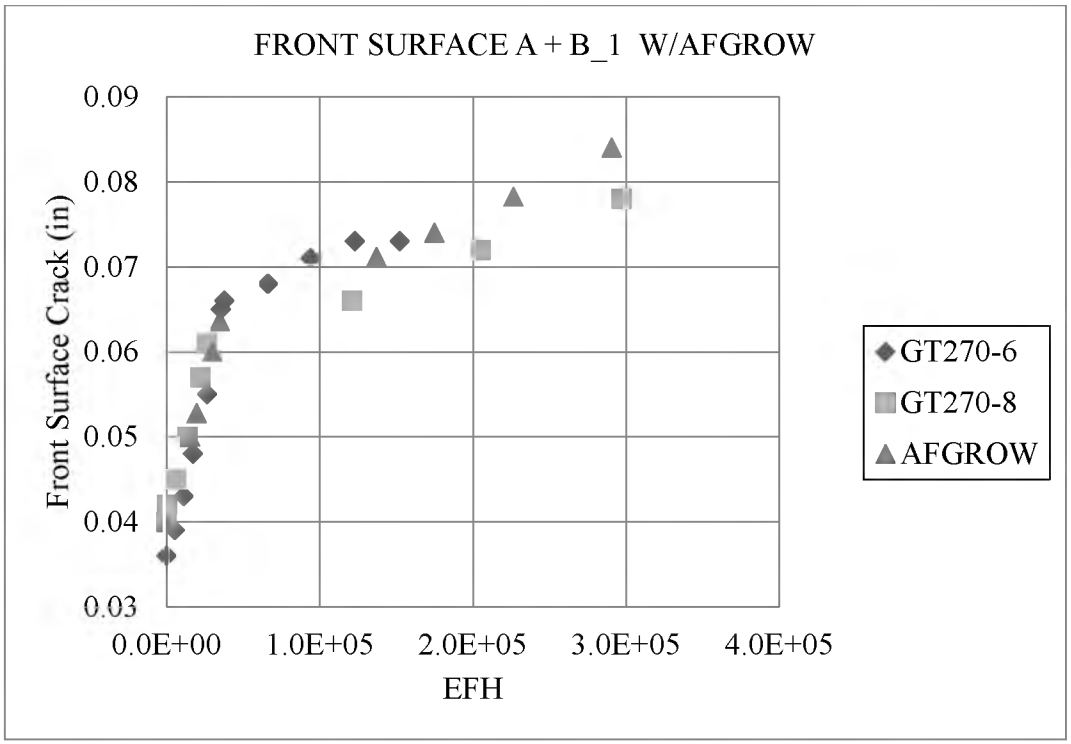

Figure 45 Front Surface Crack Simulation Results for the A + B_1 Combination

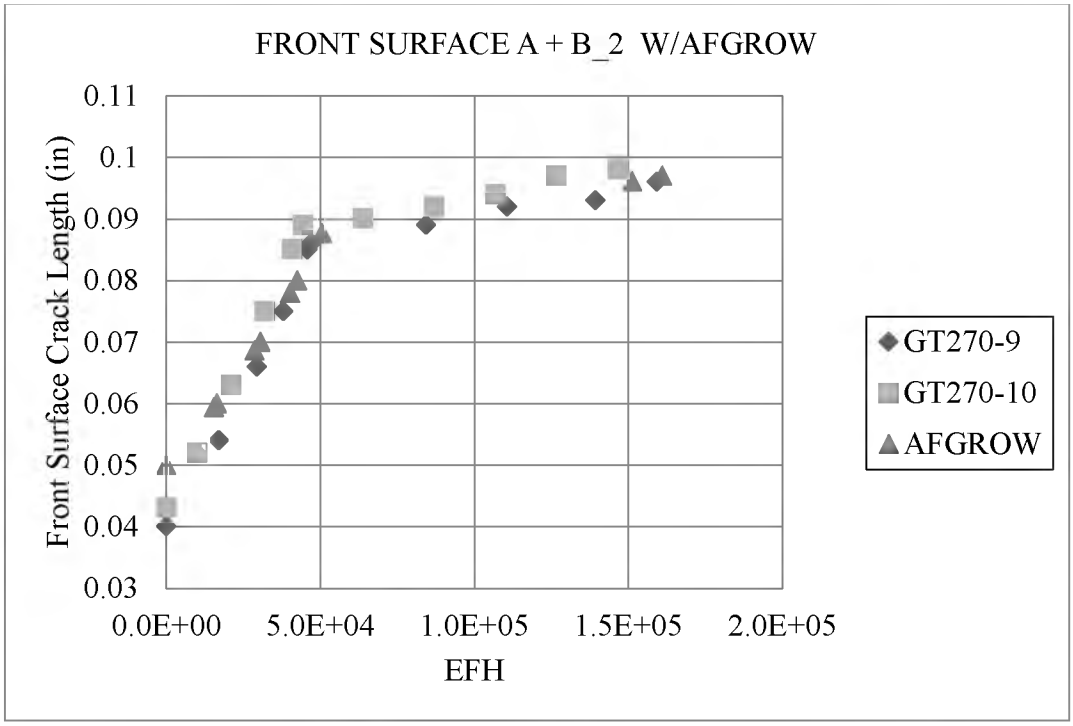

Figure 46 Front Surface Crack Simulation Results for the A + B_2 Combination

3.3.3.3 Spectrum A + Spectrum B_3 Simulation

The initial front surface and bore crack lengths used for this simulation were 0.050 and 0.070 of an inch, respectively. The initial front surface crack length again is slightly different from that recorded for these specimens for the same reasoning as was explained in the previous section. The transition to spectrum B occurred when the spectrum A portion of the simulation reached a front surface and bore crack lengths of 0.080 and 0.102 of an inch, respectively. Fig. 47 displays the results of the simulation along with spectrum A + B_3 test results. This simulation also correlated well with the test data.

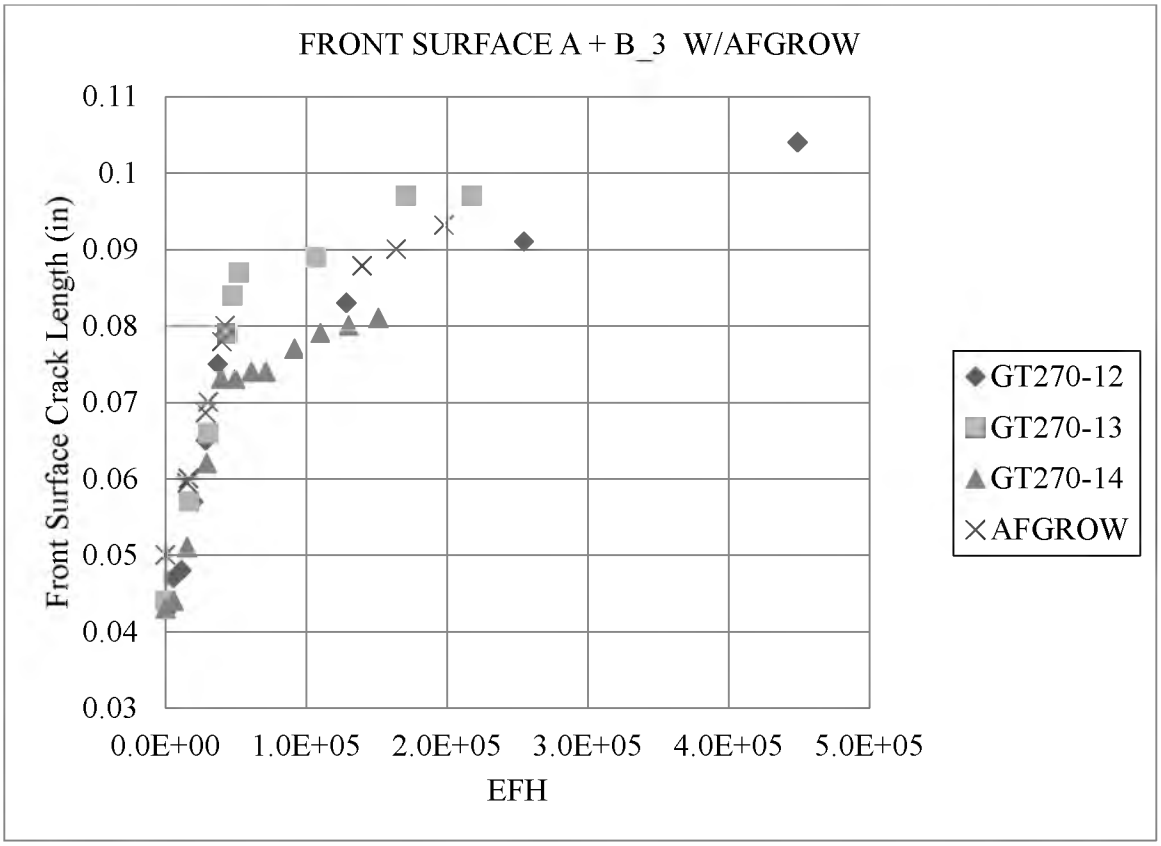

Figure 47 Front Surface Crack Simulation Results for the A + B_3 Combination

CHAPTER 4

DISCUSSION

4.1 Observations of Spectra

This study was done to compare two spectra that were observed to occur at different times in a fleet of aircraft. Data for spectrum A were gathered primarily during the 1990s while data for spectrum B have been gathered from the early 2000s to the present. Until testing is done on representative test specimens to compare the two spectra, it is impossible to quantify how different the behaviors will be. It should be noted that controlling the error on spectrum B was more difficult. The result was that testing under spectrum B had to be run at slower speeds to minimize the error. Testing actual coupons and developing analytical models from the data shows that the material in the desired location on the aircraft, in this case 17-7PH, is predictable. For a similar study using 2024-T351 aluminum, see reference [10]. The information obtained from both the testing and analysis can then be utilized in the development of best maintenance practices for the given loading condition.

4.1.1 Spectra Baseline

Baseline comparisons are essential for understanding what is occurring with the different spectra. This section will go into more detail about each of the spectra

attributes. That will be followed by a more in-depth discussion about the test results. The result will provide a better understanding about the basic and quantifiable differences between the spectra.

4.1.1.1 Spectra Attributes

Based on the spectra attributes, which was seen in Table 4, one can deduce that spectrum A was a more aggressive loading scenario than spectrum B. Spectrum A had 16,731 damage producing load points in a 240 EFH period. [8] In contrast to that, spectrum B had only 4,371 damage producing load points in a 1000 EFH period. [8] That means that spectrum A produces roughly four times the amount of load events in a quarter of the time than that of spectrum B.

As far as the loads are concerned, the max and min loads for spectrum A are 10,977 lb and 99 lb, respectively. For spectrum B, the loads are 10,977 lb for the max load and 133 lb for the min load. When the max load is applied to the test specimens, with an average cross-sectional area of 0.500 in^2, it produces a max stress of 21.954 ksi, a small fraction of the material capability in terms of yield strength. What does that mean when applied to the actual aircraft? This next section will show a side-by-side comparison of the test results.

4.1.1.2 Spectra Baseline Test Results Comparison

Fig. 48 is a plot directly comparing the front surface crack lengths results of the baseline tests. The average initial front surface crack length for all of these specimens was 0.046 of an inch. Since none of the spectrum B baseline tests were run to complete

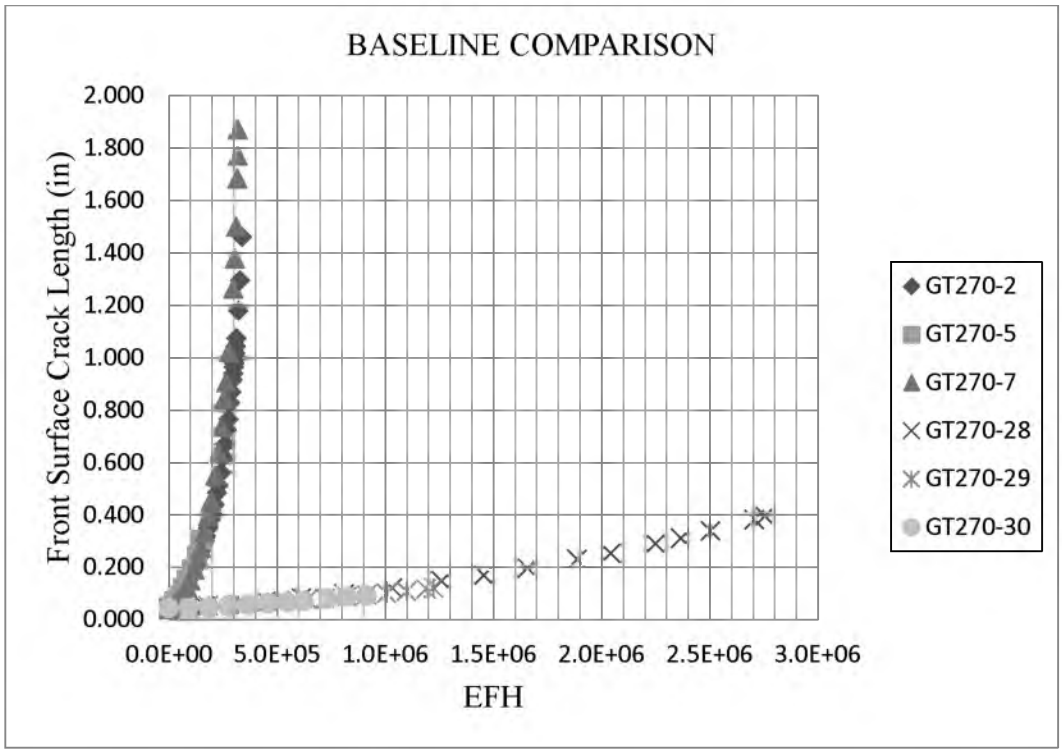

Figure 48 Plot Comparing Front Surface Crack Spectra A and B Baseline Results

failure, the crack length comparisons will focus on the smaller values. For a crack to grow 0.200 of an inch in size under spectrum A took approximately 34,200 EFH on average. For a crack to grow the same length under spectrum B took approximately 630,000 EFH on average. That is an 18 plus fold increase in expected life. Failure under spectrum A did not occur until the surface cracks were only 0.005 of an inch away from the edge of the specimen. The average time it took for the crack to grow to that length was approximately 330,000 EFH. None of the spectrum B baseline tests were run until failure. The results for aluminum specimens in a similar study had significantly less life. [10]

4.1.2 Spectra Combinations

As mentioned in previous chapters, the purpose of testing combinations of spectra was to obtain a range of data that would represent aircraft at varying stages in their usage life. Doing so would demonstrate how the material behavior might change under varying crack lengths of both spectra. The following section shows a side-by-side comparison of the three different spectra combination tests.

4.1.2.1 Spectra Combination Test Results Comparison

Figs. 49 and 50 are respectively the front surface and bore crack measurement plots directly comparing the three types of spectra combination tests. For visual purposes, not all of the data for each specimen could be plotted. The average initial front surface and bore crack lengths for all of these specimens were 0.044 and 0.077 of an inch, respectively. The initial bore crack measurements varied widely most likely due to the fact that that measurement was not the deciding factor for termination of the precracking process. The initial front surface crack measurements had little variation because it was the deciding factor on when to terminate the precracking phase. Being that the bore crack was the more critical measurement, it would have been better to make it the deciding factor for precrack termination.

The specimen that deviated the most from the average initial front surface crack measurement was GT270-1. Specimen GT270-1 was actually tested two different times. The reason for this was that GT270-1 was the first specimen to be tested and was done so under the original set of spectrum transition criteria, which was 0.070 of an inch. During the first test, the bore and front surface cracks grew to 0.084 and 0.062 of an inch,

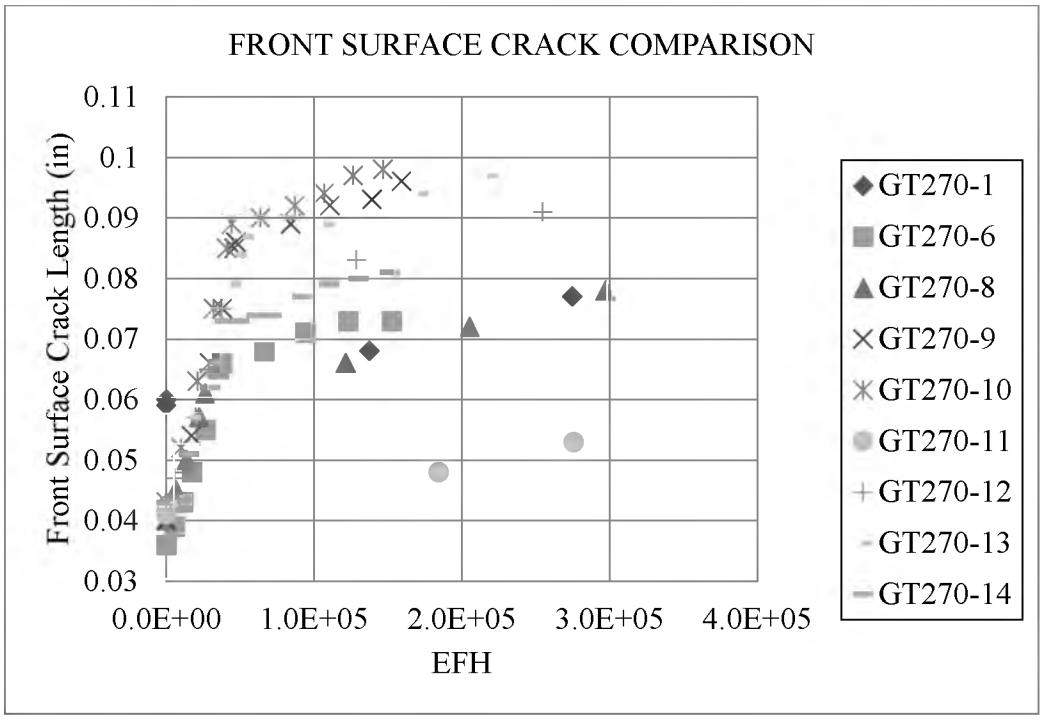

Figure 49 Plot Comparing Front Surface Crack Spectra A + B Combinations

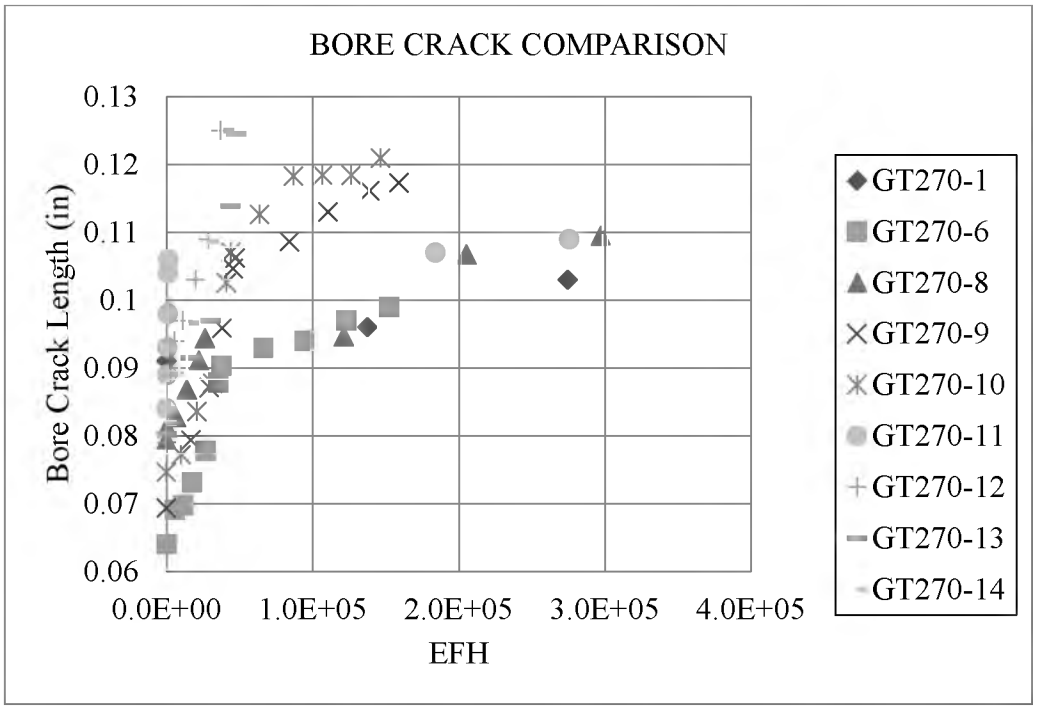

Figure 50 Plot Comparing Bore Crack Spectra A + B Combinations

respectively. Being that the bore crack had not grown to the new set of spectrum transition criteria, it was determined that the specimen should be tested again to obtain a third set of valid data. The reason the surface crack for GT270-1 started out so large is due to the fact that it finished the first test at a longer length than the other specimens.

Fig. 49 shows that, with the exception of a few outliers, the data gathered during testing under spectrum A agree very well. Once the transition to spectrum B occurred, the figure shows that the slopes of the data point are very consistent as well. The front surface crack growth under spectrum A ranged from 0.059 to 0.092 of an inch before the transition to spectrum B. Note that the even though the shortest front surface crack length was from an A + B_1 test, the longest length came from an A + B_2 test, which was unexpected. This shows that even though the transitions occurred when the bore cracks reached a certain length, the front surface cracks did not necessarily grow equally as much. In other words, the aspect ratios varied from test to test.

The data used to create Figs. 49 and 50 show that the range of time under spectrum A, for a majority of the specimens, was approximately 26,500 to 47,700 EFH, a range of 21,200 EFH. When that value is compared to the overall average life expectancy of the component, just under spectrum A, it accounts for less than 7 % of the expected life. Without a total range of data for spectrum B, one cannot quantify exactly what percentage of life 21,200 EFH would be under that spectrum. But, with the data obtained, it is safe to conclude that the percentage would be very small. Once again, the study using aluminum showed significantly different results than those produced in this study for 17-7PH. [10] The exceptions for time under spectrum A were specimens GT270-1 and GT270-11 with 286 EFH and 1291 EFH, respectively. The reason why

Specimen GT270-1 spent so little time under spectrum A can be attributed to what was discussed in the previous paragraph. The testing for specimen GT270-11 was conducted at SwRI and they did not mention any anomalies that occurred during testing. Therefore, it is unclear why that particular specimen's test results deviated from the other test data. Due to the uncertainty of the results from these two specimens, the data were not used in further analyses.

Fig. 50 shows that even though the initial bore crack lengths varied significantly, the transition crack lengths were as specified for each type of test. The range of initial bore crack lengths was 0.064 to 0.084 of an inch. Once again, it is important to remember that those are initial values, which highlights the variations that occurred during precracking.

4.2 Observations from Fractographic Examinations

The main observation that came from the fractography images of the baseline specimen was how different the appearances were between the two spectra. Spectrum A, as was seen most of the fractography images, had a consistently rougher appearance. Even though striations could be seen on both spectrum A and B fracture surfaces, they were much easier to see on spectrum A fracture surfaces.

In contrast to spectrum A, fracture surfaces produced by spectrum B had a significantly smoother appearance. Another interesting phenomenon that was observed initially in some of the spectrum B fracture surface was the appearance of cracks that formed in the L-T plane of the specimens; see Figs. 51 and 52. These cracks were seen preferentially in the middle range of the thickness. As was stated in Chapter 2 these

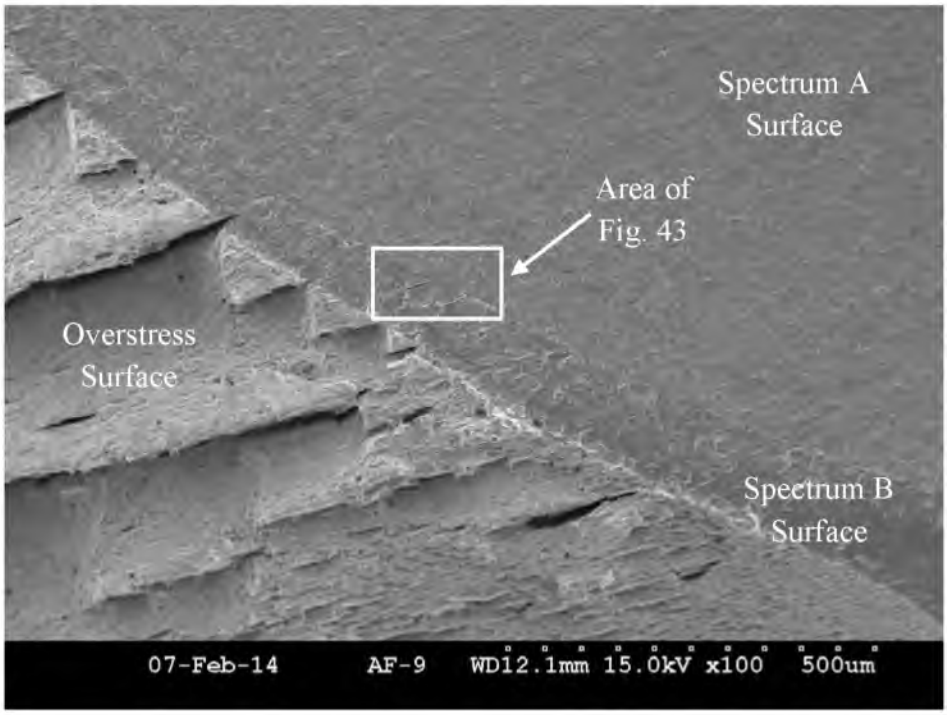

Figure 51 Wide View of Cracks in Spectrum B Fracture Surface

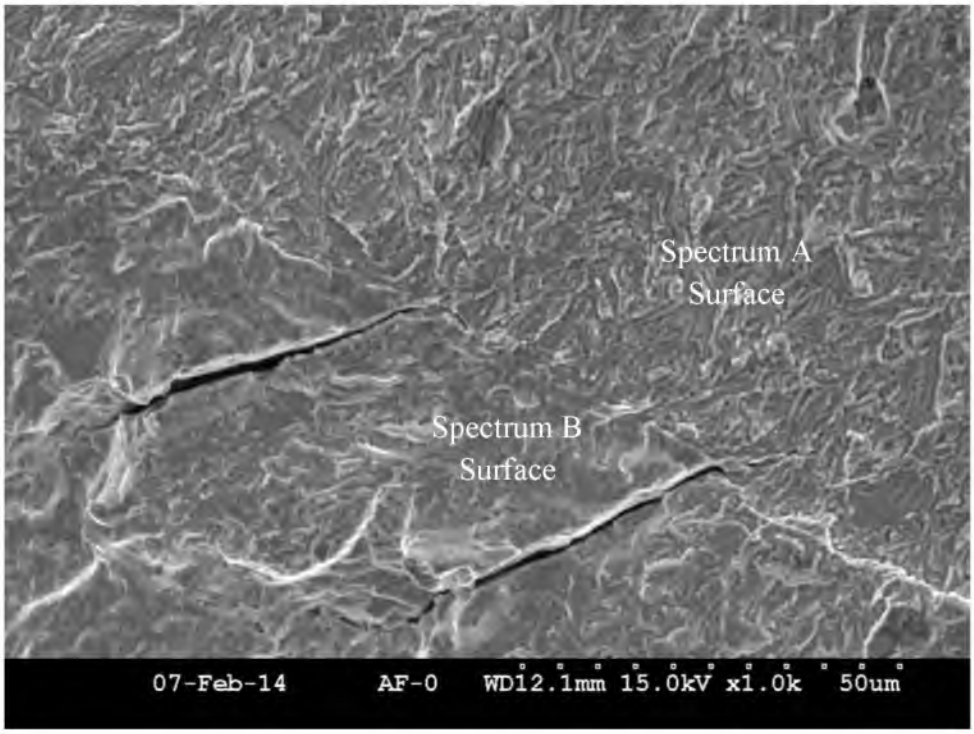

Figure 52 Crack in the Spectrum B Fracture Surface

specimens were formed out of 17-7PH sheet with the grains running preferentially in the longitudinal direction. It is believed that the cyclic loading caused the grains in the material to separate because of the Poisson effect. The cracking preferentially occurring in the middle of the thickness might be due to the plane strain condition. These cracks would also form eventually under spectrum A loading once the primary crack was sufficiently long; see Fig. 53.

The key observation in this section was that fractography measurements of transition points did not match those of bore observations with the traveling microscope. This is most likely due to the fact that the operators had difficulties obtaining accurate readings from this particular microscope. It is therefore recommended that a different microscope be used for future projects. Regardless of the difficulties experienced, a

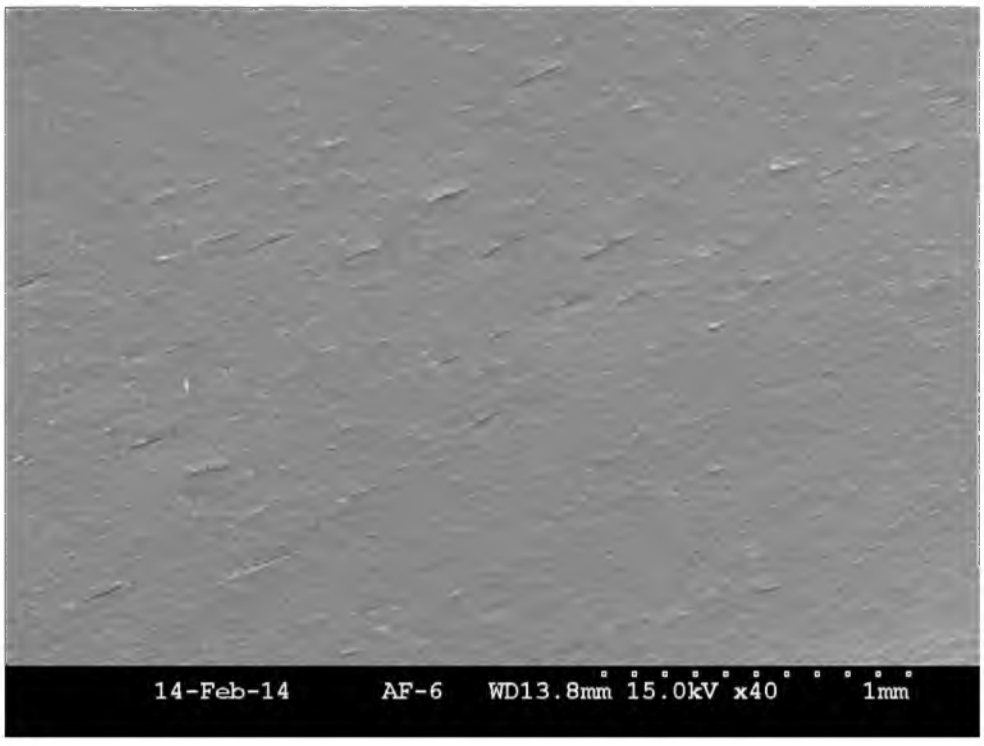

Figure 53 Cracks Forming in the L-T Plane on a Spectrum A Fracture Surface

range of life was still obtained, which showed how the material would behave under the given conditions, which was the main objective.

4.2.1 Aspect Ratios with Front and Back Surface Crack Comparisons

The aspect ratio is a term used to describe how the crack in a bore compares to the crack on the surface of the specimen. Typically, the ratio is represented in the form $^{a}/_{c}$, with a representing the bore crack and c representing the surface crack. In this study, the specimens started off with an EDM notch with an aspect ratio of $^{a}/_{c}$= 0.667. After having conducted the precracking phase of the experiment, it was observed that the bore crack had grown much more rapidly compared to the surface crack. This is to be expected as it is well known in solid mechanics that a hole is a stress concentrator, with the largest stress tangent to the edge of the hole in the direction of the load. The range of aspect ratios for this study was 1.370 to 2.018 with an average of 1.789.

Once the bore crack went through thickness, the front crack growth rate decreased slightly until the crack, now forming on the back side of the specimen, caught up. Once the crack on the back side of the specimen reached a length similar to that of the crack on the front, the two cracks remained within 0.020 of an inch of each other. This suggests that the specimens were loaded correctly into the fatigue machine and no undesired loading conditions, such as torsion or bending, were occurring.

4.3 AFGROW Simulations

When the AFGROW simulations were initially being developed, it was desired to know which material model would best simulate the test data. These models are used by

the program to simulate how the crack will grow in the given material. Thus, comparisons for both spectra were done using the Forman equation, NASGRO equation and tablular lookup file with no retardation. Figs. 54 and 55 show the results of the comparisons. These results show two things; first, that the NASGRO equation correlated the best with the data, second, that very little retardation was occurring in the material. The only 17-7 PH heat treatment condition available in the NASGRO database was TH1050. The main difference between the TH1050 condition and the TH1100 condition the test specimens were supplied in was the tensile strength. The heat treatment specification for PH stainless steels, AMS 2759/3, states that TH1050 should have a min

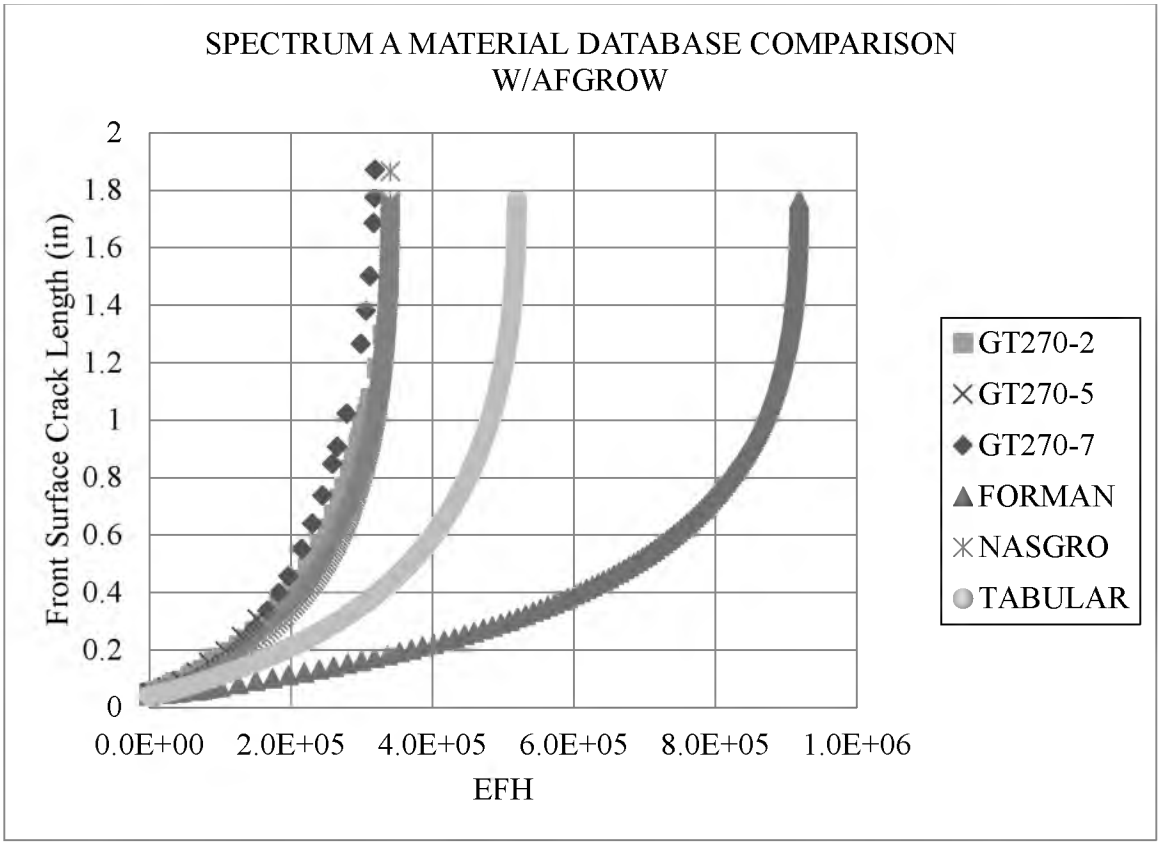

Figure 54 Spectrum A Material Database Comparison with Test Data

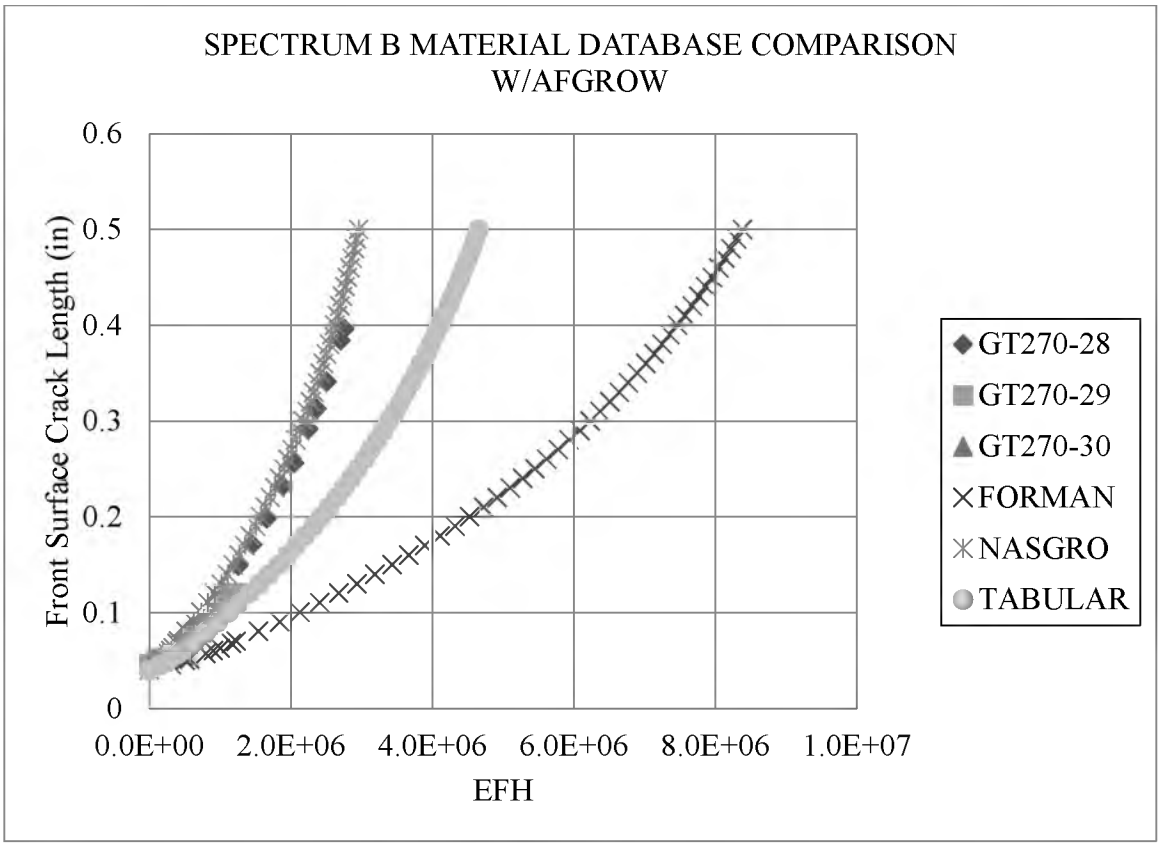

Figure 55 Spectrum B Material Database Comparison with Test Data

tensile strength of 180 ksi. [32] The average test specimen tensile strength was approximately 170 ksi, making the difference between the two conditions 10 ksi. Though the heat treatment condition in the NASGRO database differed from that of the actual test specimens, the predictions agreed very well with the test data.

The NASGRO equation uses material properties and a mathematical model to predict crack growth for a given material. The following is the NASGRO equation used in AFGROW. [30]

$$\frac{da}{dN} = C\left[\left(\frac{1-f}{1-R}\right)\Delta K\right]^{n} \frac{\left(1-\frac{\Delta K_{th}}{\Delta K}\right)^{p}}{\left(1-\frac{K_{max}}{K_{crit}}\right)^{q}}$$

where $^{da}/_{dN}$ is the crack growth rate; C, n, p, and q are empirically derived parameters, f is the ratio of K_{op}over K_{max} and R is the stress ratio. As mentioned previously, n was slightly increased from 3.4 to 3.45 because increasing the slope made the prediction conservative and conforms better to test data. See the AFGROW Users Guide for further details. [30]

The fact that very little retardation is occurring during testing is evident from the simulations. Most materials will experience some retardation when an overload occurs in the loading sequence. The degree of retardation will vary depending on the material being used and the degree of the overload. The degree of retardation observed in this study appears to be very little. For this reason, in order to obtain the best fit to the test data, no retardation models were used.

4.3.1 Spectra Combination Simulations

To match the data for each type of combination test, two simulations were developed, one for the spectrum A portion of the curve and the other for the spectrum B portion. This was done by running the spectrum A portion of the simulation until the transition point matched that of the test data. The spectrum B portion of the test was then simulated using the new front surface and bore crack lengths produced from the spectrum A portion of the simulation. The results of the two simulations were then combined in an Excel spreadsheet. Note that the aspect ratios of these simulations did not necessarily match that of the test data. These efforts focused on representing the front surface crack.

In these simulations, it was not necessary to change any of the NASGRO equation parameters. The main difference between the two portions of the crack simulation was that, to better match the spectrum A portion of the curve, the aspect ratios were not forced to remain constant, which was not done for the spectrum B portion.

CHAPTER 5

CONCLUSIONS AND RECOMMENDATIONS

5.1 Conclusions

The main objective of this study was to better understand the sensitivity of 17-7PH to the different spectra. The crack growth curves, fractographic examinations and AFGROW simulations provided the information necessary for users of this aircraft to better maintain the integrity of the structure. The following sections detail the conclusions obtained from each of those analyses performed. Now that a better understanding of the differences between the two spectra has been obtained, engineers can make alterations, based on the damage tolerant design philosophy, to maintenance practices, repair procedures and inspection intervals. This study showed that while the aircraft are under spectrum B type conditions, the component, in the location studied, will last for hundreds of thousands of effective flight hours. The alterations in procedures will reduce costs by eliminating unnecessary maintenance hours and inspections while maintaining the integrity of the aircraft.

5.1.1 Crack Growth Curve Conclusions

The main takeaway from the crack growth curves is the degree to which the two spectra differ. Before this study was conducted, the differences in crack growth behavior

between spectra A and B were suspected but unvalidated. It is now known that usage, under spectrum B type conditions, is much more benign than that of spectrum A. Again, for a crack to grow 0.200 of an inch under spectrum B takes 18 times as long as spectrum A. The combination tests showed that once the transition to spectrum B occurred, it dominated in all cases. Thus, no matter what stage in life the aircraft may be in, if the usage for that aircraft is spectrum B type conditions, the respective component's integrity will not be compromised before inspections can occur.

5.1.2 Fractographic Examination Conclusions

The fractographic examinations showed some distinct feature differences between the two spectra and the material itself. Spectrum A produced a fracture surface that had a significantly rougher appearance than that of spectrum B. Another key feature that was distinct for this material was the secondary cracks that formed in the fracture surface, preferentially in the middle thickness section. These cracks were predominately observed in the spectrum B fracture surface, but could be seen in the spectrum A fracture surface if the primary crack was sufficiently long. These examinations also showed that the bore crack measurements taken during the testing were not accurate, being off as much as 0.020 of an inch. Even though these inaccuracies occurred, the main objective of obtaining a range of life was achieved, the results of which were discussed in the previous section. The last observation obtained from the examinations has to do with the aspect ratios. The fatigue tests provided a wide range of aspect ratios, which complicated crack growth simulations.

5.1.3 AFGROW Simulation Conclusions

Simulations of crack growth for the 5 different types of tests were obtained. The NASGRO database, for 17-7PH, produced the best results of the different material databases. Initial simulations indicate that very little retardation of the crack growth occurred during testing. For the spectrum A baseline simulation, the *n* parameter had to be slightly adjusted from 3.4 to 3.45 to obtain a better fit. As far as the combination tests were concerned, the aspect ratios, for the spectrum A portion of the simulation, were not forced to remain constant to, once again, obtain a better fit. Also, the initial front surface crack size had to be slightly increased to 0.050 of an inch from 0.040 of an inch for the A + B_2 and A + B_3 simulations. Doing so was necessary to better approximate the test data.

5.2 Recommendations

The recommendations have been separated into the three following sections: test practices, potential future studies and current aircraft.

5.2.1 Test Practices

When preparing to perform a fatigue test, it is recommended that the operators take time to better understand and inspect the major components of the machine. During this study, the fatigue machine failed due to a hydraulic pump failure. If the pump had been inspected prior to testing, the deficiency may have been caught early and unnecessary delays would not have occurred. This was also true for the microscope that gave inaccurate measurements. Though those performing the testing had difficulty with the microscopes it was not known, until the fractographic examinations, that the

measurements were inaccurate. Also, knowing the limitations of the machine will reduce the amount of error that can occur. In some instances, during this study, the loading rate was increased to accelerate the testing. Though the error remained within acceptable limits, it would have been better to continue with the reduced loading rate to better maintain the error

5.2.2 Potential Future Studies

It is recommended that fatigue-prone systems, like aircraft, be continually monitored for failures. Loading conditions need to be observed, especially if usage has changed from that for which the system has been previously tested. Significant changes in usage should then be fatigue tested, as was done in this study, to determine the sensitivity of the materials in question to the changes in usage. From the data obtained, engineers can develop better models, based on the damage tolerant design philosophy, which empower them to make better determinations on how maintenance practices can be applied. As mentioned earlier, these types of studies can save time and money for the user by developing the more efficient maintenance practices while maintaining the integrity of the system and prolonging its life.

5.2.3 Current Aircraft

Though the specific aircraft for this study was not mentioned, in order to generalize the study, it is recommended that the maintenance practices be adjusted appropriately based on the information given here in. It is now known that, while usage of the aircraft are spectrum B type conditions, the respective area on the aircraft will last

significantly longer than when usage conditions more closely resemble that of spectrum A. Depending on the relationship between the normal usage and the alternative usage, this may provide economical relief to the operator while maintaining flight safety.

APPENDIX A

TEST SPECIMEN FABRICATION PROCEDURES AND MATERIAL CERTIFICATION SHEETS

PROCEDURE FOR FABRICATING THE TEST SPECIMENS

1. Northrop Grumman contracted Aero Specialties Material Corp. to machine and heat treat the specimens which they delivered on 6 November 2012.

2. Aero Specialties Material Corp. bought the raw materials from AK Steel Corp., on 14 March 2012, who certified the chemical composition and material properties. The sampling used to determine chemical composition was done in accordance with ASTM E 59, while the mechanical properties were determined in accordance with ASTM E 8 and ASTM A 370. Hardness of the material was determined using ASTM E 18. AMS 2371 was used to maintain quality assurance during all of the above mentioned tests. Certifications for these tests are seen in the following Aero Specialties Material Corp. document.

3. Once Aero Specialties received the material from AK Steel Corp., they contracted Burton Industries Incorporated to perform the heat treatment process. The heat treatment process was done in accordance with AMS 2759/3 Rev E, Heat Treatment Precipitation-Hardening Corrosion-Resistant and Maraging Steel Parts. The heat treatment certifications are seen in following AK Steel Corp. documents. The test specimens were delivered on 5 November 2012.

4. The specimens were then all manufactured from sheets of the same heat with the grains running in the longitudinal direction of the specimens.

5. After the test specimens were heat treated and fabricated, they were sent to Lawrence Ripak Co., Inc. to shot peen both ends of the specimens in accordance with AMS 2430. The shot peened specimens were then delivered on 20 November 2012. Shot peening certification is seen in the following Lawrence Ripak Co. document.

6. After the test specimens were shot peened, they were sent to Western Professional, Inc. where the EDM of the notch was performed. Western Professional, Inc. provided the measurements of the notches in their respective documents below.

7. Once the fabrications of the test specimens were complete, Northrop Grumman performed their own testing to verify mechanical properties. The results of this testing showed that the test specimen material did indeed meet the 17-7PH AMS 2759/3 heat treat specification. The certification for this testing can be seen in the following Northrop Grumman Technical Services Laboratory document.

NORTHROP GRUMMAN

Northrop Grumman Corporation
Technical Services
925 South Oyster Bay Road -M/S U03-26
Bethpage, New York 11714
Tel: 516-575-3073; Fax: 516-575-9909

To: Michael Behring
From: Robert Fidnarick / Ken Grube

Subject:
Coupon Drawing GT270KB003-13, Coupons 1-33

Enclosures:

1) Drawing GT270KB003
2) Aero Specialties Material Corp Packing Slip with Material and Heat Treatment Certification for 17-7PH 150-170 ksi
3) Technical Service Laboratory Material Property Report
4) Lawrence Ripak Co. Inc Shot Peen Certification
5) Western Professional EDM notch data sheet with Memo for Coupon 3
6) Technical Service Laboratory Coupon Measurements

Aero Specialties Material Corp.
20 Burt Drive
Deer Park, NY 11729
USA

Voice: 631-242-7200
Fax: 631-242-7652

PACKING SLIP

Invoice Number: 15566
Invoice Date: Nov 6, 2012
Page: 1

Sales Order Number: N5092-DL

Bill To:
NORTHROP GRUMMAN 925 SO. OYSTER BAY ROAD M/S U03-26 BETHPAGE, NY 11714

Ship to:
NORTHROP GRUMMAN TECH SVC. 925 SOUTH OYSTER BAY ROAD ATT: KEVIN COOK BETHPAGE, NY 11714

Customer ID	Customer PO	Sales Order
NORTHR	TA2086004	N5092-DL
Sales Rep ID	**Shipping Method**	**Payment Terms**
DONNA	ROBLIS	Prepaid

Order Qty	Item	Item Unit	Description	Shipped Qty
40.00	17-7PH .125"THK.	EA	17-7PH MIL-S-25043 H/T 155-170 KSI .125" X 4.250" X 16.250" GRAIN W/16.250" DIM	40.00
1.00	PO#	<Each>	HEAT# 7511084	1.00
1.00	SPECIAL INSTRUCT	<Each>	**BEST EFFORT FOR MATERIAL TO BE KEPT AS FLAT AS POSSIBLE **	1.00
1.00	FREIGHT CHGS	<Each>	FREIGHT CHARGES PREPAID ON THE ABOVE REFERENCED PO.	1.00

Certificate of Compliance

This is to certify that the material supplied against the above purchase order has been produced in accordance with applicable specifications

D. Donlon

Certification Clerk

Burton Industries Incorporated

"Building a Stronger Future"
www.heatreat.com

Accredited Nadcap™

CERTIFICATION

Aero-Specialities Corp.
20 Burt Drive
Deer Park, NY 11729 USA

Certification ID: **317182-1**
Date: 11/5/2012
Cert Date: 11/05/2012
Purchase Order: M19745
Material: 17-7PH

Part Number	Part Description	Additional Part Information	Qty
0.125" X 4.250" X 16.250"	SHEETS	Heat Code #: 7511084 Add'l Info: HARDNESS TESTED IAW ASTM E-18	40

Customer Requirements

Inspection Type	U Of M	Lower Spec	Upper Spec
Hardness	HRC	35.0	38.0

Results

Inspection Type	Scale	Min	Max	Quantity	Quantity Passed	Quantity Rejected
Hardness	HRC	36.8	38.0	40	40	0

Process Performed

Austenitize in Vacuum atmosphere/ N2 Cool:
Start:Oct 26 2012 8:36AM End:Oct 26 2012 10:07AM. Time:1 hrs 31 mins. Eq:1000 (1000 Vacuum Atmosphere Furnace)
Austenitizing temperature: **1400F**
Cold Stabilize 17-7PH:
Start:Oct 26 2012 12:36PM End:Oct 26 2012 1:18PM. Time:0 hrs 42 mins. Eq:700B (700B Air Atmosphere Freezer)
Temperature:+60F

Temper:
Start:Oct 27 2012 5:38AM End:Oct 27 2012 7:11AM. Time:1 hrs 33 mins. Eq:400 (Air Atmosphere Furnace)
Temperature:: **1100F**

Certification Statement

Process: 17-7PH TH1100, **In Accordance with Spec(s):** AMS2759/3 Rev E (Heat Treatment Precipitation-Hardening Corrosion-Resistant and Maraging Steel parts)

We hereby certify that the articles stipulated above have been processed in conformance with all applicable specifications , drawings, and/or written instructions. Test and/or Inspection Reports indicating conformance are on file for examination.

AERO SPECIALITIES CERTIFY THIS IS A TRUE COPY OF THE MILL TEST REPORT - USED TO FILL YOUR ORDER.
Company ARMOR BRASTER
PO# 1A5208600/4
Our Order # 150724X
QTY 40 PCS
Q.C. asst. D. Dwyer
Authorized Signature

Riadh Hameed

BII QUALITY ASSURANCE 13

Certified By: Riadh Hameed
Title: Quality Administrator
Date: 11/05/2012
Burton Industries Incorporated

AK Steel Corporation
Metallurgical Test Report
Coshocton Works
17400 State Route 16
Coshocton, OH 43812 U.S.A.

Page 1

Load No. 7503282
Srn No. 7503282

CUSTOMER

SHIP TO

MILL ORDER NO. 230987-0417
PROCESSOR ORDER NO. 009260-003
BUYERS ORDER NO. 009260-003

PART NO.
1707SAN112D

ENGLISH UNITS -:PRODUCT:- METRIC UNITS
.1250 NOM 36.0000 X 120.0000

LIFT ID	PIECE	HEAT	PARENT LIFT ID	NET WEIGHT	OUTSIDE PROCESSOR ID	
705536-06-001	22	7511084	705536-06	3,306 LBS. 1,500 KG.	735146A	
705536-06-002	22	7511084	705536-06	3,306 LBS. 1,500 KG.	735146B	
705536-06-003	15	7511084	705536-06	2,254 LBS. 1,022 KG.	735146C	
TOTAL LIFTS	TOTAL PIECES			TOTAL NET WEIGHT		
3	59			8,866 LBS. 4,022 KG.		

L-Ladle Analysis of Heat P-Product Analysis of Parent Coil

CHEMICAL ANALYSIS

ID	C	MN	P	S	SI	CR	NI	AL								
L 7511084	.07	.67	.024	.0001	.45	16.68	7.27	1.14								

SHIPPING DATE: 03/14/2012

REMARKS
NO WELD REPAIRS (WITH OR WITHOUT FILLER METAL) HAVE BEEN MADE.
THIS MATERIAL WAS MELTED AND MANUFACTURED IN THE U.S.A. (DFARS COMPLIANT).
THIS MATERIAL WAS SOLUTION HEAT TREATED TO 1950 +- 25F FOR AN APPROPRIATE TIME NECESSARY TO ACHIEVE MECHANICAL PROPERTY REQUIREMENTS.
BALANCE OF CHEMICAL COMPOSITION NOT REPORTED IS IRON AND MINOR RESIDUAL ELEMENTS.
NO INTENTIONAL ADDITIONS OF MERCURY OR MERCURY COMPOUNDS, RADIUM, ALPHA SOURCE, AND LOW MELTING ALLOYS OR ELEMENTS CAPABLE OF FORMING LOW MELTING ALLOYS WERE MADE THROUGHOUT THE PROCESSING OF THIS MATERIAL.
COILED PRODUCTS CONTAIN NO WELDS

PRODUCT DESCRIPTION

CR SHT 17-7 PH(R) STAINLESS #2D FINISH COND A SLIT EDGE * ASTM A 693-06 * ASME SA-693 SECTION II PART A (2004 ED) * AMS 5528H * MIL-S-25043C CANCELLED 5/9/1997 EX 3.2 WAIVE SOAK REQ; EX 3.6/3.6.1/5.3 PER AK STEEL/CUSTOMER AGREEMENT; EX 4.3.1 WAIVE SAMPLE SIZE; EX 4.4.1 SAMPLING PER ASTM E 59; EX 4.5.1/4.6.1 AK STEEL SAMPLING METH; EX 4.5.2 PREP PER ASTM E 8; EX 4.5.3 TEST PER ASTM A 370; EX 4.6.4 TEST PER ASTM E 18; EX 4.7.1 AMS 2371 3.3.5.3.1 APPLIES * AL 1.05 MIN

*** CONTINUED ON NEXT PAGE ***

AERO SPECIALTIES CERTIFY THIS IS A TRUE COPY OF THE MILL TEST REPORT - USED TO FILL YOUR ORDER.
Company LOCKING SYSTEMS TECH
PO# TL-0R54897 SOLUTIONS
Our Order # 4R5022C
QTY 4R5022C
Q.C. asst
Authorized Signature

AK Steel

AK Steel Corporation
Metallurgical Test Report
Coshocton Works
17400 State Route 16
Coshocton, OH 43812 U.S.A.

Load No. 7S03282
Srl No. 7S03282

CUSTOMER

SHIP TO

MILL ORDER NO. 230987-0417
PROCESSOR ORDER NO. 009260-003
BUYERS ORDER NO. 009260-003

PART NO.
1707SAN112D

ENGLISH UNITS <-PRODUCT:- METRIC UNITS
.1250 NOM 36.0000 X 120.0000

PARENT LIFT ID	POS	DIR (L, T, D)	COND	% ELONG	ELONG METHOD	ELONG GAUGE LENGTH	TENSILE STRENGTH (KSI)	Y.S. .2% OFFSET (KSI)	ROCKWELL HARDNESS Tail	ROCKWELL HARDNESS Front
705536-06	T	T	COND A	36.6	MEASURED	2 Inch	121.5	45.0	BW 88	BW 87
705536-06	T	T	TH 1050	9.0	MEASURED	2 Inch	199.6	191.0	C 45	C 44
705536-06	T	T	RH 950	7.7	MEASURED	2 Inch	232	195.9	C 51	C 50

PARENT LIFT ID	POS	DIR (L, T, D)	COND	BEND 180 1T
705536-06	T		COND A	PASS

PARENT LIFT ID	POS	DIR (L, T, D)	COND	% ELONG	ELONG METHOD	ELONG GAUGE LENGTH	TENSILE STRENGTH (KSI)	Y.S. .2% OFFSET (KSI)	ROCKWELL HARDNESS Tail	ROCKWELL HARDNESS Front
705536-06	F	T	COND A	35.6	MEASURED	2 Inch	123.6	45.3	BW 88	BW 87
705536-06	F	T	TH 1050	10.4	MEASURED	2 Inch	198.4	186.4	C 45	C 44
705536-06	F	T	RH 950	7.1	MEASURED	2 Inch	231	203.0	C 51	C 50

PARENT LIFT ID	POS	DIR (L, T, D)	COND	BEND 180 1T
705536-06	F		COND A	PASS

THE CHEMICAL ANALYSIS AND PHYSICAL OR MECHANICAL TESTS REPORTED ABOVE ARE CORRECT AS CONTAINED IN THE RECORDS OF THE CORPORATION.

ALL TESTING IS DONE IN ACCORDANCE WITH A.S.T.M. STANDARDS UNLESS OTHERWISE NOTED

AK Steel Corporation

MWQCP0049.SRS
Program Version LM438B 1.11

THIS CERTIFIED TEST REPORT HAS BEEN DELIVERED TO A CONSIGNEE OF MATERIAL PURCHASED FROM AK Steel Corporation. TO AVOID THE POSSIBILITY OF ITS MISUSE ON DELIVERY OF THE REPORT TO A THIRD PARTY IT MUST BE RECERTIFIED BY AND UNDER THE NAME OF SUCH CONSIGNEE.

SIGNED: Eric Raymond DATE 03/15/2011 TIME 05:36 AM
ERIC RAYMOND APPLICATION ENGINEER

TECHNICAL SERVICES LABORATORY
Northrop Grumman Corporation
925 South Oyster Bay Road, M/S U03-26
Bethpage, New York 11714-3582

LABORATORY REQUEST NUMBER: 37340-12
DATE: 12/04/2012

DIRECTED TO: (√) ☐ CHEMISTRY LABORATORY ☒ METALLURGY LABORATORY ☐ ADV-DEV TECH-OPS ☐ NDT LABORATORY ☐ OPERATIONS

PART NAME/PART NUMBER: Crack Growth Option 1 For Drawing GT270KB003

TYPE OF MATERIAL: 17-7 PH MIL-S-25043 H/T 155-170 ksi 0.125 inch Thick

PROGRAM	PURCHASE ORDER NO.	JOB NUMBER/IOS	QUANTITY	Heat NO.
				7511084

SPECIFICATIONS	SELLER OR CUSTOMER
MIL-S-25043	

TYPE OF TEST OR ANALYSIS REQUIRED
Mechanical Properties of an IATP Control Points Test Material

PURPOSE OF TEST/BACKGROUND

SAMPLE DESCRIPTION/CONDITION/REMARKS

REQUESTED BY	MAIL STA.-BLDG	FAX	PHONE	LAB APPROVAL
Ken Grube/ Bob Fidnarick	Plant 26		516.346.9232	*John Callori*

FINDING OR RESULTS
THE ABOVE MATERIAL IS: (√) ☒ **SATISFACTORY** ☐ UNSATISFACTORY ☐ INFORMATION ONLY

REMARKS:

Properties	Test Results			Requirements, min.
Specimen Number	1	2	AVG	
Tensile Strength, ksi	169.0	168.7	168.9	155 - 170
Yield Strength, ksi	156.6	156.9	156.8	
% Elongation in 2 inches	13.0	12.0	12.5	

Al Sinowitz
SIGNATURE

Kevin Cook
APPROVED

(TECHNICAL SERVICES LABORATORY FAX 516-575-9909)
All Signatures on File
FORM 1512 REV. May 11
REFERENCE NO.

Lawrence Ripak Co., Inc.

Certification

Order No.: 287137 - 274083
Date: 11/20/2012
Entry Date: 11/15/2012

To: NGRUMNY
NORTHROP GRUMMAN
925 South Oyster Bay Rd
M/S U03-26
Bethpage NY 11714-3582

Purchase Order No.: 50712
Packing List No.:

We are pleased to provide you with the following Certification

Quantity	Part Number / Part Name / Part Description	Pounds
33	GT270KB003-13 MAT'L: 17-7PH	

Process Steps

Step: 1 **Process: Sp** **Equipment #:**

Comment: Note: Certification is void if material removal exceeds 10% of nominal Almen A intensity

Shot Peen per AMS2430 Rev S (s/s AMS-S-13165 Rev A) Machine #: 1 OD Shot: ASR230 Hardness: 45-52Rc Coverage: 100% Intensity: .008-.012A2 Actual: .0102A2 Technique Card: GT270KB003-13 REV N/C 11-19-12

Step: 2 **Process: Cl** **Equipment #:**

Acid clean per AMS2430 Rev S (s/s AMS-S-13165 Rev A) to remove shot peen residue Nitric Acid clean to remove shot peen residue

We certify that the processes listed have been performed in accordance with the specifications shown. Records are being maintained and are available for review.

Deborah Castellano
Planning/Cert Supervisor
Lawrence Ripak Co., Inc.

WESTERN PROFESSIONAL, INC.
3460 BRADY CT. NE
SALEM, OR 97301
PHONE (503)585-6263
FAX (503)585-6577
www.westprolab.com

ULTRASONICS / PHASED ARRAY / EDM
RESEARCH & DEVELOPEMENT

WWW.WESTPROLAB.COM

CUSTOMER:	NORTHRUP GRUMMAN IT
P.O. #:	7500109433
S/N:	PLATES 1 THRU 33
SIZE:	16" X 4" X .125"
HEAT #:	UNKNOWN
MATERIAL:	17-7 PH
DWG#:	GT270KB003
DATE:	11-30-12

PLATE #	DEPTH	LENGTH	WIDTH	TYPE
1	.0201"	.0297"	.0044"	CORNER NOTCH
2	.0209"	.0317"	.0043"	CORNER NOTCH
*3	.0217"	.0313"	.0040"	CORNER NOTCH
4	.0217"	.0342"	.0041"	CORNER NOTCH
5	.0201"	.0307"	.0044"	CORNER NOTCH
6	.0202"	.0285"	.0044"	CORNER NOTCH
7	.0206"	.0304"	.0041"	CORNER NOTCH
8	.0215"	.0303"	.0041"	CORNER NOTCH
9	.0202"	.0295"	.0043"	CORNER NOTCH
10	.0215"	.0314"	.0043"	CORNER NOTCH
11	.0209"	.0296"	.0039"	CORNER NOTCH
12	.0208"	.0309"	.0039"	CORNER NOTCH
13	.0205"	.0304"	.0040"	CORNER NOTCH
14	.0209"	.0321"	.0039"	CORNER NOTCH
15	.0224"	.0331"	.0041"	CORNER NOTCH
16	.0220"	.0331"	.0041"	CORNER NOTCH
17	.0206"	.0304"	.0037"	CORNER NOTCH

PLATE #	DEPTH	LENGTH	WIDTH	TYPE
18	.0253"	.0374"	.0041"	CORNER NOTCH
19	.0206"	.0305"	.0037"	CORNER NOTCH
20	.0200"	.0298"	.0037"	CORNER NOTCH
21	.0209"	.0308"	.0038"	CORNER NOTCH
22	.0209"	.0293"	.0038"	CORNER NOTCH
23	.0207"	.0328"	.0039"	CORNER NOTCH
24	.0222"	.0347"	.0036"	CORNER NOTCH
25	.0213"	.0313"	.0041"	CORNER NOTCH
26	.0211"	.0316"	.0039"	CORNER NOTCH
27	.0205"	.0308"	.0039"	CORNER NOTCH
28	.0206"	.0313"	.0038"	CORNER NOTCH
29	.0202"	.0313"	.0037"	CORNER NOTCH
30	.0208"	.0311"	.0043"	CORNER NOTCH
31	.0219"	.0330"	.0041"	CORNER NOTCH
32	.0203"	.0290"	.0043"	CORNER NOTCH
33	.0217"	.0333"	.0043"	CORNER NOTCH

* SEE ATTACHED NOTE

NOTE: SEE ATTACHED CUSTOMER DRAWING FOR NOTCH REQUIREMENTS AND LOCATION.

ALL DIMENSIONS ARE MEASURED WITH DIMENSIONAL EQUIPMENT WHICH IS CERTIFIED AND TRACEABLE TO **NIST (#708) #5084918** AND **NIST (#783183) #5830553.** NUCLEAR REGULATORY COMMISSION RULES AND REGULATIONS 10 CFR PART 21 APPLIES TO THIS ORDER. ALL NOTCHES MANUFACTURED PER WESTPRO PROCEDURE WQC-IV.

FABRICATED BY: S. CHAMBERLAIN

APPROVED BY: Mitchell A Dale

Crack growth Option 1 12/4/2012

Material: 17-7 PH (155 -170 ksi)
Heat number: 7511084
Drawing No: GT270KB003
Coupon ID 1-33

Coupon ID	Thickness in	Width in	Hole dia in
1	0.125	4.003	0.157
2	0.125	4.003	0.156
3 (1)	0.125	4.003	0.164
4	0.125	4.002	0.156
5	0.125	4.003	0.156
6	0.125	4.003	0.156
7	0.125	4.003	0.156
8	0.125	4.003	0.156
9	0.125	4.004	0.156
10	0.125	4.002	0.156
11	0.125	4.002	0.156
12	0.125	4.004	0.156
13	0.125	4.004	0.156
14	0.124	4.002	0.156
15	0.125	4.003	0.156
16	0.124	4.001	0.156
17	0.125	4.002	0.156

Coupon ID	Thickness in	Width in	Hole dia in
18	0.125	4.004	0.156
19	0.125	4.002	0.156
20	0.125	4.004	0.156
21	0.124	4.001	0.156
22	0.124	4.004	0.156
23	0.124	4.005	0.156
24	0.125	4.002	0.156
25	0.125	4.003	0.156
26	0.125	4.002	0.156
27	0.124	4.004	0.156
28	0.125	4.001	0.156
29	0.124	4.001	0.156
30	0.124	4.004	0.156
31	0.125	4.002	0.156
32	0.124	4.001	0.156
33	0.125	4.003	0.156

Note: (1) Coupon 3 had .004 inch EDM notch 180° from the required notch. It was removed by drilling the hole to .164 inches. The new EDM notch measures .027 inches in length.

APPENDIX B

POLISHING, REAMING AND SEM PROCEDURES

PROCEDURE FOR POLISHING SURFACE OF TEST SPECIMENS

1. A progression of 500, 800 and 1200 grit sandpaper was used to remove the mill finish.

2. A Struers Tanspol-2 polisher was then used with a progression of polishing paste of 3 micron and 1 micron to polish the surface from the 1200 grit sand paper.

PROCEDURE FOR REAMING THE BORE OF THE TEST SPECIMENS

1. Find the center of the hole using a hole dial indicator mounted in the spindle of the mill.

2. Using a 15/64" drill bit, drill out the bore starting on the opposite side of where the precrack is located. This will help prevent the bit from catching on the crack. [26] The spindle, in high gear, was set at a speed of 700 rpm.

3. Using a 12 straight flute 0.25" reamer, slowly ream out the bore also starting on the side opposite the precrack. The spindle, in low gear, was set at 80 rpm.

PROCEDURE FOR POLISHING THE BORE OF THE TEST SPECIMENS

1. Use a 84922 silicon carbide sanding stone to remove reaming marks

2. Use a 462 rubber polishing cone point to remove the defects created by the sanding stone.

3. Apply 3 micron polishing paste to a polishing cloth wrapped around a 402 rotary tool mandrel.

PROCEDURE FOR USING THE SEM

1. Turn on the chiller to the SEM and wait for it to reach a temperature of 68°F.

2. Turn on power to the SEM.

3. Place the specimen in the vibrating cleaner containing a lacquer solution for 10 minutes.

4. Replace the lacquer solution with one of alcohol for another 10 minutes.

5. Release the vacuum from the observation chamber.

6. Using rubber gloves, place the cleaned specimen into the holding mount, close the chamber and turn on the vacuum pump.

7. Once the vacuum indicator signals that conditions are sufficient, the electron beam is turned on.

8. Adjust the focus, contrast and brightness until the image is clear. Initially keep a working distance of 15 to 20 mm to obtain a wide view of the surface.

9. Pick a desired location on the surface and magnify the image to 3,000X to 4,000X and focus the image. This will help produce higher quality pictures at smaller magnifications.

10. Once the image is focused, zoom back out to obtain the widest view desired.

11. Progressively take pictures by incrementally increasing the magnification until the desired amount of detail is obtained.

12. Once the examinations are complete, turn off the electron beam and the pump to release the vacuum from the observation chamber.

13. Using rubber gloves, open the observation chamber and remove the specimen.

14. Close the observation chamber and turn on the pump once more. This will help prevent contaminants from entering the chamber.

15. Once the observation chamber has sufficient vacuum applied, the power may then be turned off to both the SEM and chiller.

APPENDIX C

SOUTHWEST RESEARCH INSTITUTE EQUIPMENT INFORMATION

Pump Information

Motor:	Baldor (2)
HP:	100 (each)
Flow Rate:	50 GPM (each), 100 GPM total
Pressure:	3000 psi
History:	Designed and implemented by SwRI staff in the 1980's; not a commercially produced system. Primary Cooling: refrigerant based heat exchanger (compressor/evaporator). Secondary Cooling: air over water heat exchanger (radiator)

Frame Information

Model #:	Instron A393-499
Serial #:	1322-23
Servo Valve:	1 (5GPM)
Capacity:	50 kip
Load Cell:	Lebow 3117-101
Grips:	SATEC 55 Kip 185480-3
FTA version:	V3.12.08

Traveling Microscopes

Magnification Scope:	Gaetner Scopes (2 per test fram); 10X eyepiece, 38mm EFL
Measurement Device:	6" Digital Scales (certification provided by SwRI calibration laboratory; annually)
Mounting Hardware:	SwRI custom brackets anchored to frame posts

Testing Procedures

The overall test setup included a fatigue rated test frame, matching load cell rated to the frame capacity, hydraulic wedge grips (flats), a MTS 458 analog controller, and a Windows based software package from Fracture Technology Associates (FTA). The system is a closed-loop command-feedback system and commonly used in the fatigue testing community. The specific application within the FTA software package was the variable amplitude fatigue crack growth option. FTA is based in Bethlehem, PA and owned and operated by Mr. Keith Donald (www.fracturetech.com). The Solid and Fracture Mechanics Laboratory has been using the FTA software for fatigue testing for the past 20+ years.

The FTA variable amplitude software utilizes a read-in approach for application of variable amplitude loading. The software has multiple options with regards to spectrum file format. For the testing performed herein, the files were provided in sequential format (max, min, max, min, etc.) and the maximum stress for the spectrum. During the

software read-in, it is determined whether or not the spectrum is an acceptable form and a simple summary of the spectrum is provided (number of points, maximum value within the spectrum, etc). During the test setup, the maximum load corresponding to the maximum stress is inputted and from there all of the spectrum file endpoints are scaled accordingly.

The FTA software is adaptive and learns during the first spectrum pass. A matrix is established for the particular spectrum content and loading parameters for the current test. The matrix contains information regarding the command signal needed for the multitude of loading segments within the spectrum file. During the first pass of the spectrum the matrix is populated with parameters associated with the command parameters and are used during subsequent passes as the test progress. In addition, the matrix is updated as specimen compliance changes thus requiring command parameter changes.

The backbone of variable amplitude testing is how well the system can achieve the target load level during each cycle; for spectra that have rather aggressive and deviating content, this becomes extremely important. The FTA system monitors the target and feedback values during the course of a test as a way to monitor and assess the performance. An absolute voltage level is entered as a parameter into the system as an acceptable threshold. Any difference between the target and feedback that is greater than this value and the event is archived in a file correlate to that test. It is important to note that this approach is an absolute difference (voltage) and not a relative difference (%). During the setup of a test and establishing the control parameters, the threshold value can be set to 0 volts such that every event is logged and can be post-test assessed to establish a history of error for a multiple spectrum passes. Furthermore, this history can be the basis for whether or not the current parameters are acceptable in terms of system performance and the frame is able to maintain under a certain acceptable amount of target/feedback error.

The FTA software controls test rate by utilizing both load rate and frequency as controlling parameters. The overall rate is bounded by these two parameters by inputting upper limits for both in terms of volts/time (loading rate) and frequency (cyclic rate). The system operates within these two bounds and depending the current cyclic content of the spectrum, is typically governed by one or the other. For example, during extreme events in a spectrum, the frequency limit may not be achievable and thus the loading rate becomes the controlling parameter during application of those events. Similarly, during low excursion events in a spectrum, the system may be easily able to handle a higher loading rate but is bound by an upper limit frequency. As previously mentioned, these two rate parameters are established during pretest exercises and are dependent on: the test frame, the spectrum content, coupon material, coupon geometry, load frame compliance, and acceptable error between target and feedback. During the testing of the 17-7PH SS, the frame was evaluated based on the above considerations when establishing the loading

rate and frequency limits. For the 17-7PH SS testing, the limits were 100 kips/sec and 20 Hz.

Testing was executed by the Solid and Fracture Mechanics technical staff with guidance and test documentation provided by a test engineer. The technical personnel are responsible for test frame setup which includes configuration of the proper load train components (connections, grips, etc), integration of the control hardware, and overall shakedown of the system after setup.

Alignment of the grips was based on ASTM E1012 and involves the use of a strain gaged alignment coupon to determine the amount of bending (misalignment) for an uniaxial setup. The alignment consists of four strain gages with two on each side at the mid-length location. On each side, the gages are placed at the 1/3 and 2/3 width locations such that there is an opposing pair on the front and back. During the alignment process, the strain gaged coupon is rotated and flipped to the four possible configurations and a post-exercise evaluation summarizes the in-plane and out-of-plane bending for those four orientations. The objective is get all of those below a certain level; ASTM recommends less than 5% while the Solid and Fracture Mechanics Lab typically seeks for 2% or less. If the results of the analysis indicate unsatisfactory alignment, adjustments are made to the load train for correction until an acceptable level is achieved. Once aligned, the load is not altered during the course of testing. It is important to note that the alignment approach does not take into account specimen to specimen variability. The frame is aligned by using an alignment coupon and not adjusted thereafter unless the load train has to be dissembled in anyway.

Prior to applying spectrum loading to a test article, the FTA system is configured to feed itself the command signal (essentially the load frame is taken out of the control-feedback loop). During this step, the spectrum is fed through the system to ensure the file is read correctly and there are no errors during a pass. Once complete and checked out, the frame is reinserted into the loop and the setup is considered ready for testing.

The operation of the FTA system is rather straight forward regards to performing a test. The software steps through a series of inputs needed to configure a test. After completing this task, they are reviewed and confirmed for the current test in the frame. FTA has multiple options regarding startup and SwRI has historically used a soft-start in which it requires approximately 10 cycles to full achieve the full amplitude control (in analog this would be full span). In simpler terms, the test does not start out going to target end-point but instead gradually ramps up over the course of a few cycles. During a test stop/halt, the frame will go to a predetermined hold level defined by a voltage input. The lab historically has set this value to correspond to 100-200 lbs of tensile load. The frame will go to this level during both a manual stop and an interval stop (reaching a certain crack length or cycle count as examples). This go to hold level is chosen such that the applied

load during the hold has no potential to induce load history effects into the test history. During the course of these testing, technicians were responsible for crack length measurements which happened multiple times a day during the work week. During the weekends, on occasion there was a technician available to monitor the test and maintain cycling. However, during a non-active weekend, the specimen would hold at the input level until a technician addressed the frame.

Both surface (c) and bore (a) measurements were made during the test effort. Traveling microscopes were used to monitor and measure crack lengths. Surface measurements were rather straightforward with the scope and travel setup orthogonal and perpendicular to the face of the coupon. Bore measurements, however, were accomplished by angling the scope into the bore and making the required geometric corrections to account for the non-orthogonal measurement by the angled view.

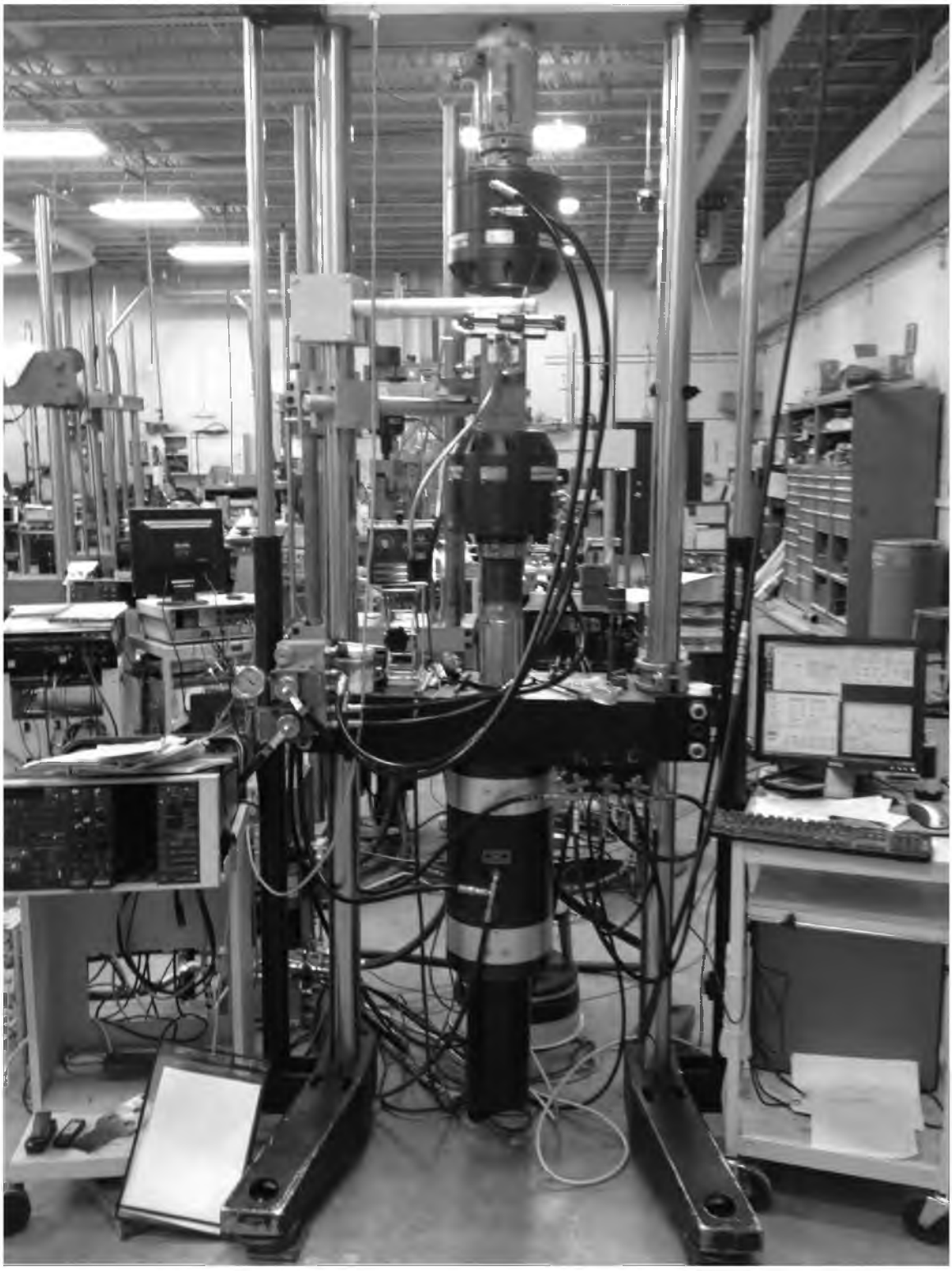

Figure 56 50 kip Instron Fatigue Machine

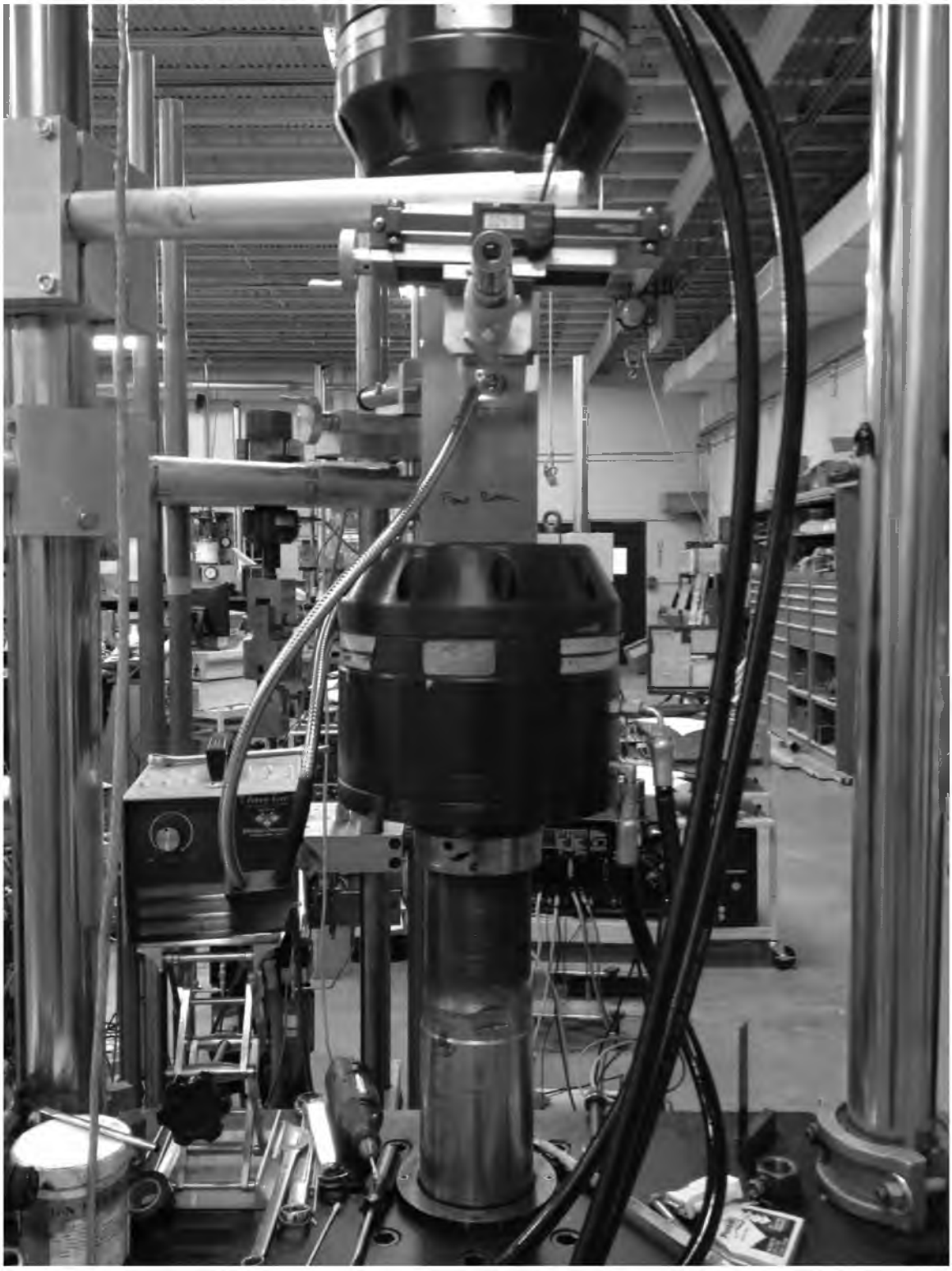

Figure 57 Close up of Measurement Equipment

APPENDIX D

FATIGUE MACHINE AND LOAD CELL CALIBRATION CERTIFICATIONS

CERTIFICATE OF CALIBRATION

ISSUED BY: INSTRON CALIBRATION LABORATORY

DATE OF ISSUE: 02-May-13 CERTIFICATE NUMBER: **95041613090507C**

NVLAP
Lab code: 200301-0

Instron
825 University Avenue
Norwood, MA 02062-2643
Telephone: (800) 473-7838
Fax: (781) 575-5750
Email: service_requests@instron.com

APPROVED SIGNATORY

Type of Calibration:	**Force**
Relevant Standard:	**ASTM E4-10**
Date of Calibration:	**16-Apr-13**

Customer Requested Due Date: 16-Apr-14

Customer

Name:	Hill AFB
Address:	7278 4th Street, Bldg. 100, Bay D Hill AFB, UT 84056 cody.hone@hill.af.mil
P.O./Contract No.:	CO8616
Contact:	Cody Hone

Machine

Manufacturer:	Interlaken
Serial Number:	880RJ3037
System ID:	8800RCJ3037
Range Type:	Single

Transducer

Manufacturer:	Interface
Transducer ID:	1032AF-50K-B/376010A
Capacity:	50 kips
Type:	Tension/Compression

Classification

1. Digital Readout - PASSED

Certification Statement

This certifies that the forces verified with machine indicator(s) (listed above) that passed are WITHIN ± 1 % accuracy, 1 % repeatability, and zero return tolerance.
All machine indicators were verified on-site at customer location by Instron in accordance with ASTM E4.
The certification is based on runs 1 and 2 only. A third run is taken to satisfy uncertainty requirements according to ISO 17025 specifications.
The verification and equipment used conform to a controlled Quality Assurance program which meets the specifications outlined in ANSI/NCSL Z540-1, ISO 10012, ISO 9001:2008 and ISO/IEC 17025:2005.

Method

The testing machine was verified in the 'as found' condition with no adjustments carried out.

CERTIFICATE OF CALIBRATION

ISSUED BY : INSTRON CALIBRATION LABORATORY

DATE OF ISSUE : **16-Apr-2013** CERTIFICATE NUMBER: **95041613130159B**

NVLAP
Lab code: 200301-0

APPROVED SIGNATORY

INSTRON
Instron
825 University Avenue
Norwood, MA 02062-2643
Telephone: (800) 473 - 7838
Fax: (781) 575 - 5755
Email: service_requests@instron.com

Type of Calibration: **Linear Stroke**
Relevant Standard: **Linear Stroke**
Date of Calibration: **16-Apr-2013** **Customer Requested Due Date: 16-Apr-2014**

Customer	Hill AFB 7278 4th St Bldg 100, Bay D Hill AFB, UT 84056
P.O. Number :	CO8616
Contact :	Cody Hone

Machine	
Serial No :	880RJ3037
Make :	Interlaken
Model :	8800
Ambient Temperature :	79.3 °F

Readout Verified

1. Digital Readout (in)

Certification Statement

This certifies that the displacements verified with machine indicator 1 (listed above) were verified by Instron in accordance with Instron work instruction ICA-8-07.

The acceptable field calibration tolerance for certification is ± 1.0% full travel for Instron machines. For other machines, check the manufacturers specifications.

Method of Verification

The verification and equipment used conform to a controlled Quality Assurance program which meets the specifications outlined in ANSI/NCSL Z540-1, ISO 10012, ISO 9001:2008, and ISO/IEC 17025:2005. The Instron measurement equipment used for verification is traceable to NIST.

The testing machine was verified on-site at customer location. The testing machine was verified in the 'As Found' condition with no adjustments or repairs carried out. This is also the 'As Left' condition.

CERTIFICATE OF CALIBRATION

ISSUED BY : INSTRON CALIBRATION LABORATORY

DATE OF ISSUE : **16-Apr-2013** CERTIFICATE NUMBER : **95041613145249E**

NVLAP
Lab code: 200301-0

APPROVED SIGNATORY

Instron
825 University Avenue
Norwood, MA 02062-2643
Telephone: (800) 473 - 7838
Fax: (781) 575 - 5755
Email: service_requests@instron.com

Type of Calibration: Speed
Relevant Standard: ASTM E2658-11
Date of Calibration: 16-Apr-2013 **Customer Requested Due Date: 16-Apr-2014**

Customer	Hill AFB 7278 4th St Bldg 100, Bay D Hill AFB, UT 84056	**Machine**	
		Serial No :	880RJ3037
		Make :	Interlaken
		Model :	8800
P.O. Number :	CO8616	Ambient Temperature :	79.7 °F
Contact :			

Readout Verified

1. Digital Readout (in/min)

Resolution of Indicator: .001 in/min

Certification Statement

This certifies that each speed verified with machine indicator 1 (listed above) was verified by Instron in accordance with ASTM E2658 (Start and Stop Method) and Instron work instruction ICA-8-07, and that the ASTM E2658 classification for each speed was:

PASSED Class A - for 1 in/min speed
PASSED Class A - for .25 in/min speed
PASSED Class A - for 1 in/min speed

Method of Verification

The verification and equipment used conform to a controlled Quality Assurance program which meets the specifications outlined in ANSI/NCSL Z540-1, ISO 10012, ISO 9001:2008, and ISO/IEC 17025:2005. The Instron measurement equipment used for verification is traceable to NIST.

The testing machine was verified on-site at customer location. The testing machine was verified in the 'As Found' condition with no adjustments or repairs carried out. This is also the 'As Left' condition.

APPENDIX E

EXAMPLE OF PRECRACK CALCULATIONS

DIMENSIONS REQUIRED FOR CALCULATIONS

Crack Length in Hole (a) = 0.0510 in,Crack Length on Surface (c) = 0.0765 in,

Thickness (t)= 0.1250 in, Hole Diameter (d) = 0.1570 in, Hole Radius (r) = 0.0785 in,

Specimen Width (W) = 4.003 in, b = w/2 = 2.002 in

PRELIMINARY STEP CALCULATIONS

$$a/c = 0.667,\ Q = 1 + 1.464\left(a/c^{1.65}\right) = 1.750,\ a/t = 0.408,\ r/t = 0.628$$

CONSTANTS AND APPLIED STRESS

for tension loads $\mu = 0.85$, for single crack $n = 1$, $St = 15.4\ ksi$, bending correction factor $H_{ch} = 0$ since there are no bending stresses

MAIN EQUATIONS FOR CALCULATING THE STRESS INTENSITY IN A SINGLE CORNER CRACK OF A HOLE

$$K_{one\ crack} = \sqrt{\left(\frac{4}{\pi} + \frac{ac}{2tr}\right) \Big/ \left(\frac{4}{\pi} + \frac{ac}{tr}\right)}\, K_{two\ cracks}$$

$$K_{two\ cracks} = (St + H_{ch}S_b)\sqrt{\pi \frac{a}{Q}}\, F_{ch}\left(\frac{a}{c}, \frac{a}{t}, \frac{r}{t}, \frac{r}{b}, \frac{c}{b}, \frac{c}{b}, \phi\right)$$

for $0.2 < a/c < 2, a/t < 1, 0.5 < r/t < 2, (r+c)/b < 0.5$, and $0 < \phi < \pi/2$

$$F_{ch} = \left[M_1 + M_2\left(\frac{a}{t}\right)^2 + M_3\left(\frac{a}{t}\right)^4\right] g_1 g_2 g_3 g_4 f_\phi f_w$$

for $a/c < 1$: $M_1 = 1.13 - 0.09(a/c),\ M_2 = -0.54 + 0.89/(0.2 + a/c),$

$$M_3 = 0.5 - 1/(0.65 + a/c) + 14(1 - a/c)^{24},$$

$$g_1 = 1 + \left[0.1 + 0.35(a/t)^2\right](1 - \sin\phi)^2,$$

$$g_2 = \frac{1 + 0.358\lambda + 1.425\lambda^2 - 1.578\lambda^3 + 2.156\lambda^4}{1 + 0.13\lambda^2},$$

$$\text{where } \lambda = 1/(1 + {}^{c}/_{r}\cos(\mu\phi)),$$

$$g_3 = (1 + 0.04\,{}^{a}/_{c})[1 + 0.1(1 - \cos\phi)^2]\left[0.85 + .15({}^{a}/_{c})^{1/4}\right],$$

$$g_4 = 1 - 0.7\left(1 - {}^{a}/_{t}\right)({}^{a}/_{c} - 0.2)(1 - {}^{a}/_{c}),\ f_\phi = [({}^{a}/_{c})^2(\cos\phi)^2 + (\sin\phi)^2]^{1/4}$$

$$f_w = \left\{\sec\left(\frac{\pi r}{2b}\right)\sec\left[\frac{\pi(2r + nc)}{4(b - c) + 2nc}\sqrt{\frac{a}{t}}\right]\right\}^{1/2}$$

These equations were input into an Excel spread to calculate the max stress intensities. Knowing the applied stress with the stress intensities the plastic zone sizes could then be calculated. The following is a printout of the spreadsheet used for the calculations.

Stress Intensity Solution of a Corner Crack From a Hole

Dimensions

a=	0.0510 in	M1=	1.07
c=	0.0765 in	M2=	0.486923
t=	0.1250 in	M3=	-0.25949
d=	0.1570 in	g4=	0.935538
r=	0.0785 in	fw=	1.001842
W=	4.003 in		
b=	2.002 in		
Q=	1.750		
a/c=	0.667		
a/t=	0.408		
r/t=	0.628		
μ=	0.85		
n=	1		

Stresses

St=	15.4 ksi

Crack Lengths

c	a	k	St	Plastic (in)
0.091	0.061	11.0	15.4	0.005
0.084	0.056	13.2	19.2	0.0075
0.075	0.05	17.1	24	0.011
0.06	0.04	19.7	30	0.0145
0.045	0.03	22.2	37.5	0.018
0.03	0.020			

Fch=	fϕ=	g3=	g2=	λ=	g1=	ϕ=	K two	K one	Deg
1.450	0.816	0.996	1.436	0.506	1.158	0.000	6.755	6.340244	0
1.421	0.818	0.996	1.437	0.507	1.132	0.087	6.621	6.214858	5
1.404	0.824	0.996	1.440	0.509	1.108	0.175	6.541	6.139361	10
1.397	0.833	0.996	1.445	0.513	1.087	0.262	6.510	6.110445	15
1.400	0.845	0.996	1.452	0.518	1.069	0.349	6.525	6.124361	20
1.412	0.859	0.997	1.462	0.524	1.053	0.436	6.581	6.177512	25
1.433	0.874	0.998	1.475	0.532	1.040	0.524	6.677	6.266933	30
1.461	0.890	0.999	1.490	0.542	1.029	0.611	6.808	6.390613	35
1.497	0.906	1.001	1.509	0.553	1.020	0.698	6.976	6.547671	40
1.541	0.922	1.004	1.531	0.566	1.014	0.785	7.179	6.738468	45
1.592	0.937	1.008	1.559	0.582	1.009	0.873	7.420	6.964716	50
1.653	0.951	1.014	1.591	0.600	1.005	0.960	7.702	7.229661	55
1.723	0.963	1.021	1.630	0.620	1.003	1.047	8.031	7.538384	60
1.806	0.974	1.029	1.678	0.643	1.001	1.134	8.415	7.898313	65
1.902	0.983	1.039	1.736	0.669	1.001	1.222	8.864	8.320011	70
2.016	0.991	1.050	1.807	0.699	1.000	1.309	9.395	8.818406	75
2.152	0.996	1.064	1.895	0.733	1.000	1.396	10.030	9.414656	80
2.318	0.999	1.079	2.007	0.771	1.000	1.484	10.802	10.139	85
2.523	1.000	1.095	2.148	0.815	1.000	1.571	11.757	11.03517	90

	Plastic	0.005168 in
		0.001706

APPENDIX F

PROCEDURES FOR AFGROW ANALYSIS

STEP BY STEP PROCESS TO USE AFGROW BASED ON THE GUIDELINES PREPARED BY THE UNITED STATES AIR FORCE [31]

1. Create Title: Brief description of model.

2. Select Material: This analysis used a file containing material properties and parameters for the Forman equation to simulate the 17-7PH in the AFGROW program. The information in the file is a general guide and some material properties may need to be adjusted based on manufacturing thicknesses or other factors. Reference the Metallic Materials Properties Development and Standardization (MMPDS) to verify correct material properties.

3. Create Model: From a selection of "Classic Models", choose the appropriate geometric model. For this analysis, the "Single Corner Crack at Hole" model was chosen.
   a. Enter problem geometric factors including: thickness, width, hole diameter, initial flaw size (IFS), offset, etc.
      i. Check: keep A/C constant
      ii. Uncheck: Oblique through crack
      iii. IFS: Unless otherwise specified, the initial flaw size should be the same in both the "A" and "C" directions. For this analysis an average of the precrack sizes, for each type of test conducted, were used.
   b. Select Load Type: Ratio of tension or bearing stress to reference stress must be input for each load case (tension stress fraction = 1.0 if bearing stress is zero). The test for this analysis was purely tensile.

4. Open Spectrum File: For this analysis the A and B spectrum files, specifically created to be used in AFGROW, were utilized. AFGROW require that the files be normalized with the greatest value given a value of 1.0 and all other loads be represented as a fraction of the highest load.
   a. Stress Multiplication Factor (SMF): Enter the max stress of the spectrum. Since the values in the spectrum files are representative of loads the SMF had to include a conversion factor to make the values in the spectrum files convert to stresses.

5. Select a Retardation Model: For this analysis several retardation models were attempted to obtain the best fit to the test data.

6. Predict Function Preferences: Used for establishing various analysis criteria and outputs.
   a. Select Growth Increments: Cycle by Cycle Beta and Spectrum calculation. Use a Max Growth Increment of 0.25%
   b. Enter Output Intervals: Specify crack growth increments. Increment = 0.01"
      i. Enter Number of Hours per Pass: Conversion factor for calculating effective flight hours (EFH) from segment count.
   c. Select Output Options: Typically the user will select the data file and plot file options for crack growth data.

d. Select Propagation Limits: Unless otherwise specified use the K_{max} and the Net Section Section Yield failure criteria.
    i. If using Forman, as was done for this analysis, select User-Defined K_{max} and enter an appropriate value for the material.
e. Enter Transition to Through Crack: Use default unless otherwise specified.

7. Select Stress State: Use default unless otherwise specified.

8. Select Beta Criteria: Use AFGROW standard solution betas for standard geometries.

9. At this point the user is ready to run the analysis.

APPENDIX G

CRACK GROWTH DATA SHEETS

GT270KB003-13-1 Fatigue Crack Growth Data Sheet

Width: 4.003 in. Thick: 0.125 in. Area: 0.500 in^2

Pre-crack Information

Pre-crack Date: 5/31/13 Loading Condition: Constant Amplitude R=0.05

Hole Dia.: 0.156 in. Surface EDM: 0.0295 in.

Pre-crack Tuning Data

Tuning Step	Frequency (Hz)	Tuning Cycles	Max Stress (ksi)
1	13	1057	37.5
2	13	420	30
3	15	550	24
4	20	1000	15.4
5	18	1279	15.4

Pre-crack Run Data

Cycles	Stress (ksi)	Frequency (Hz)	Crack Length (in.)
0	0	0	0.1075
9800	37.5	13	0.1093
26564	37.5	13	0.1118
47564	30	13	0.1218
84580	24	15	0.1353
118698	19.2	15	0.1407
274222	15.4	18	0.1551

Experiment Information

Exp. Date: SwRI 01/14 Loading Condition: Variable Amplitude

Exp. Type: Spec. A & B1 Loading Rate: 100 kip/s Hole Dia.: 0.256 in.

Max Stress (Sp. A&B): 21.953 ksi Surface Crack: 0.059 in. Bore Crack: 0.084 in.

Experiment Run Data

		Crack Length (in.)			
Spectrum	EFH	Front	Bore	Back	Comments
A	0	0.059	0.084		
	286.89	0.060	0.091		
B	0	0.060	0.091		
	137299.80	0.068	0.096		
	274599.50	0.077	0.103		
	411899.30	0.085	0.118		
	456292.90	0.088	0.125	0.020	
	503432.50	0.090		0.032	
	549199.10	0.093		0.042	

Continued on the next page

Spectrum	EFH	Crack Length (in.)			Comments
		Front	Bore	Back	
B	617849.00	0.098		0.052	
	663615.60	0.101		0.059	
	709382.20	0.104		0.066	
	755148.70	0.108		0.072	

This sample was tested twice. The first test was conducted before the transition points were changed and the bore crack only grew to 0.084 inches. Since the new transition point was changed to a range of 0.090 to 0.095 inches the test was ran a second time. The table here represents the data gathered from the test conducted by SwRI. Due to the lack of data during testing of spectrum A this data was not used for analysis purposes.

GT270KB003-13-2 Fatigue Crack Growth Data Sheet

Width: 4.001 in. Thick: 0.124 in. Area: 0.496 in^2

Pre-crack Information

Pre-crack Date: 6/3/13 Loading Condition: Constant Amplitude R=0.05

Hole Dia.: 0.155 in. Surface EDM: 0.0293 in.

Pre-crack Tuning Data

Tuning Step	Frequency (Hz)	Tuning Cycles	Max Stress (ksi)
1	13	544	37.5
2	15	1341	24
3	18	913	15.4

Pre-crack Run Data

Cycles	Stress (ksi)	Frequency (Hz)	Crack Length (in.)
0	0	0	0.1068
34020	37.5	13	0.1208
55159	30	13	0.1346
90705	24	15	0.1535
120816	19.2	15	0.1612
167765	15.4	18	0.1677

Experiment Information

Exp. Date: SwRI 01/14 Loading Condition: Variable Amplitude

Exp. Type: Spec. A Loading Rate: 100 kip/s Hole Dia.: 0.249 in.

Max Stress (Sp. A): 21.953 ksi Surface Crack: 0.046 in. Bore Crack: 0.063 in.

Experiment Run Data

Spectrum	EFH	Crack Length (in.)			Comments
		Front	Bore	Back	
A	0	0.046	0.063		100 kip/s
	860.68	0.048	0.068		
	1721.36	0.050	0.072		
	9171.10	0.055	0.074		
	20082.48	0.064	0.077		
	31558.19	0.077	0.085		
	36178.88	0.085	0.089		
	45902.82	0.091	0.096		
	57378.52	0.106	0.125	0.034	
	63596.20	0.115		0.050	
	74592.07	0.128		0.074	
	86067.78	0.143		0.098	

Continued on the next page

Spectrum	EFH	Crack Length (in.)			Comments
		Front	Bore	Back	
A	91231.85	0.152		0.109	100 kip/s
	103281.30	0.170		0.132	
	114757.00	0.190		0.157	
	126232.70	0.212		0.181	
	137708.40	0.236		0.207	
	149184.10	0.262		0.233	
	160659.90	0.289		0.263	
	172135.60	0.318		0.291	
	183611.30	0.350		0.323	
	195087.00	0.383		0.358	
	201445.00	0.403		0.378	
	212300.50	0.439		0.416	
	223776.20	0.484		0.461	
	230485.20	0.512		0.490	
	240989.80	0.561		0.538	
	252465.50	0.621		0.599	
	261072.30	0.670		0.650	
	269679.00	0.725		0.704	
	275766.60	0.765		0.746	
	284023.70	0.827		0.806	
	289761.50	0.869		0.850	
	295499.40	0.915		0.897	
	298368.30	0.939		0.920	
	301237.20	0.964		0.945	
	302970.40	0.979		0.961	
	306975.10	1.016		0.997	
	309844.00	1.043		1.026	
	312712.90	1.074		1.058	
	321659.60	1.179		1.163	
	329926.50	1.295		1.281	
	338533.30	1.460		1.449	

GT270KB003-13-3 Fatigue Crack Growth Data Sheet

Width: 4.003 in. Thick: 0.125 in. Area: 0.500 in^2

Pre-crack Information

Pre-crack Date: NA Loading Condition: Constant Amplitude R=0.05

Hole Dia.: 0.164 in. Surface EDM: 0.0295 in.

Test coupon was manufacture with an oversized hole. The coupon was used as a trial specimen for setting up the machine. The information for this coupon is not valid.

GT270KB003-13-4 Fatigue Crack Growth Data Sheet

Width: 4.001 in. Thick: 0.1245 in. Area: 0.498 in^2

Pre-crack Information

Pre-crack Date: 6/4/13 Loading Condition: Constant Amplitude R=0.05

Hole Dia.: 0.157 in. Surface EDM: 0.033 in.

Pre-crack Tuning Data

Tuning Step	Frequency (Hz)	Tuning Cycles	Max Stress (ksi)
1	13	986	37.5
2	15	1556	24
3	18	NA	15.4

Pre-crack Run Data

Cycles	Stress (ksi)	Frequency (Hz)	Crack Length (in.)
0	0	0	0.1115
33814	37.5	13	0.1271
53933	30	13	0.1430
90716	24	13	0.1565
125924	19.2	15	0.1657
164676	15.4	15	0.1803

This specimen was not used for testing due to the fact that the precrack grew longer than the previously determined range.

GT270KB003-13-5 Fatigue Crack Growth Data Sheet

Width: 4.004 in. Thick: 0.125 in. Area: 0.501 in^2

Pre-crack Information

Pre-crack Date: 6/4/13 Loading Condition: Constant Amplitude R=0.05

Hole Dia.: 0.157 in. Surface EDM: 0.0298 in.

Pre-crack Tuning Data

Tuning Step	Frequency (Hz)	Tuning Cycles	Max Stress (ksi)
1	13	1977	37.5
2	15	1923	24
3	18	2940	15.4

Pre-crack Run Data

Cycles	Stress (ksi)	Frequency (Hz)	Crack Length (in.)
0	0	0	0.1083
32759	37.5	13	0.1233
54099	30	13	0.1397
92092	24	15	0.1529
128284	19.2	15	0.1620
173327	15.4	18	0.1687

Experiment Information

Exp. Date: 2/11/14 Loading Condition: Variable Amplitude

Exp. Type: Spec. A Loading Rate: 400 to 500 kip/s Hole Dia.: 0.253 in.

Max Stress (Sp. A): 21.953 ksi Surface Crack: 0.046 in. Bore Crack: 0.082 in.

Experiment Run Data

Spectrum	EFH	Crack Length (in.)			Comments
		Front	Bore	Back	
A	0	0.046	0.082		500 kip/s
	4497.77	0.048	0.082		
	25347.35	0.069	0.098		
	45425.05	0.090	0.116		Reduced to 400 kip/s due to limit trip
	66581.12	0.120	0.125	0.073	
	84059.44	0.153		0.109	
	107210.63	0.193		0.163	
	129839.13	0.244		0.221	
	152402.17	0.305		0.284	

GT270KB003-13-6 Fatigue Crack Growth Data Sheet

Width: 4.003 in. Thick: 0.125 in. Area: 0.500 in^2

Pre-crack Information

Pre-crack Date: 6/5/13 Loading Condition: Constant Amplitude R=0.05

Hole Dia.: 0.157 in. Surface EDM: 0.0298 in.

Pre-crack Tuning Data

Tuning Step	Frequency (Hz)	Tuning Cycles	Max Stress (ksi)
1	13	1116	37.5
2	15	1722	24
3	18	2452	15.4

Pre-crack Run Data

Cycles	Stress (ksi)	Frequency (Hz)	Crack Length (in.)
0	0	0	0.1083
30533	37.5	13	0.1241
49551	30	13	0.1375
82597	24	15	0.1521
122787	19.2	15	0.1625
168845	15.4	18	0.1681

Experiment Information

Exp. Date: 9/6/13 Loading Condition: Variable Amplitude

Exp. Type: Spec. A&B1 Loading Rate: 100 to 150kip/s Hole Dia.: 0.256 in.

Max Stress (Sp. A&B): 21.953 ksi Surface Crack: 0.036 in. Bore Crack: 0.064 in.

Experiment Run Data

Spectrum	EFH	Crack Length (in.)			Comments
		Front	Bore	Back	
A	0	0.036	0.064		150 kip/s
	5697.86	0.039	0.069		
	11386.16	0.043	0.070		
	17492.24	0.048	0.073		
	26767.95	0.055	0.078		
	35850.07	0.065	0.088		
	37998.09	0.066	0.090		
B	0	0.066	0.090		100 kip/s
	124387	0.068	0.093		
	246174	0.071	0.094		
	371934	0.073	0.097		
	501119	0.073	0.099		

GT270KB003-13-7 Fatigue Crack Growth Data Sheet

Width: 4.003 in. Thick: 0.1245 in. Area: 0.498 in^2

Pre-crack Information

Pre-crack Date: 6/6/13 Loading Condition: Constant Amplitude R=0.05

Hole Dia.: 0.157 in. Surface EDM: 0.0253 in.

Pre-crack Tuning Data

Tuning Step	Frequency (Hz)	Tuning Cycles	Max Stress (ksi)
1	13	350	37.5
2	15	832	24
3	18	410	15.4

Pre-crack Run Data

Cycles	Stress (ksi)	Frequency (Hz)	Crack Length (in.)
0	0	0	0.1038
38424	37.5	13	0.1187
62624	30	13	0.1330
106732	24	15	0.1478
154756	19.2	15	0.1568
219891	15.4	18	0.1637

Experiment Information

Exp. Date: 8/24/13 Loading Condition: Variable Amplitude

Exp. Type: Spec. A Loading Rate: 100 to 150kip/s Hole Dia.: 0.253 in.

Max Stress (Sp. A): 21.953 ksi Surface Crack: 0.040 in. Bore Crack: 0.076 in.

Experiment Run Data

Spectrum	EFH	Crack Length (in.)			Comments
		Front	Bore	Back	
A	0	0.040	0.076		100 kip/s
	2859.62	0.041	0.077		
	5260.20	0.041	0.077		150 kip/s
	22985.25	0.053	0.092		
	39056.60	0.067	0.106		
	52335.35	0.082	0.125	0.020	
	68996.72	0.101		0.075	
	84989.02	0.124		0.115	
	100052.62	0.150		.153	
	119197.68	0.191		0.203	
	135309.67	0.233		0.247	
	148845.95	0.273		0.289	

Continued on the next page

Spectrum	EFH	Crack Length (in.)			Comments
		Front	Bore	Back	
A	167102.83	0.334		0.352	
	182659.39	0.395		0.412	
	196825.52	0.455		0.474	
	215270.53	0.549		0.567	
	230360.42	0.638		0.655	
	244995.32	0.736		0.756	
	258654.02	0.846		0.862	Rebalance
	265458.86	0.905		0.921	Load Cell
	279101.18	1.020		1.035	Rebalance
	298946.59	1.262		1.275	Load Cell
	306206.81	1.378		1.374	
	311863.55	1.498		1.491	Back
	317324.04	1.683		1.664	Microscope
	318635.21	1.771		1.796	Malfunction
	318796.41	1.869		1.869	

GT270KB003-13-8 Fatigue Crack Growth Data Sheet

Width: 4.003 in. Thick: 0.124 in. Area: 0.496 in^2

Pre-crack Information

Pre-crack Date: 6/6/13 Loading Condition: Constant Amplitude R=0.05

Hole Dia.: 0.156 in. Surface EDM: 0.0279 in.

Pre-crack Tuning Data

Tuning Step	Frequency (Hz)	Tuning Cycles	Max Stress (ksi)
1	13	937	37.5
2	15	1700	24
3	18	383	15.4

Pre-crack Run Data

Cycles	Stress (ksi)	Frequency (Hz)	Crack Length (in.)
0	0	0	0.1059
38130	37.5	13	0.1227
60172	30	13	0.1369
97933	24	15	0.1527
138001	19.2	15	0.1610
191535	15.4	18	0.1664

Experiment Information

Exp. Date: 2/10/14 Loading Condition: Variable Amplitude

Exp. Type: Spec. A&B1 Loading Rate: 200 to 500 kip/s Hole Dia.: 0.256 in.

Max Stress (Sp. A&B): 21.953 ksi Surface Crack: 0.034 in. Bore Crack: 0.079 in.

Experiment Run Data

Spectrum	EFH	Crack Length (in.)			Comments
		Front	Bore	Back	
A	0	0.040	0.079		500 kip/s
	485.00	0.042	0.081		
	6532.19	0.045	0.083		
	13961.59	0.050	0.087		
	22326.25	0.057	0.091		
	26544.85	0.061	0.094		
B	0	0.061	0.094		
	94951.50	0.066	0.095		200 kip/s to reduce error
	178876.00	0.072	0.107		
	270864.79	0.078	0.110		

GT270KB003-13-9 Fatigue Crack Growth Data Sheet

Width: 4.004 in. Thick: 0.1245 in. Area: 0.498 in^2

Pre-crack Information

Pre-crack Date: 6/11/13 Loading Condition: Constant Amplitude R=0.05

Hole Dia.: 0.157 in. Surface EDM: 0.0275 in.

Pre-crack Tuning Data

Tuning Step	Frequency (Hz)	Tuning Cycles	Max Stress (ksi)
1	13	688	37.5
2	15	1924	24
3	18	223	15.4

Pre-crack Run Data

Cycles	Stress (ksi)	Frequency (Hz)	Crack Length (in.)
0	0	0	0.1060
34752	37.5	13	0.1222
57045	30	13	0.1359
94318	24	15	0.1507
136224	19.2	15	0.1603
201320	15.4	18	0.1679

Experiment Information

Exp. Date: 9/14/13 Loading Condition: Variable Amplitude

Exp. Type: Spec. A&B2 Loading Rate: 100 kip/s Hole Dia.: 0.255 in.

Max Stress (Sp. A&B): 21.953 ksi Surface Crack: 0.041 in. Bore Crack: 0.069 in.

Experiment Run Data

Spectrum	EFH	Crack Length (in.)			Comments
		Front	Bore	Back	
A	0	0.040	0.069		
	16995.52	0.054	0.079		
	29381.79	0.066	0.087		
	38063.86	0.075	0.096		
	45886.61	0.085	0.105		
	47109.23	0.086	0.106		
B	0	0.086	0.106		
	37267.90	0.089	0.109		
	63537.18	0.092	0.113		
	92216.88	0.093	0.116		
	112156.03	0.096	0.117		

GT270KB003-13-10 Fatigue Crack Growth Data Sheet

Width: 4.002 in. Thick: 0.124 in. Area: 0.496 in^2

Pre-crack Information

Pre-crack Date: 6/11/13 Loading Condition: Constant Amplitude R=0.05

Hole Dia.: 0.157 in. Surface EDM: 0.0275 in.

Pre-crack Tuning Data

Tuning Step	Frequency (Hz)	Tuning Cycles	Max Stress (ksi)
1	13	2575	37.5
2	15	327	24
3	18	881	15.4

Pre-crack Run Data

Cycles	Stress (ksi)	Frequency (Hz)	Crack Length (in.)
0	0	0	0.1060
35670	37.5	13	0.1214
60268	30	13	0.1388
87563	24	15	0.1510
120311	19.2	15	0.1599
174995	15.4	18	0.1680

Experiment Information

Exp. Date: 9/19/13 Loading Condition: Variable Amplitude

Exp. Type: Spec. A&B2 Loading Rate: 100 kip/s Hole Dia.: 0.255 in.

Max Stress (Sp. A&B): 21.953 ksi Surface Crack: 0.043in. Bore Crack: 0.075 in.

Experiment Run Data

Spectrum	EFH	Crack Length (in.)			Comments
		Front	Bore	Back	
A	0	0.043	0.075		
	10049.92	0.052	0.077		
	20994.60	0.063	0.084		
	31833.67	0.075	0.088		
	40897.89	0.085	0.103		
	44327.75	0.089	0.107		
B	0	0.089	0.107		
	19453.21	0.090	0.113		
	42645.85	0.092	0.118		
	62569.66	0.094	0.118		
	82260.81	0.097	0.118		
	102329.90	0.098	0.121		

GT270KB003-13-11 Fatigue Crack Growth Data Sheet

Width: 4.001 in. Thick: 0.124 in. Area: 0.496 in^2

Pre-crack Information

Pre-crack Date: 6/12/13 Loading Condition: Constant Amplitude R=0.05

Hole Dia.: 0.157 in. Surface EDM: 0.0263 in.

Pre-crack Tuning Data

Tuning Step	Frequency (Hz)	Tuning Cycles	Max Stress (ksi)
1	13	841	37.5
2	15	539	24
3	18	1133	15.4

Pre-crack Run Data

Cycles	Stress (ksi)	Frequency (Hz)	Crack Length (in.)
0	0	0	0.1048
42758	37.5	13	0.1199
69354	30	13	0.1347
108354	24	15	0.1489
158150	19.2	15	0.1581
230195	15.4	18	0.1662

Experiment Information

Exp. Date: SwRI 01/14 Loading Condition: Variable Amplitude

Exp. Type: Spec. A&B2 Loading Rate: 100 kip/s Hole Dia.: 0.251 in.

Max Stress (Sp. A&B): 21.953 ksi Surface Crack: 0.166in. Bore Crack: 0.084 in.

Experiment Run Data

Spectrum	EFH	Crack Length (in.)			Comments
		Front	Bore	Back	
A	0	0.041	0.084		
	286.89	0.042	0.089		
	573.79	0.042	0.093		
	860.68	0.042	0.098		
	1147.57	0.043	0.104		
	1291.02	0.043	0.106		
B	0	0.043	0.106		
	187315.50	0.048	0.107		
	275827.70	0.053	0.109		
	367340.00	0.058	0.118		
	413096.10	0.060	0.125	0.005	
	458852.20	0.063		0.022	

Continued on the next page

Spectrum	EFH	Crack Length (in.)			Comments
		Front	Bore	Back	
B	504608.30	0.065		0.030	
	550364.50	0.067		0.039	
	584462.80	0.069		0.044	
	641876.70	0.073		0.054	
	687632.80	0.076		0.060	
	733388.90	0.079		0.067	
	779145.10	0.084		0.074	
	824901.20	0.085		0.079	
	870657.30	0.088		0.086	
	916413.40	0.096		0.092	
	962169.50	0.096		0.099	
	1007926.00	0.100		0.105	
	1053682.00	0.104		0.110	
	1099438.00	0.109		0.116	
	1145194.00	0.112		0.122	
	1190950.00	0.116		0.128	
	1236706.00	0.120		0.134	
	1282462.00	0.125		0.140	
	1328218.00	0.129		0.146	
	1373975.00	0.135		0.152	
	1419731.00	0.139		0.158	

Due to the uncertainty that occurred during the data recording with this test specimen the data was not used for analysis purposes.

GT270KB003-13-12 Fatigue Crack Growth Data Sheet

Width: 4.003 in. Thick: 0.125 in. Area: 0.500 in^2

Pre-crack Information

Pre-crack Date: 6/14/13 Loading Condition: Constant Amplitude R=0.05

Hole Dia.: 0.157 in. Surface EDM: 0.0263 in.

Pre-crack Tuning Data

Tuning Step	Frequency (Hz)	Tuning Cycles	Max Stress (ksi)
1	13	1933	37.5
2	15	575	24
3	18	853	15.4

Pre-crack Run Data

Cycles	Stress (ksi)	Frequency (Hz)	Crack Length (in.)
0	0	0	0.1048
33275	37.5	13	0.1228
53135	30	13	0.1363
80881	24	15	0.1494
109655	19.2	15	0.1586
154643	15.4	18	0.1644

Experiment Information

Exp. Date: SwRI 01/14 Loading Condition: Variable Amplitude

Exp. Type: Spec. A&B3 Loading Rate: 100 kip/s Hole Dia.: 0.253 in.

Max Stress (Sp. A&B): 21.953 ksi Surface Crack: 0.043in. Bore Crack: 0.079 in.

Experiment Run Data

Spectrum	EFH	Crack Length (in.)			Comments
		Front	Bore	Back	
A	0	0.043	0.079		
	2868.93	0.043	0.089		
	5737.85	0.047	0.094		
	11475.70	0.048	0.097		
	20082.48	0.057	0.103		
	28689.26	0.065	0.109		
	37296.04	0.075	0.125		
B	0	0.075	0.125		
	91512.24	0.083		0.012	
	217561.66	0.091		0.041	
	411805.08	0.104		0.072	
	594829.56	0.122		0.097	

Continued onto next page

Spectrum	EFH	Crack Length (in.)			Comments
		Front	Bore	Back	
B	777854.04	0.141		0.123	
	960878.52	0.162		0.150	
	1143903.00	0.186		0.177	
	1326927.48	0.213		0.206	
	1509951.96	0.242		0.237	
	1692976.44	0.275		0.271	
	1876000.92	0.309		0.307	
	2059025.40	0.348		0.347	
	2242049.87	0.388		0.387	
	2425074.35	0.431		0.43	
	2608098.83	0.478		0.477	
	2791123.31	0.528		0.528	
	2974147.79	0.584		0.583	
	3157172.27	0.645		0.645	

GT270KB003-13-13 Fatigue Crack Growth Data Sheet

Width: 4.003 in. Thick: 0.1245 in. Area: 0.498 in^2

Pre-crack Information

Pre-crack Date: 6/17/13 Loading Condition: Constant Amplitude R=0.05

Hole Dia.: 0.157 in. Surface EDM: 0.0275 in.

Pre-crack Tuning Data

Tuning Step	Frequency (Hz)	Tuning Cycles	Max Stress (ksi)
1	13	1299	37.5
2	15	495	24
3	18	1686	15.4

Pre-crack Run Data

Cycles	Stress (ksi)	Frequency (Hz)	Crack Length (in.)
0	0	0	0.1060
43161	37.5	13	0.1237
63551	30	13	0.1359
100966	24	15	0.1513
141206	19.2	15	0.1602
197463	15.4	18	0.1671

Experiment Information

Exp. Date: 2/17/14 Loading Condition: Variable Amplitude

Exp. Type: Spec. A&B3 Loading Rate: 100 kip/s Hole Dia.: 0.252 in.

Max Stress (Sp. A&B): 21.953 ksi Surface Crack: 0.042in. Bore Crack: 0.080 in.

Experiment Run Data

Spectrum	EFH	Crack Length (in.)			Comments
		Front	Bore	Back	
A	0	0.042	0.080		
	16794.60	0.055	0.092		
	30331.40	0.065	0.097		
	43958.80	0.078	0.114		
	47717.70	0.083	0.124		
B	0.	0.083	0.124	0.003	
	4710.40	0.085		0.016	
	59157.70	0.087		0.028	
	123226.30	0.093		0.044	
	169943.60	0.096		0.048	

GT270KB003-13-14 Fatigue Crack Growth Data Sheet

Width: 4.001 in. Thick: 0.124 in. Area: 0.496 in^2

Pre-crack Information

Pre-crack Date: 6/17/13 Loading Condition: Constant Amplitude R=0.05

Hole Dia.: 0.158 in. Surface EDM: 0.0295 in.

Pre-crack Tuning Data

Tuning Step	Frequency (Hz)	Tuning Cycles	Max Stress (ksi)
1	10	2400	37.5
2	15	524	24
3	18	337	15.4

Pre-crack Run Data

Cycles	Stress (ksi)	Frequency (Hz)	Crack Length (in.)
0	0	0	0.1085
37026	37.5	10	0.1248
59778	30	10	0.1379
103860	24	15	0.1539
144403	19.2	15	0.1620
204573	15.4	18	0.1684

Experiment Information

Exp. Date: 8/23/13 Loading Condition: Variable Amplitude

Exp. Type: Spec. A&B3 Loading Rate: 100 kip/s Hole Dia.: 0.255 in.

Max Stress (Sp. A&B): 21.953 ksi Surface Crack: 0.043in. Bore Crack: 0.075 in.

Experiment Run Data

Spectrum	EFH	Crack Length (in.)			Comments
		Front	Bore	Back	
A	0	0.043	0.082		100 kip/s
	5904.84	0.044	0.089		
	15502.10	0.051	0.097		
	29465.78	0.062	0.109		
	39610.59	0.073	0.125		
B	0	0.073	0.125	0.016	75 kip/s
	10111.42	0.073		0.019	
	21657.97	0.074		0.024	100 kip/s
	31714.48	0.074		0.025	Error recording error data
	52194.01	0.077		0.031	
	70644.48	0.079		0.034	
	90735.30	0.080		0.037	
	111876.69	0.081		0.041	

GT270KB003-13-15 to 26 Fatigue Crack Growth Data Sheets

These test specimens were reserved for another test and are not included in this report.

GT270KB003-13-27 Fatigue Crack Growth Data Sheet

Width: 4.003 in. Thick: 0.124 in. Area: 0.496 in^2

Pre-crack Information

Pre-crack Date: 7/16/13 Loading Condition: Constant Amplitude R=0.05

Hole Dia.: 0.157 in. Surface EDM: 0.0295 in.

Pre-crack Tuning Data

Tuning Step	Frequency (Hz)	Tuning Cycles	Max Stress (ksi)
1	10	672	37.5
2	15	451	24
3	18	2362	15.4

Pre-crack Run Data

Cycles	Stress (ksi)	Frequency (Hz)	Crack Length (in.)
0	0	0	0.1080
35244	37.5	10	0.1276
53520	30	10	0.1423
80243	24	15	0.1564
103940	19.2	15	0.1624
216223	15.4	18	0.1624

This specimen was not used for testing due to the fact that the experimenter induced a large load between the second to the last and last load shedding step. He did so in an attempt to obtain a more accurate measurement of the crack. During the last load shedding step the experimenter observed that the crack was not growing and concluded that the crack must have arrested.

GT270KB003-13-28 Fatigue Crack Growth Data Sheet

Width: 4.001 in. Thick: 0.124 in. Area: 0.496 in^2

Pre-crack Information

Pre-crack Date: 7/17/13 Loading Condition: Constant Amplitude R=0.05

Hole Dia.: 0.156 in. Surface EDM: 0.0268 in.

Pre-crack Tuning Data

Tuning Step	Frequency (Hz)	Tuning Cycles	Max Stress (ksi)
1	10	1000	37.5
2	15	450	24
3	18	1605	15.4

Pre-crack Run Data

Cycles	Stress (ksi)	Frequency (Hz)	Crack Length (in.)
0	0	0	0.1048
38424	37.5	13	0.1187
62624	30	13	0.1330
106732	24	15	0.1478
154756	19.2	15	0.1568
219891	15.4	18	0.1637

Experiment Information

Exp. Date: NA Loading Condition: Variable Amplitude

Exp. Type: Spec. B Loading Rate: 80 to 100kip/s Hole Dia.: 0.255 in.

Max Stress (Sp. B): 21.953 ksi Surface Crack: 0.044 in. Bore Crack: 0.089 in.

Experiment Run Data

Spectrum	EFH	Crack Length (in.)			Comments
		Front	Bore	Back	
B	0	0.044	0.089		100 kip/s
	166891.79	0.051	0.097		
	451462.59	0.071	0.121		
	613967.28	0.083	0.125	0.042	
	812228.55	0.098		0.078	
	1035320.29	0.120		0.111	
	1260340.20	0.147		0.145	
	1456623.43	0.169		0.176	80 kip/s
	1659405.86	0.196		0.207	Had to slow down due to high error
	1888527.57	0.230		0.243	
	2043777.40	0.254		0.270	
	2250640.59	0.290		0.307	

Continued on the next page

Spectrum	EFH	Crack Length (in.)			Comments
		Front	Bore	Back	
B	2366726.38	0.311		0.327	
	2504731.41	0.339		0.356	
	2707055.36	0.382		0.400	
	2755073.67	0.395		0.411	

GT270KB003-13-29 Fatigue Crack Growth Data Sheet

Width: 4.001 in. Thick: 0.124 in. Area: 0.496 in^2

Pre-crack Information

Pre-crack Date: 7/18/13 Loading Condition: Constant Amplitude R=0.05

Hole Dia.: 0.159 in. Surface EDM: 0.0264 in.

Pre-crack Tuning Data

Tuning Step	Frequency (Hz)	Tuning Cycles	Max Stress (ksi)
1	10	717	37.5
2	15	1392	24
3	18	679	15.4

Pre-crack Run Data

Cycles	Stress (ksi)	Frequency (Hz)	Crack Length (in.)
0	0	0	0.1059
35584	37.5	10	0.1224
58294	30	10	0.1376
94920	24	15	0.1529
129022	19.2	15	0.1607
193587	15.4	18	0.1687

Experiment Information

Exp. Date: SwRI 01/14 Loading Condition: Variable Amplitude

Exp. Type: Spec. B Loading Rate: 100 kip/s Hole Dia.: 0.252 in.

Max Stress (Sp. B): 21.953 ksi Surface Crack: 0.046 in. Bore Crack: 0.075 in.

Experiment Run Data

Spectrum	EFH	Crack Length (in.)			Comments
		Front	Bore	Back	
B	0	0.046	0.075		
	91512.24	0.048	0.098		
	183024.48	0.052	0.102		
	320292.84	0.057	0.105		
	457561.20	0.067	0.111		
	594829.56	0.073	0.121		
	640585.68	0.076	0.125	0.007	
	721333.33	0.081		0.025	
	823610.16	0.088		0.044	
	915122.40	0.095		0.059	
	1006634.64	0.101		0.071	
	1098146.88	0.108		0.085	

Continued on the next page

Spectrum	EFH	Crack Length (in.)			Comments
		Front	Bore	Back	
B	1189659.12	0.117		0.098	
	1223881.49	0.120		0.103	

GT270KB003-13-30 Fatigue Crack Growth Data Sheet

Width: 4.003 in. Thick: 0.123 in. Area: 0.492 in^2

Pre-crack Information

Pre-crack Date: 7/22/13 Loading Condition: Constant Amplitude R=0.05

Hole Dia.: 0.158 in. Surface EDM: 0.0250 in.

Pre-crack Tuning Data

Tuning Step	Frequency (Hz)	Tuning Cycles	Max Stress (ksi)
1	10	396	37.5
2	15	715	24
3	18	8410	15.4

Pre-crack Run Data

Cycles	Stress (ksi)	Frequency (Hz)	Crack Length (in.)
0	0	0	0.1040
45131	37.5	10	0.1205
67917	30	10	0.1349
110346	24	15	0.1533
135828	19.2	15	0.1596
188058	15.4	18	0.1671

Experiment Information

Exp. Date: SwRI 01/14 Loading Condition: Variable Amplitude

Exp. Type: Spec. B Loading Rate: 100kip/s Hole Dia.: 0.251 in.

Max Stress (Sp. B): 21.953 ksi Surface Crack: 0.045 in. Bore Crack: 0.079 in.

Experiment Run Data

Spectrum	EFH	Crack Length (in.)			Comments
		Front	Bore	Back	
B	0	0.045	0.079		
	91512.24	0.046	0.093		
	183024.48	0.049	0.095		
	274536.72	0.052	0.097		
	366048.96	0.057	0.098		
	457561.20	0.063	0.099		
	549073.44	0.067	0.099		
	623477.92	0.071	0.109		
	732097.92	0.079	0.125	0.006	
	823610.16	0.087		0.034	
	915122.40	0.091		0.052	

APPENDIX H

ADDITIONAL CRACK GROWTH CURVES

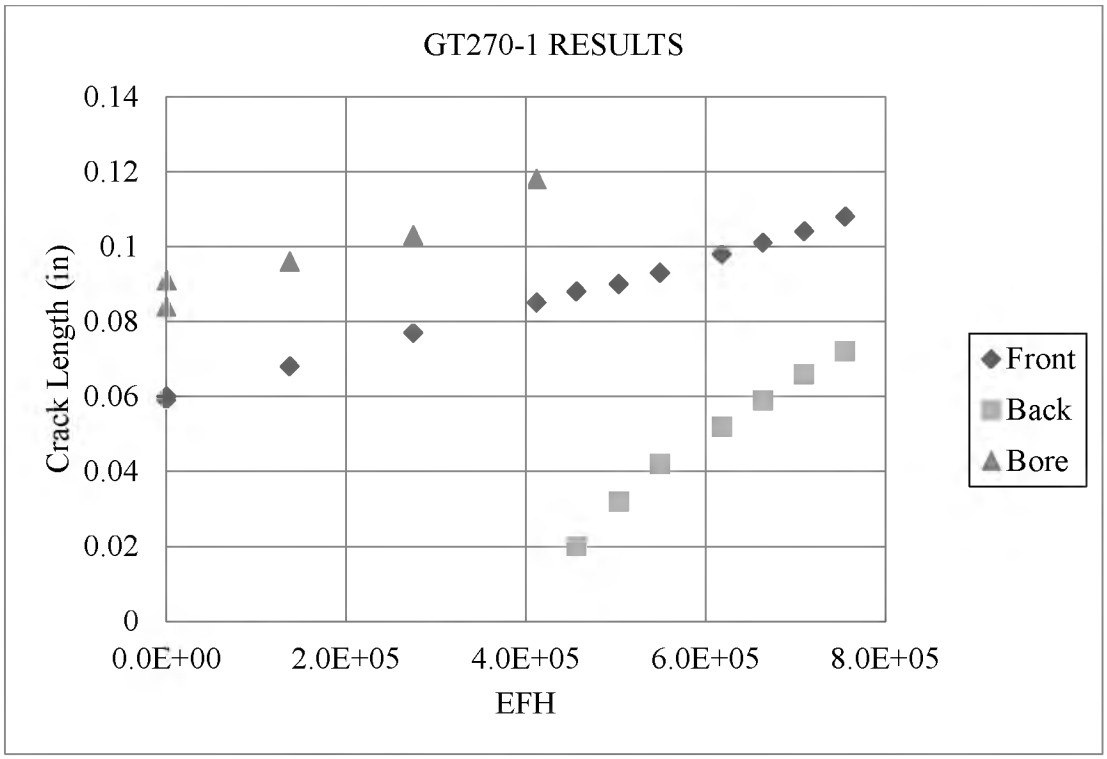

Figure 58 GT270-1 Crack Growth Data

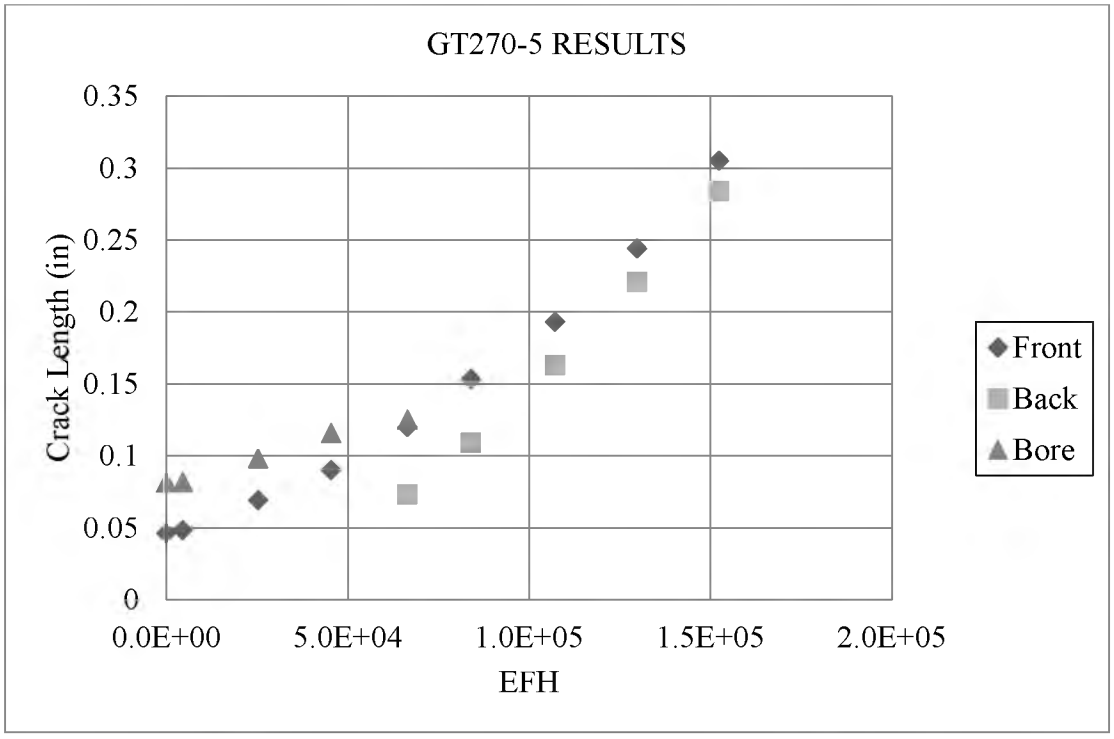

Figure 59 GT270-5 Crack Growth Data

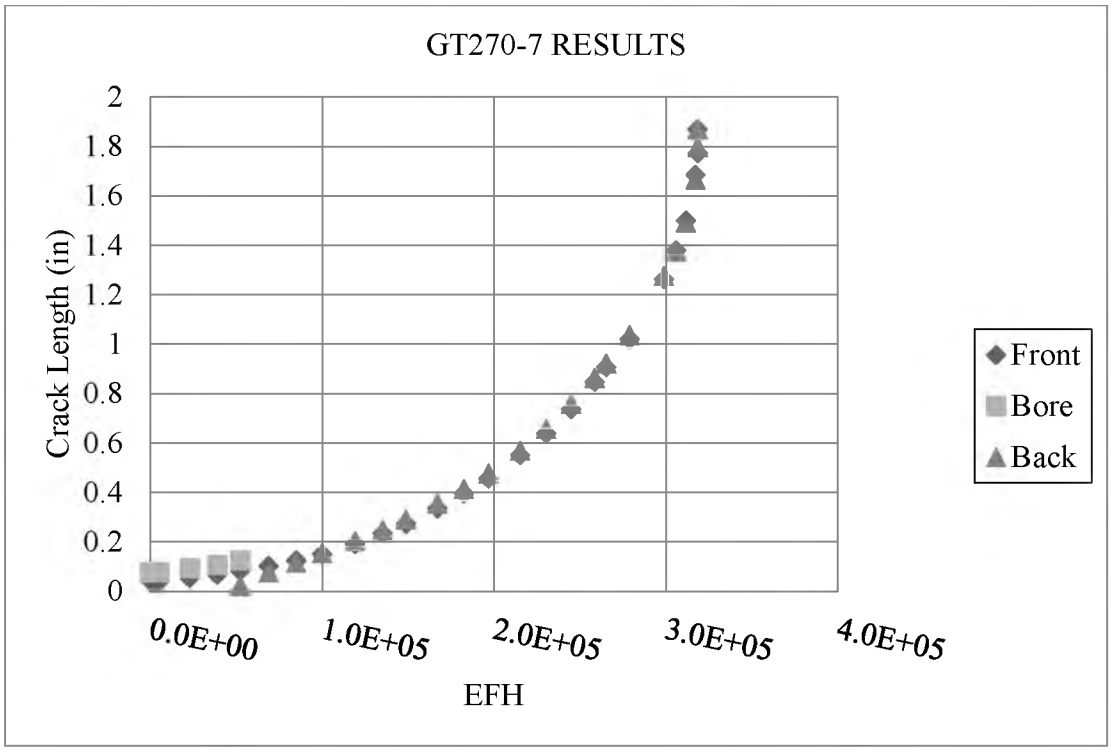

Figure 60 GT270-7 Crack Growth Data

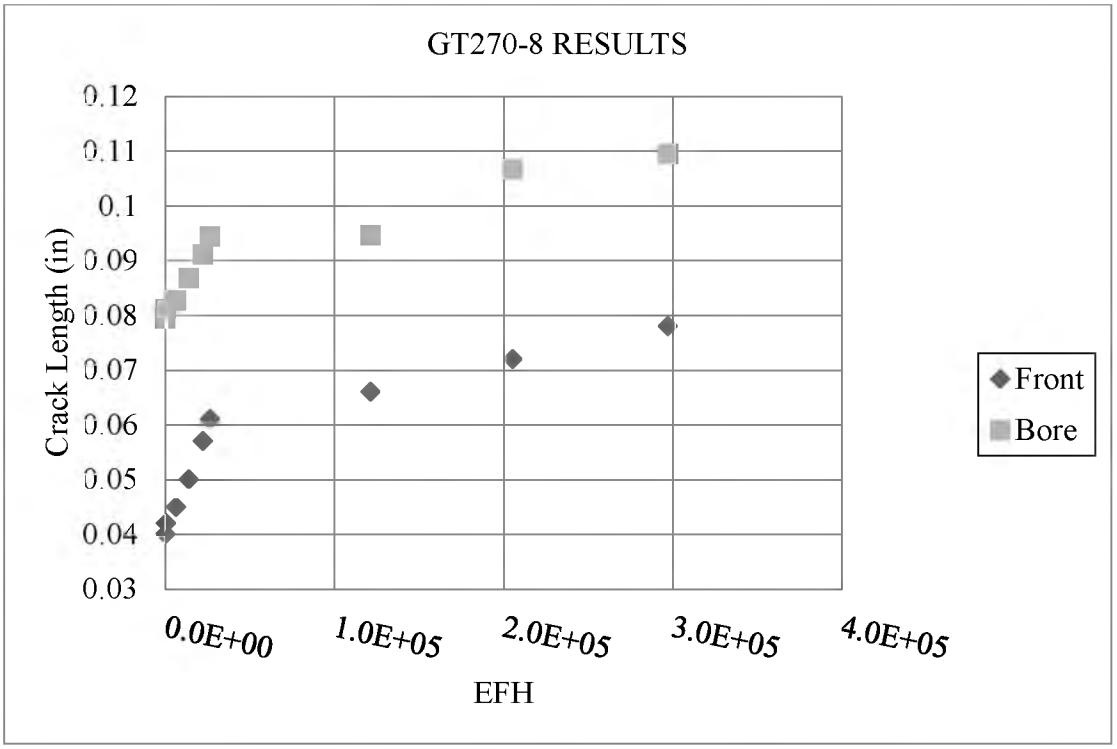

Figure 61 GT270-8 Crack Growth Data

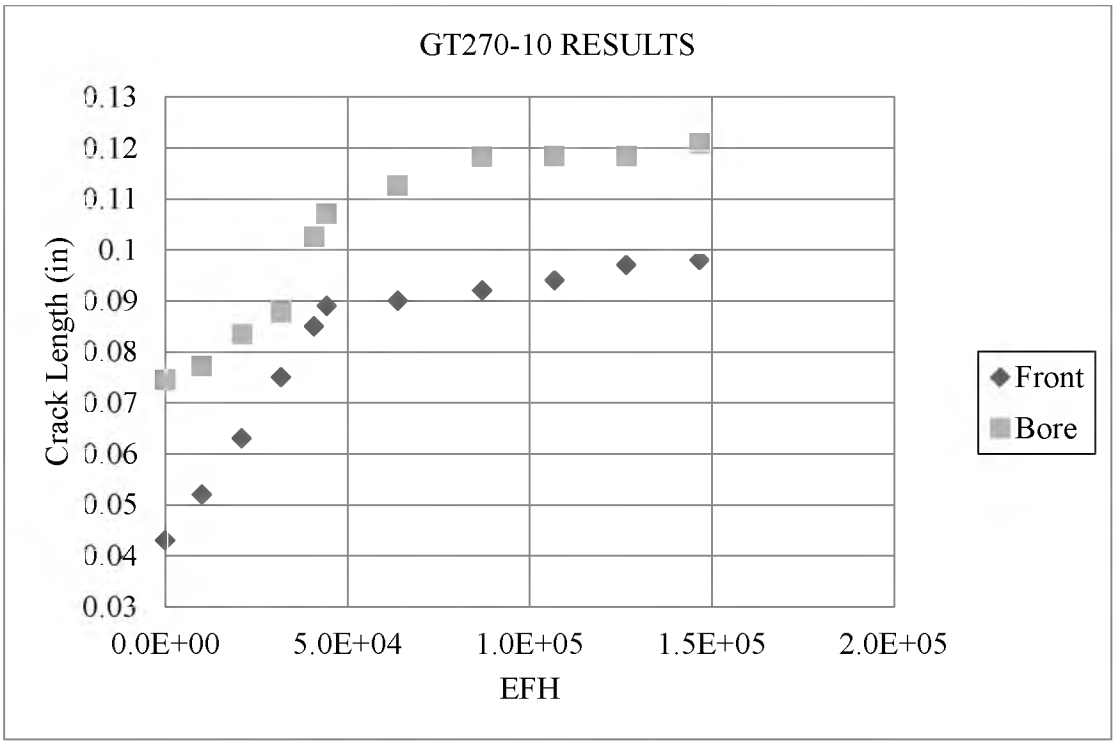

Figure 62 GT270-10 Crack Growth Data

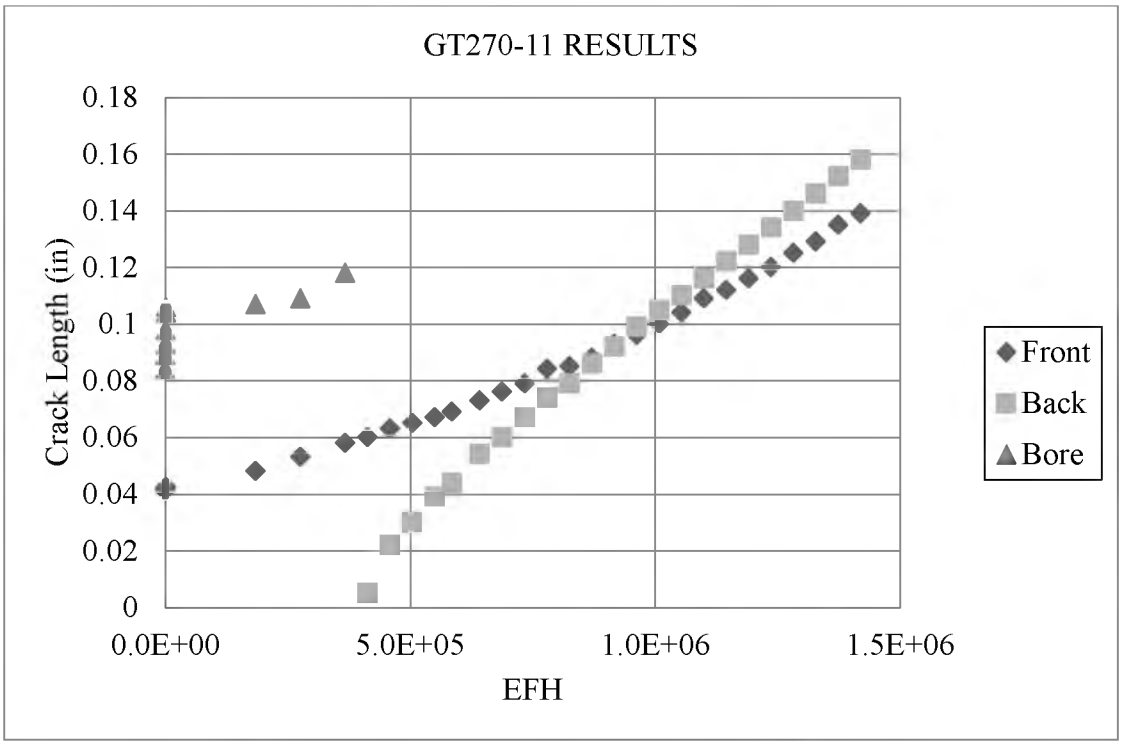

Figure 63 GT270-11 Crack Growth Data

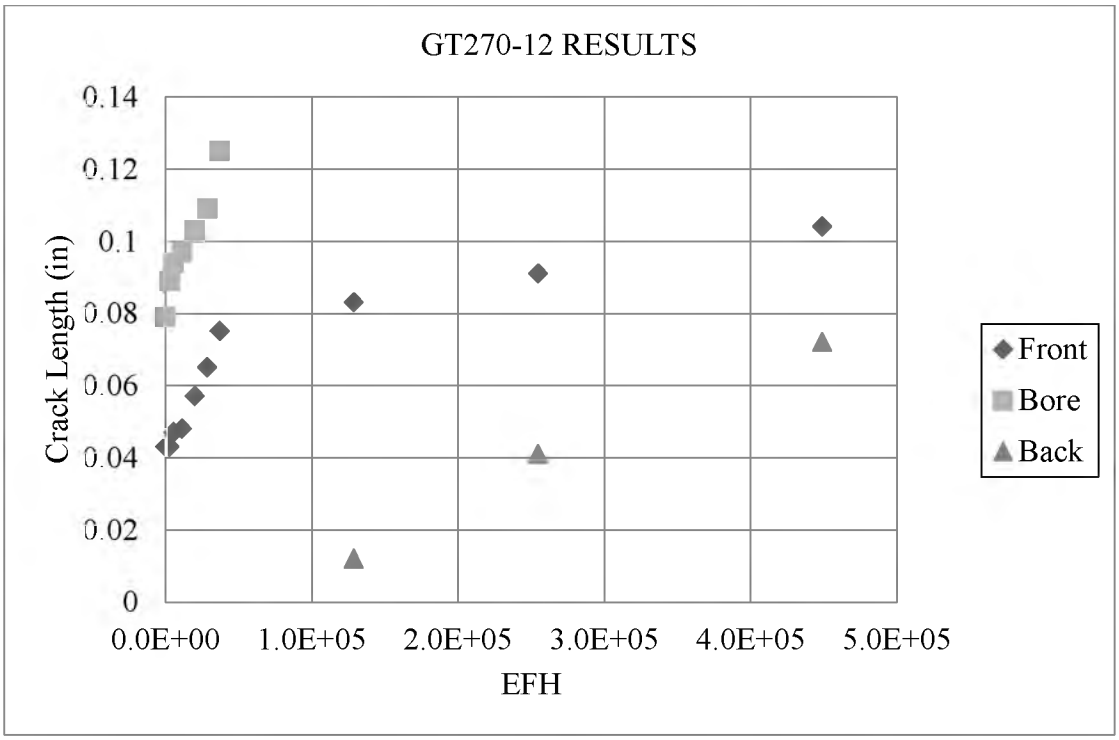

Figure 64 GT270-12 Crack Growth Data

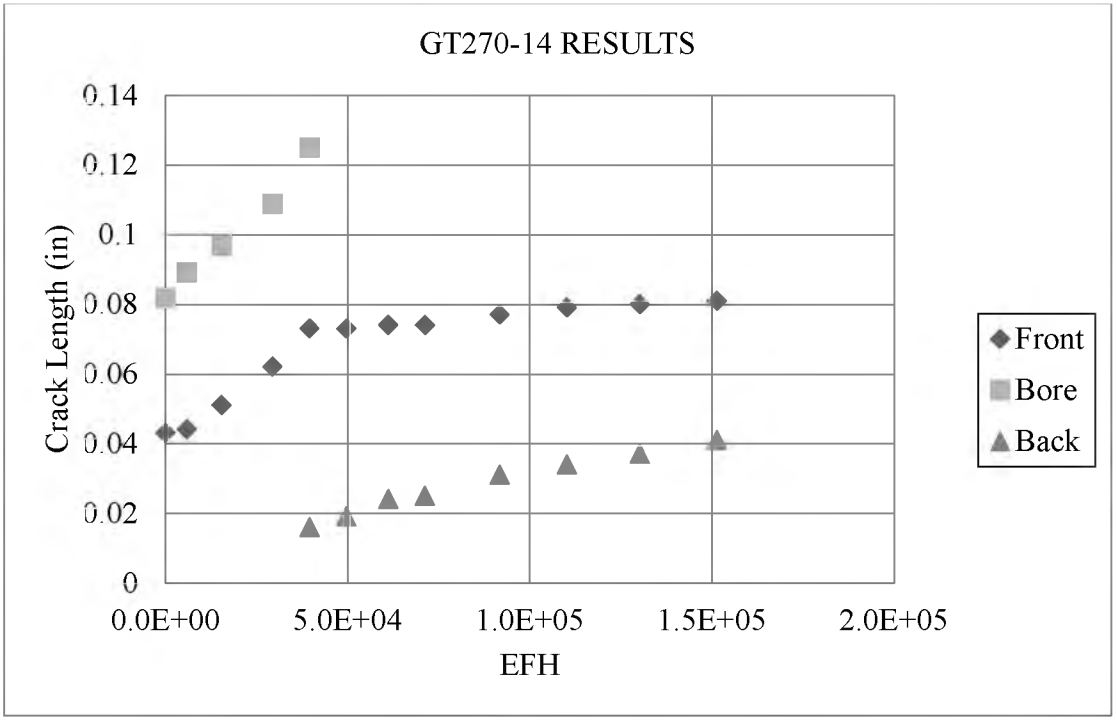

Figure 65 GT270-14 Crack Growth Data

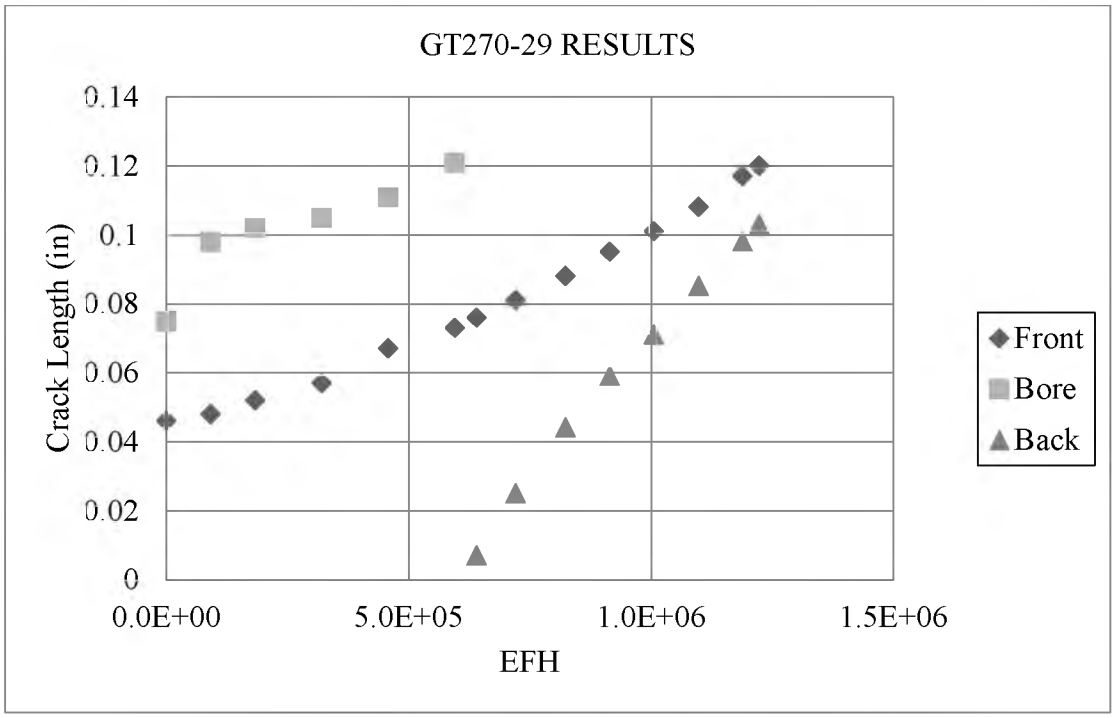

Figure 66 GT270-29 Crack Growth Data

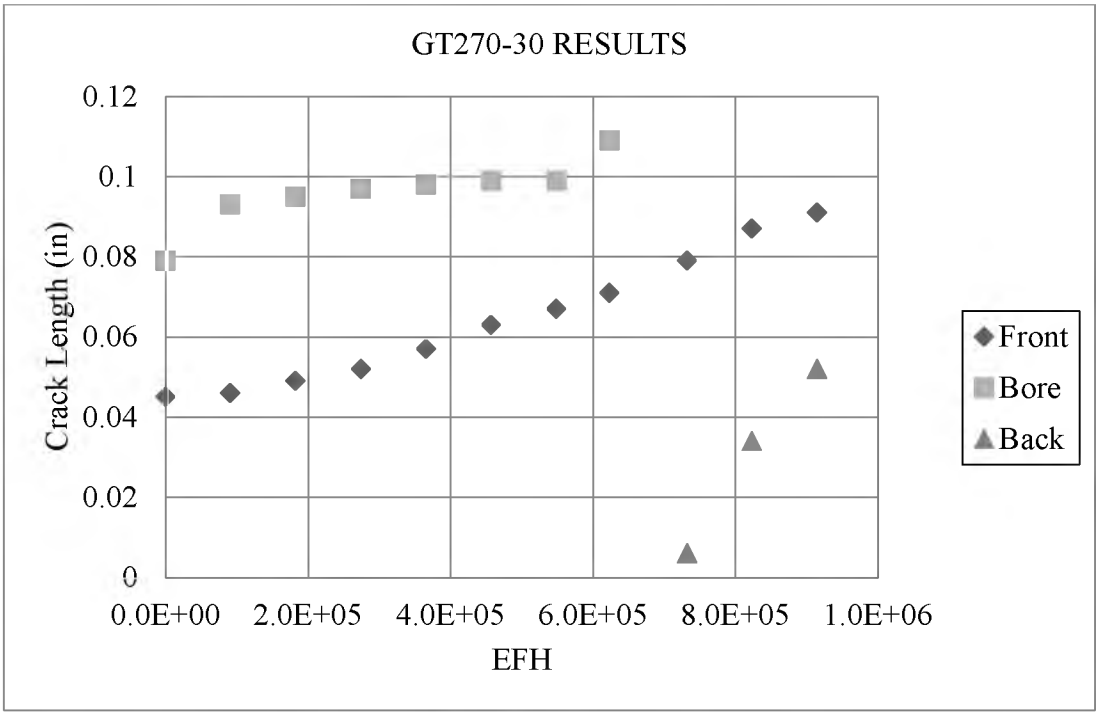

Figure 67 GT270-30 Crack Growth Data

APPENDIX I

ADDITIONAL SEM IMAGES OF TEST SPECIMEN FRACTURE SURFACES

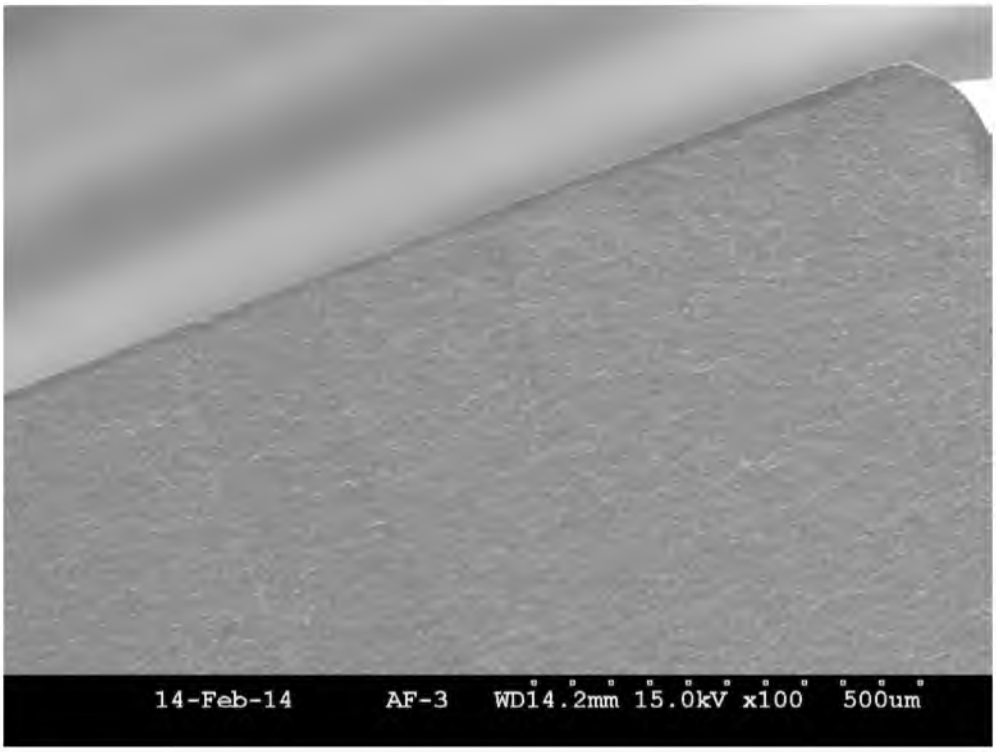

Figure 68 GT270-7 100x Image of the Precrack Load Steps

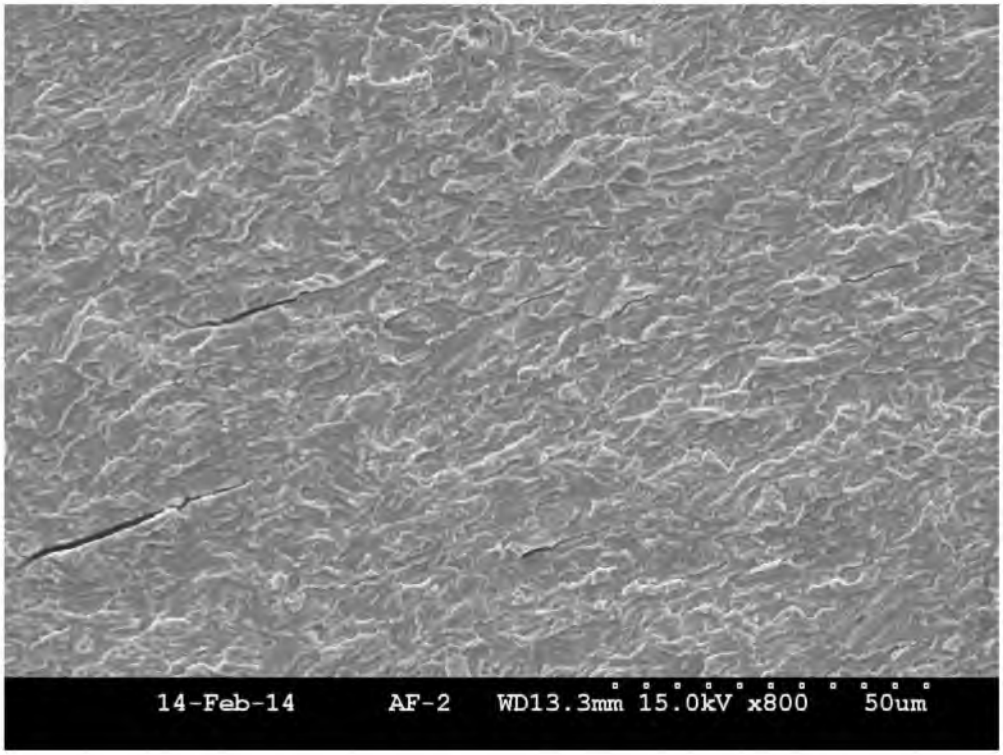

Figure 69 GT270-7 800x Image of Multiple Crack Formations

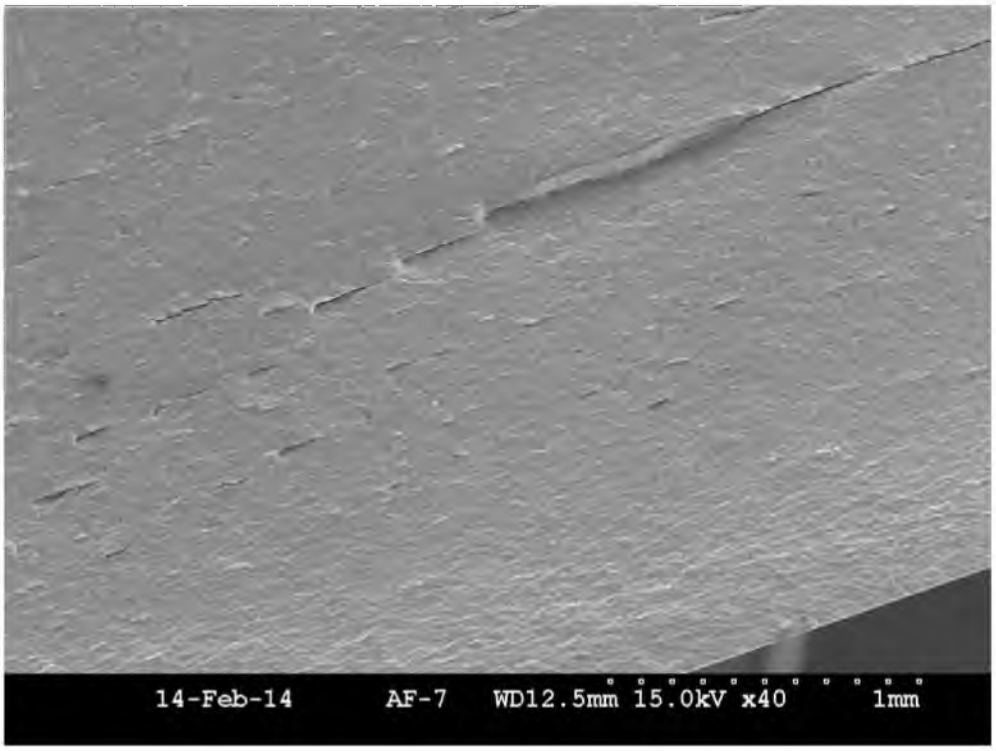

Figure 70 GT270-7 40x Image of Secondary Cracks Near End of Fatigue Crack

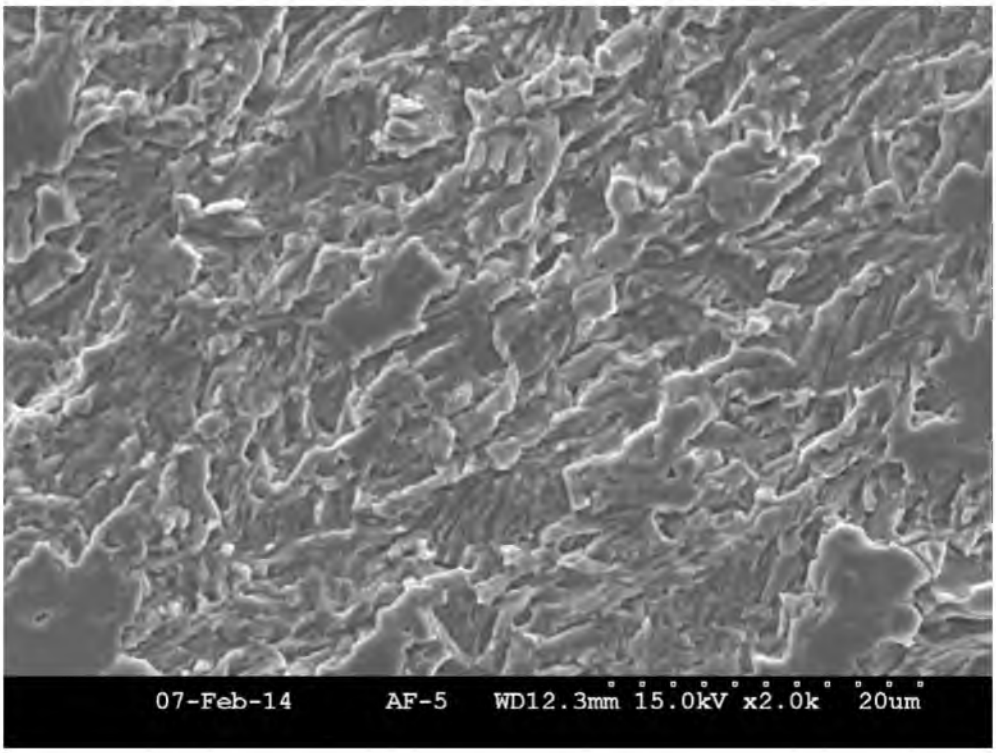

Figure 71 GT270-28 2,000x Precrack Surface Image

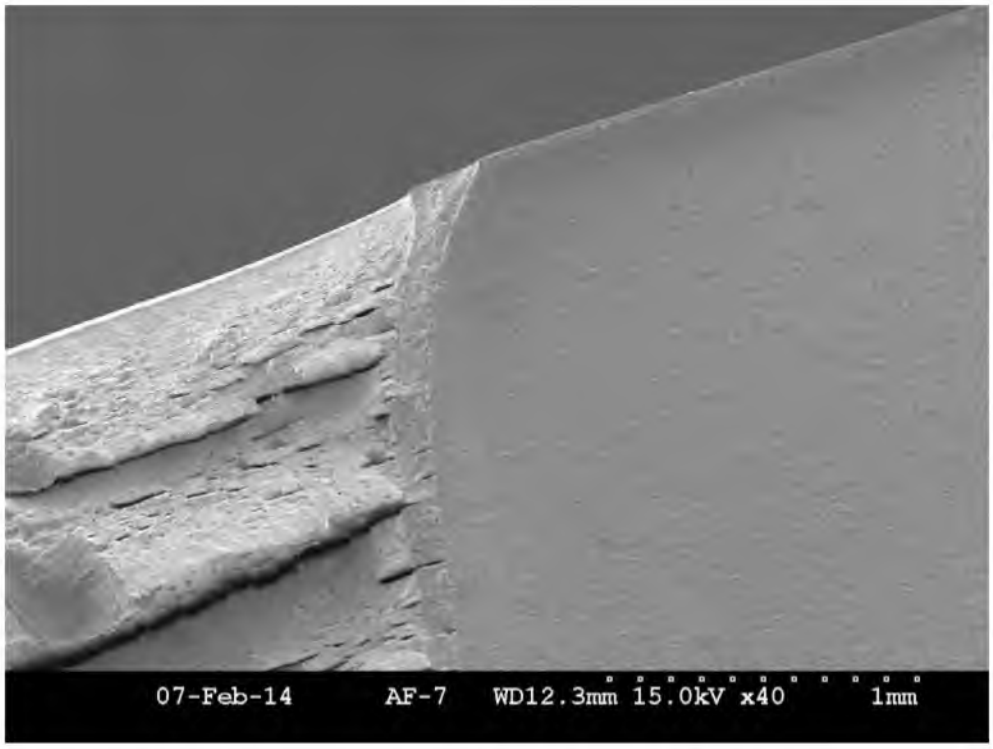

Figure 72 GT270-28 40x End of Fatigue Crack Image

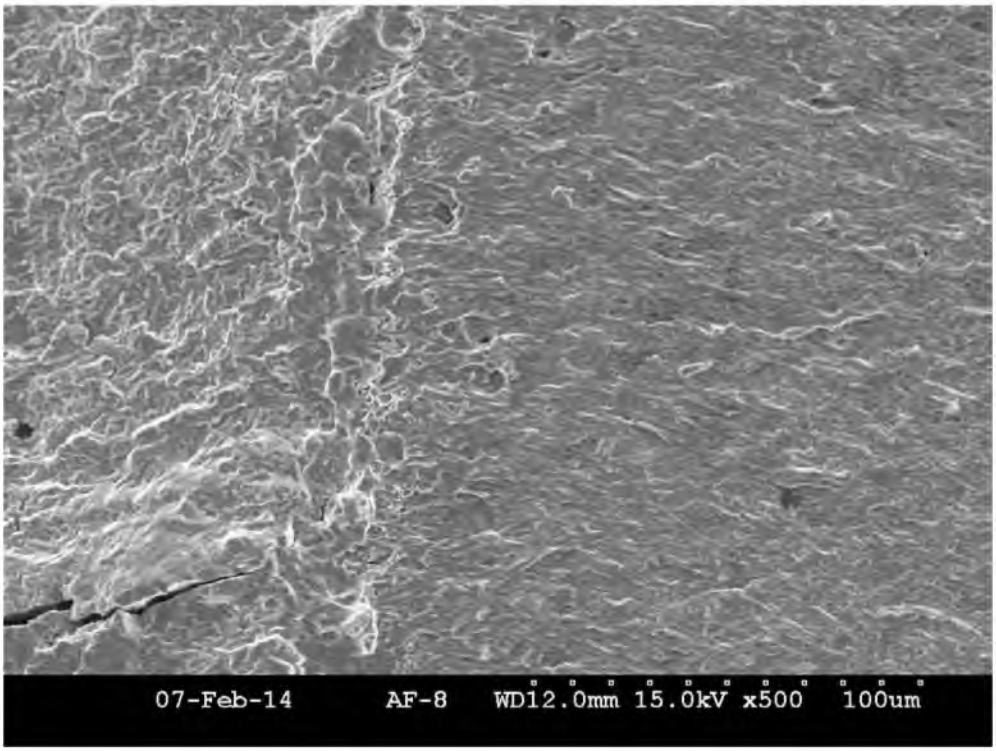

Figure 73 GT270-28 500x End of Fatigue Crack Image

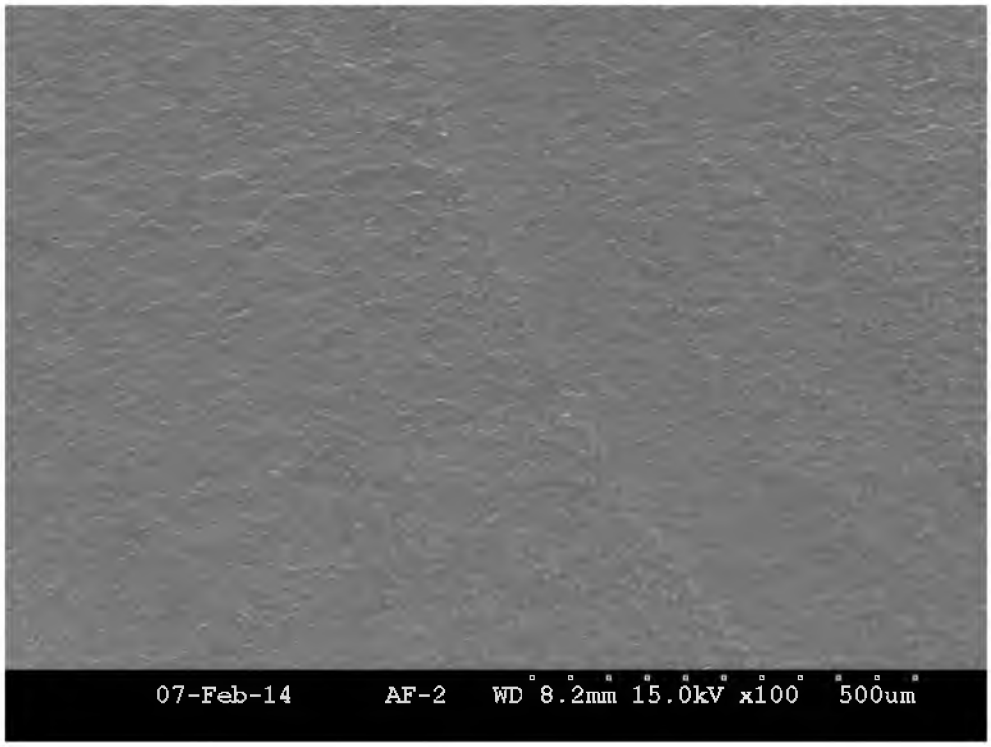

Figure 74 GT270-6 100x Image of Precrack to Spectrum A Transition

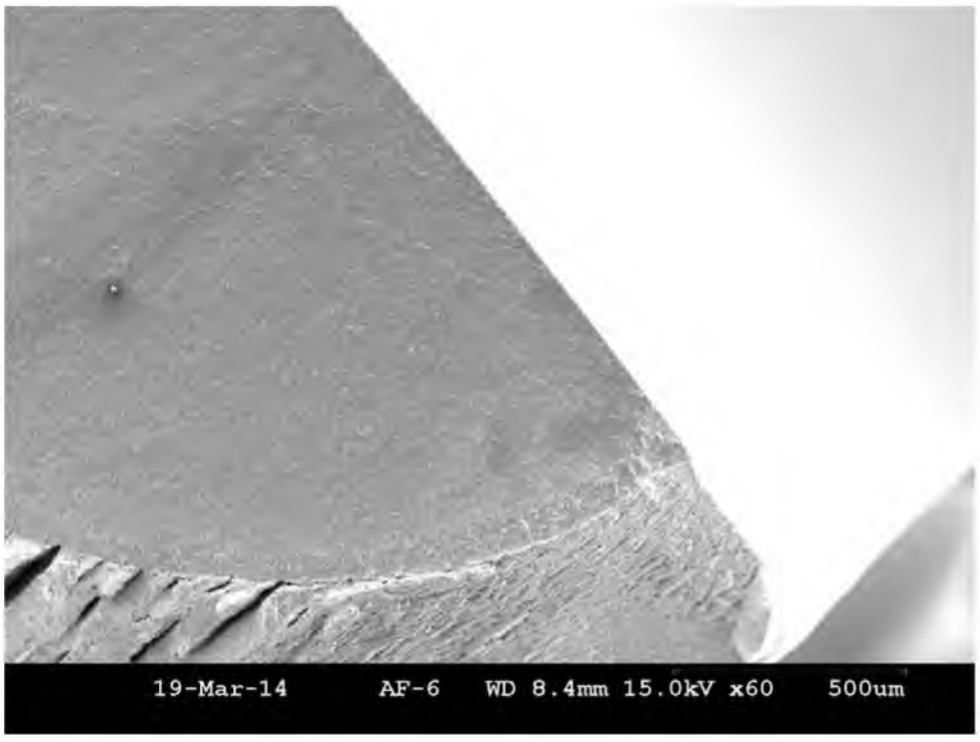

Figure 75 View of GT270-6 Transitions

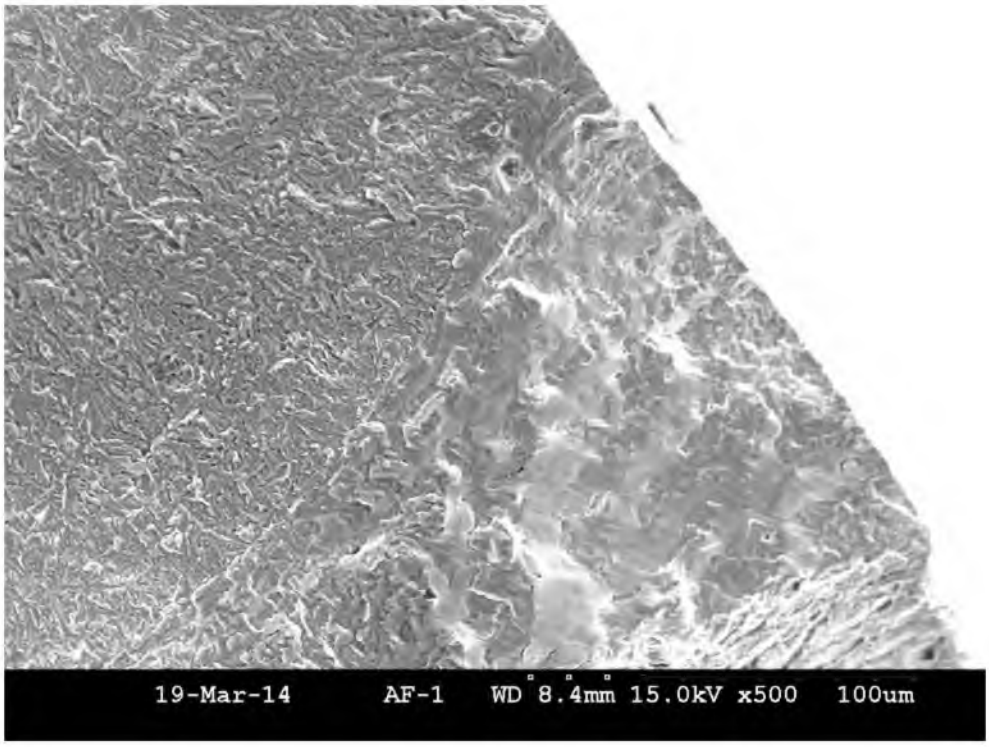

Figure 76 500x View of GT270-6 Transition from Spectrum A to B

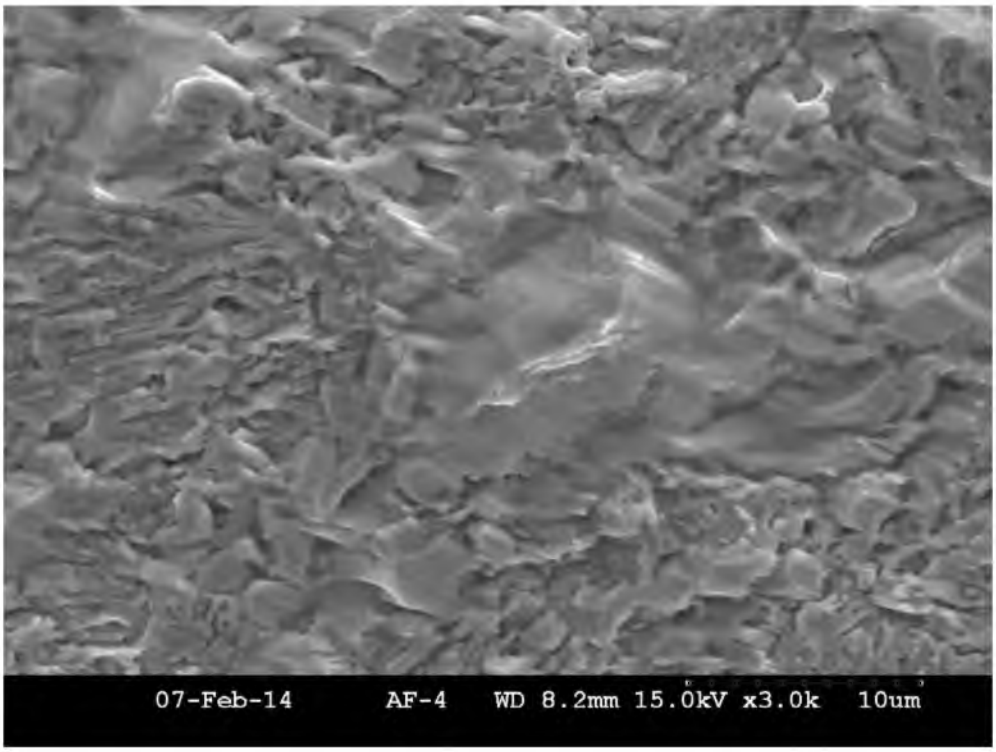

Figure 77 GT270-6 3,000x Image of Spectrum A Striations

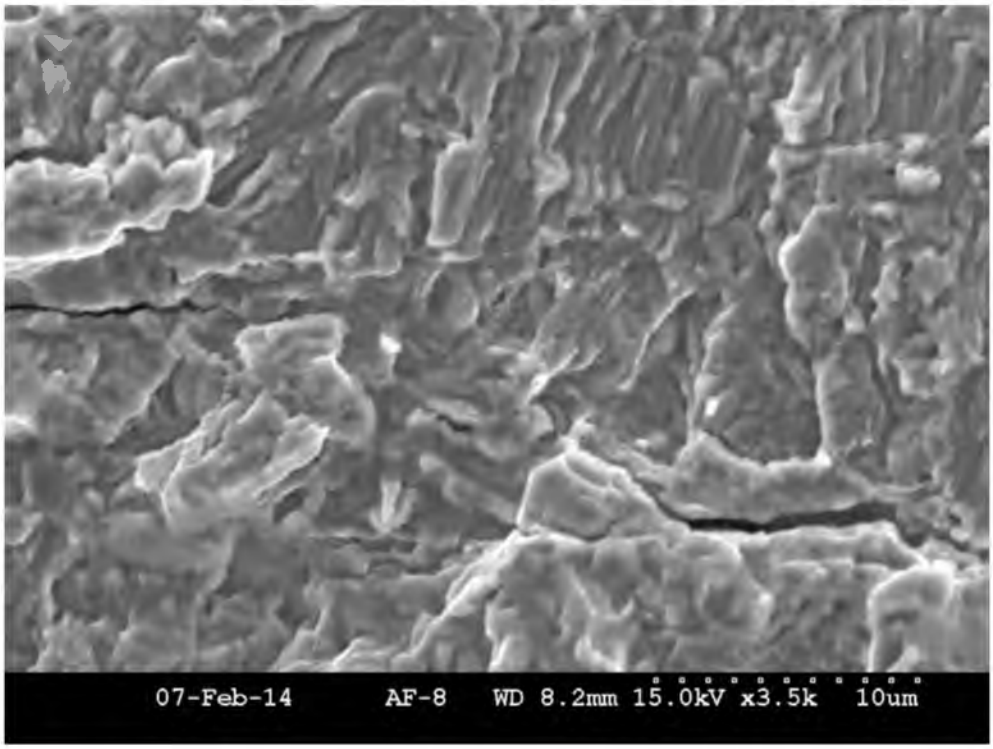

Figure 78 GT270-6 3,500x Image of Spectrum A to B Transition

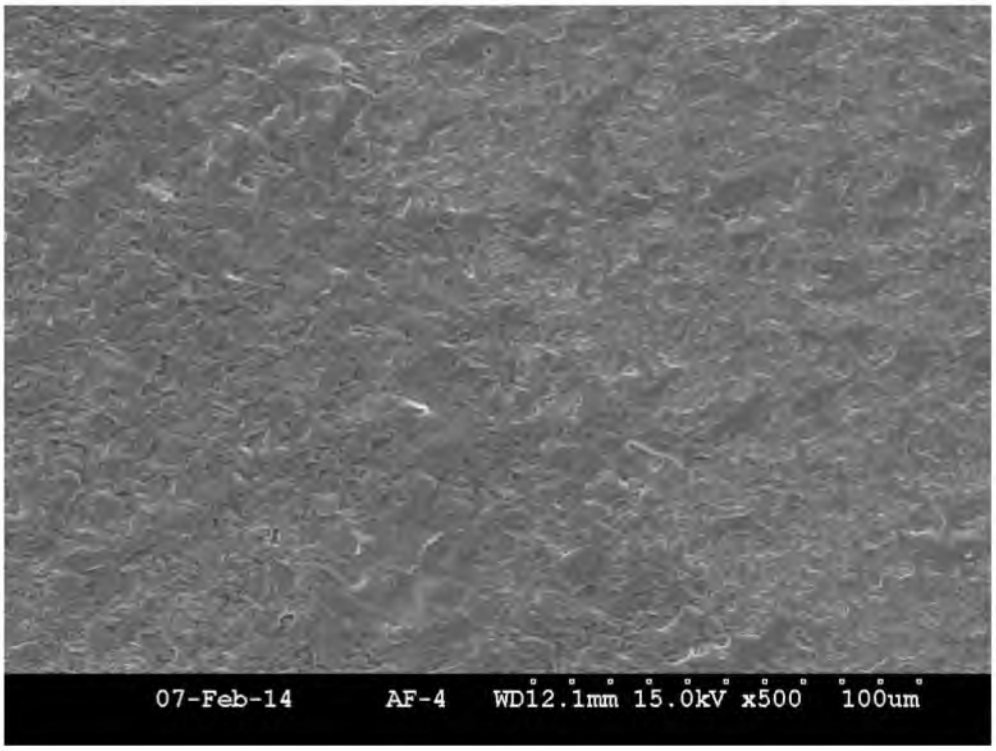

Figure 79 GT270-9 500x Precrack to Spectrum A Transition

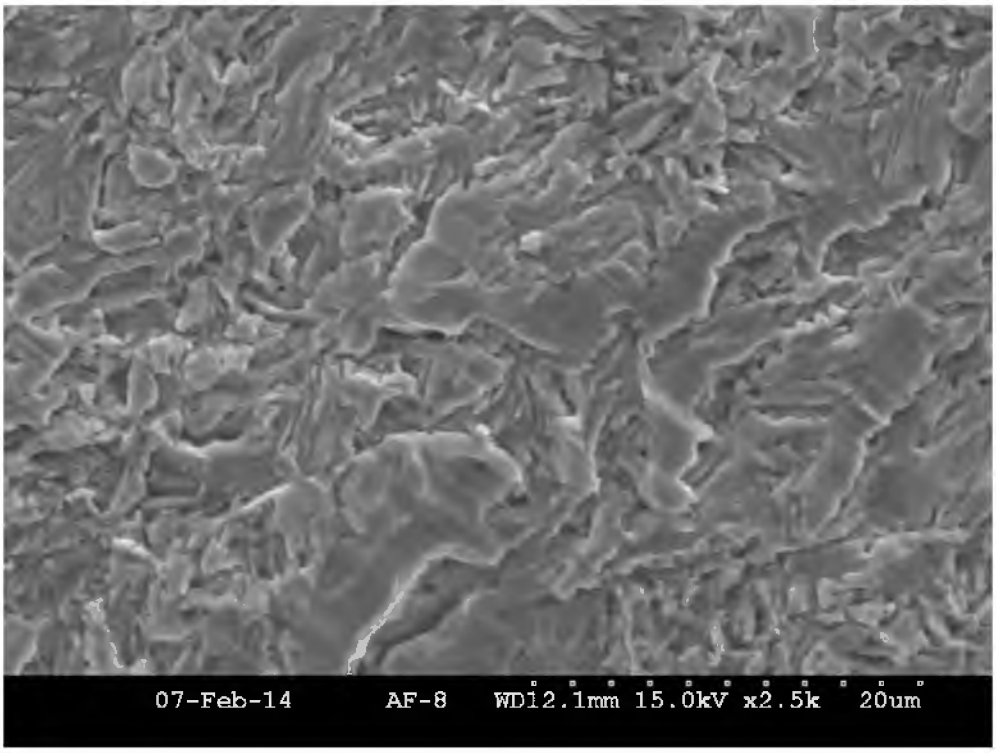

Figure 80 GT270-9 2,500x Image of Spectrum A Striations

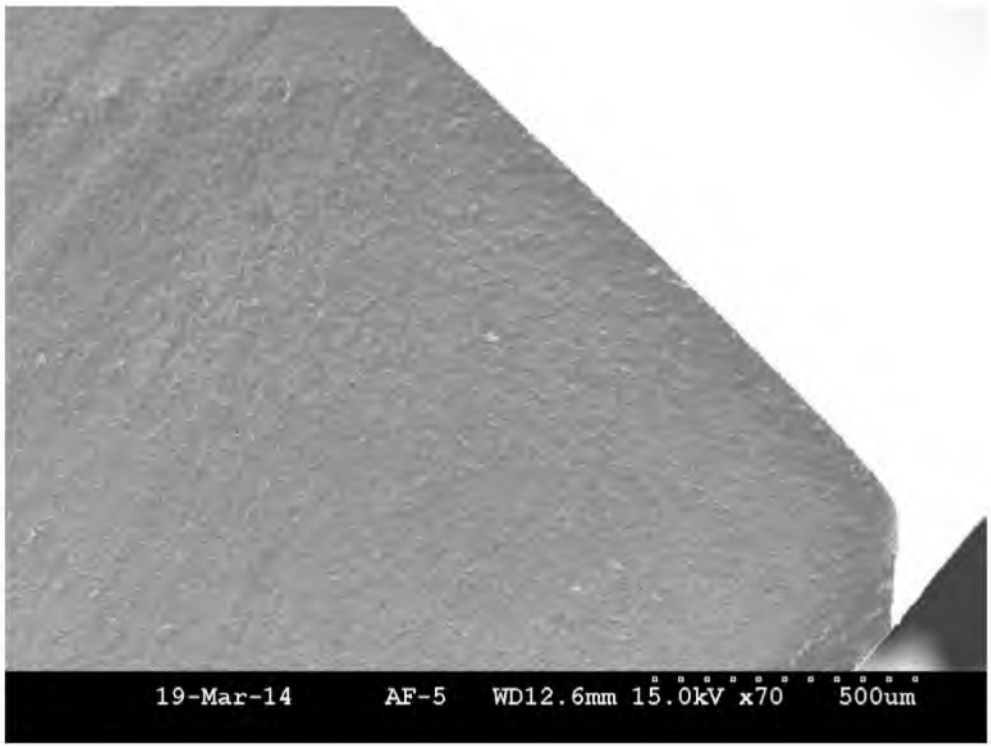

Figure 81 View of GT270-9 Transitions

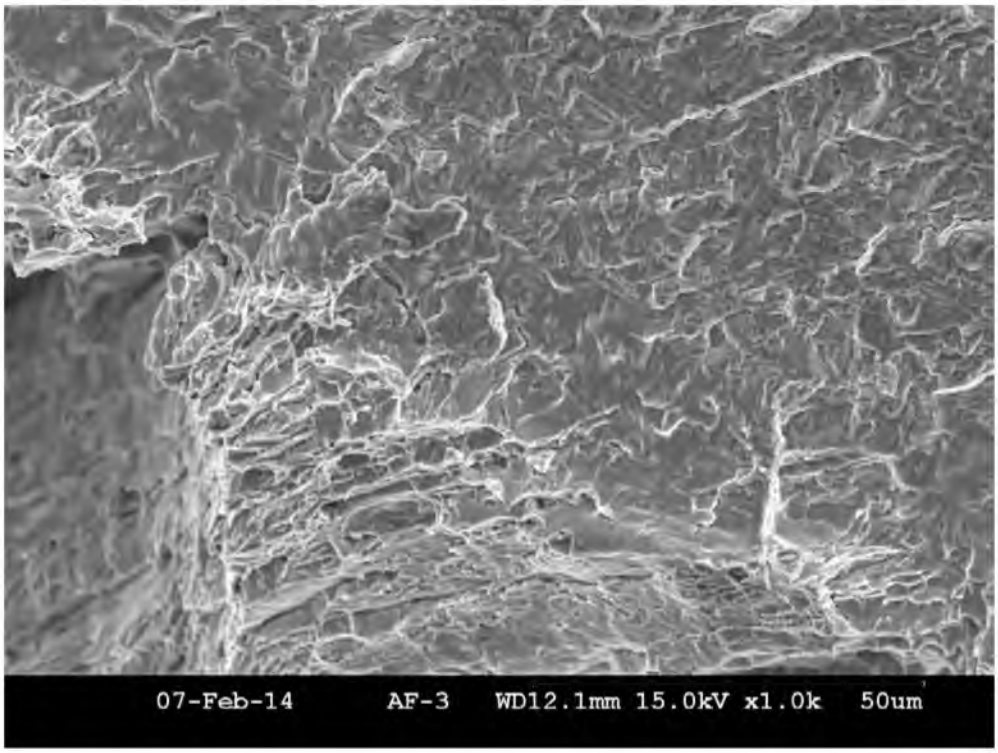

Figure 82 GT270-9 1,000x End of Spectrum B Image

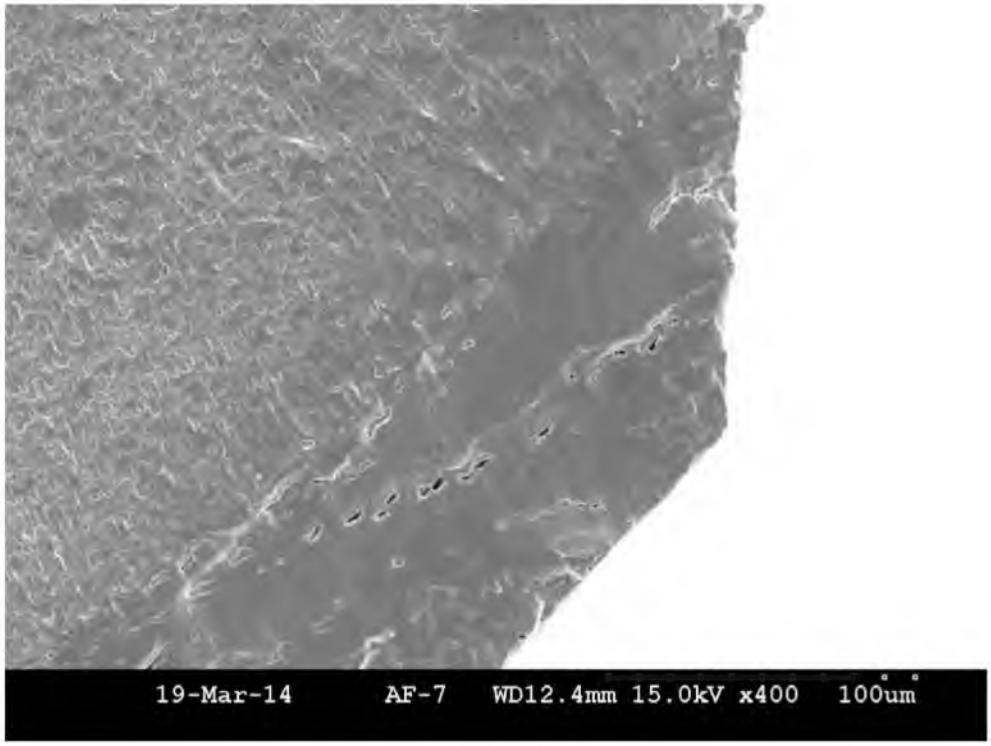

Figure 83 400x View of GT270-9 Transition from Spectrum A to B

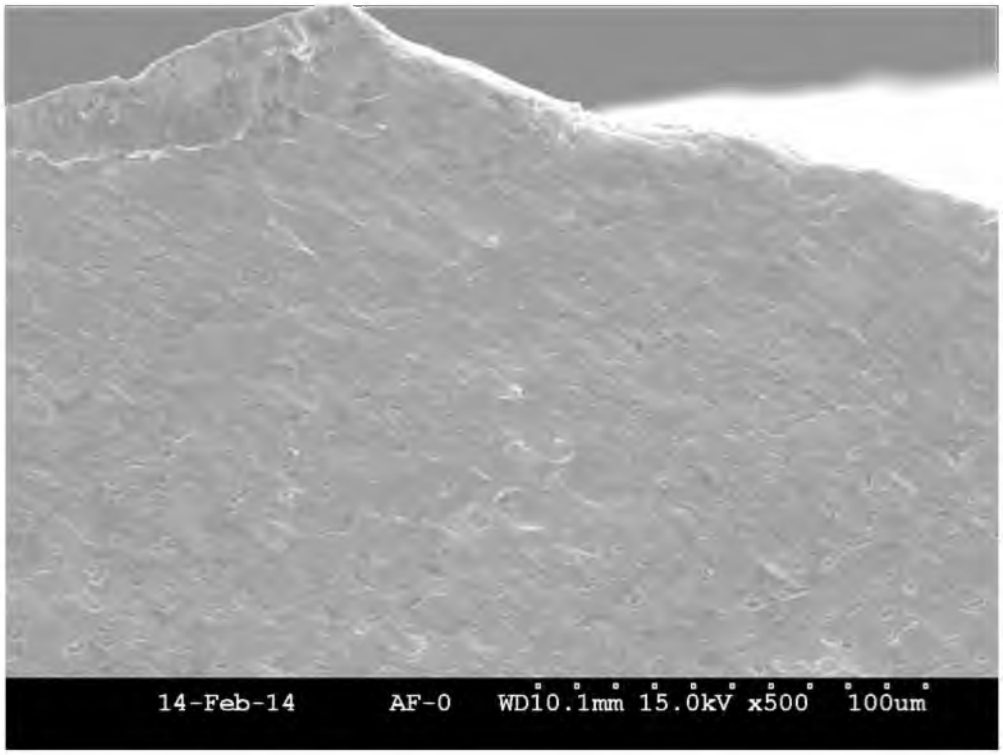

Figure 84 GT270-14 500x Image of Crack Nucleation Site

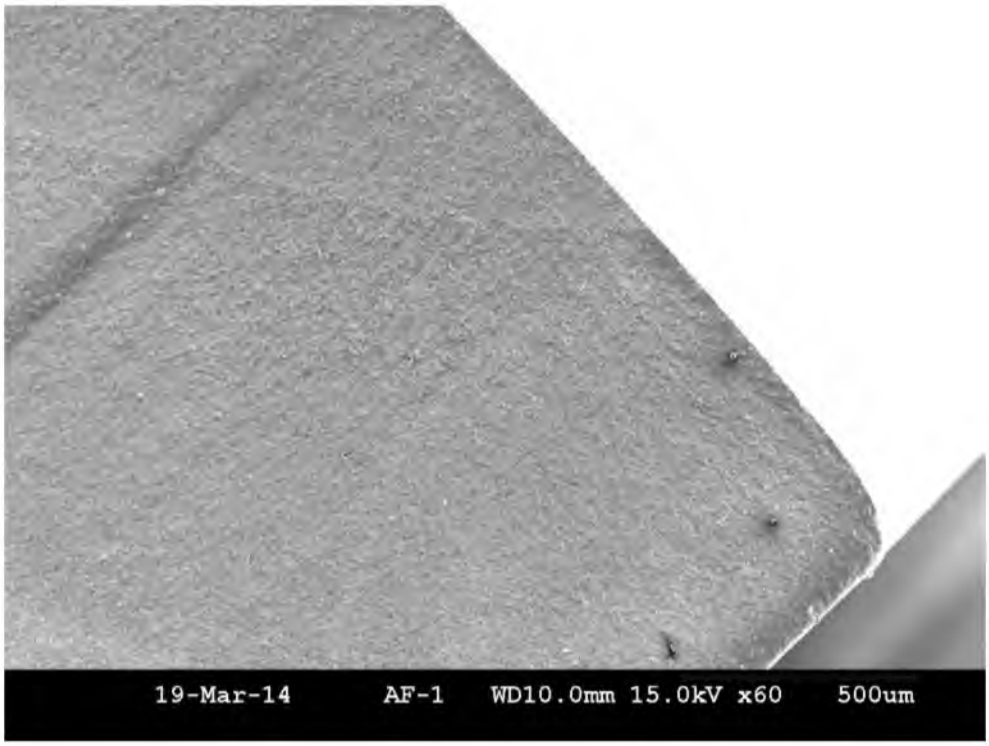

Figure 85 View of GT270-14 Transitions

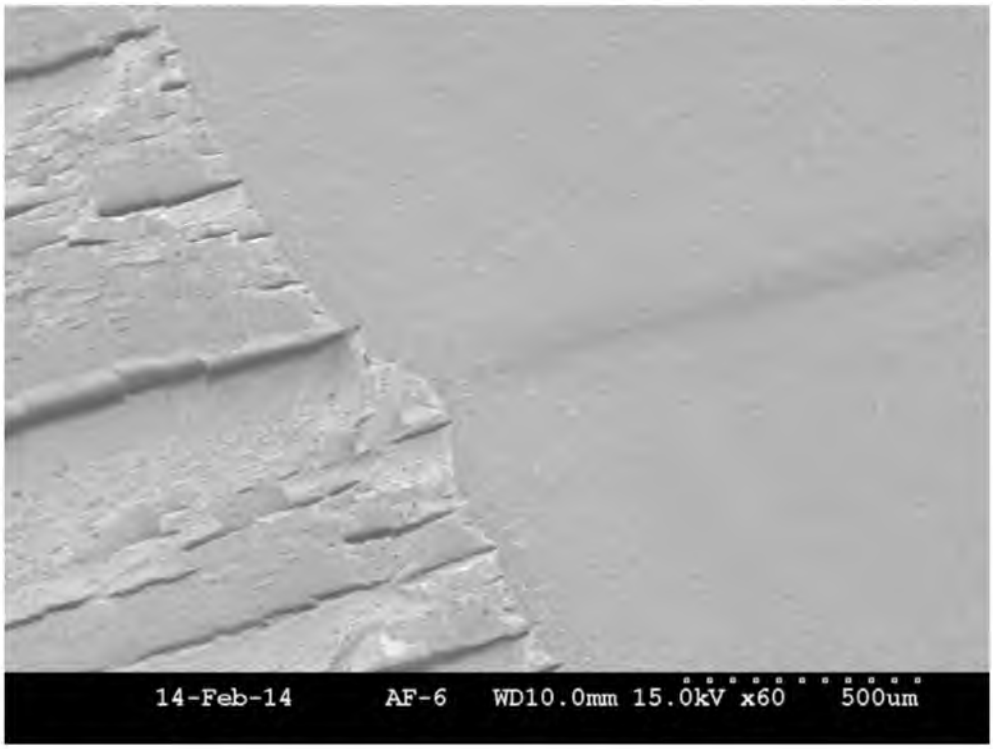

Figure 86 GT270-14 60x Image of Crack Surface Midway Through Thickness

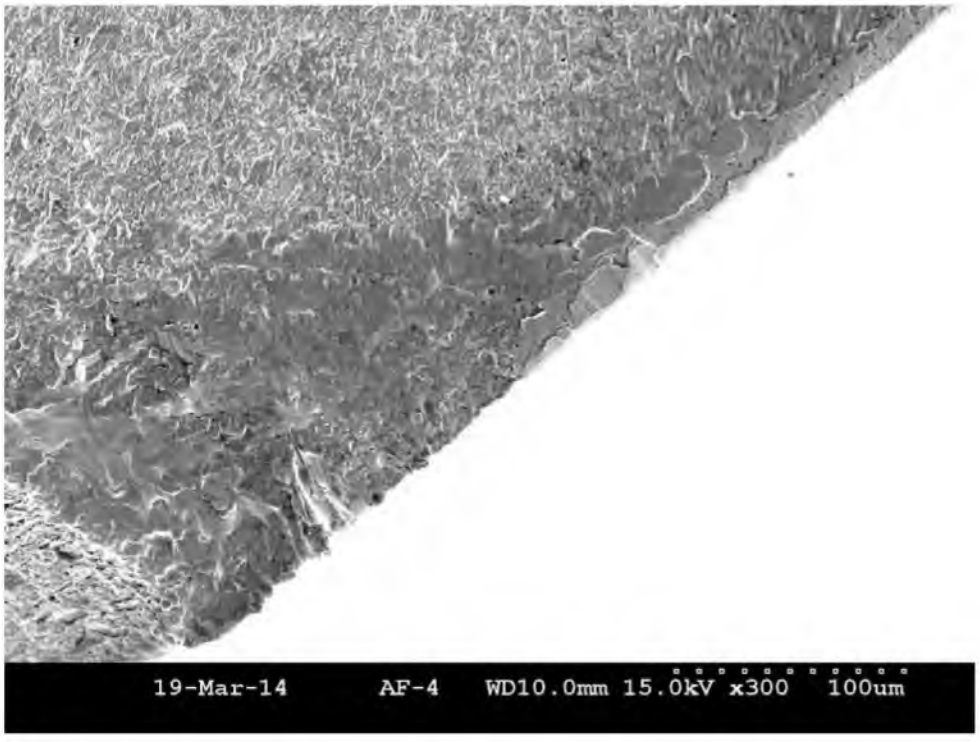

Figure 87 300x End of GT270-14 Fatigue Crack Image

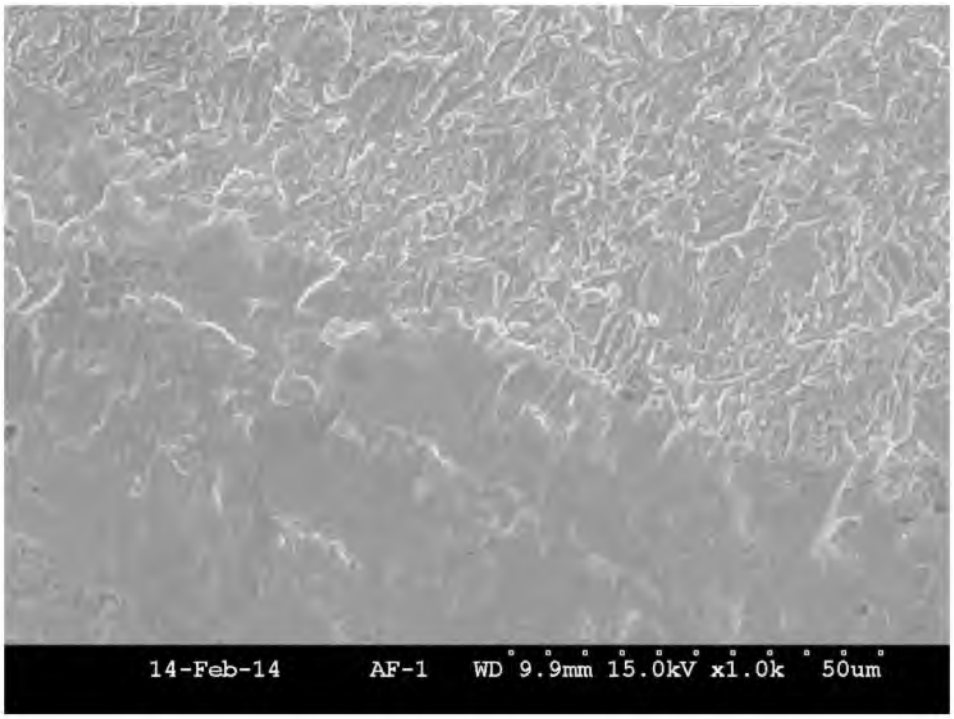

Figure 88 GT270-14 1,000x Image of Spectrum A to B Transition

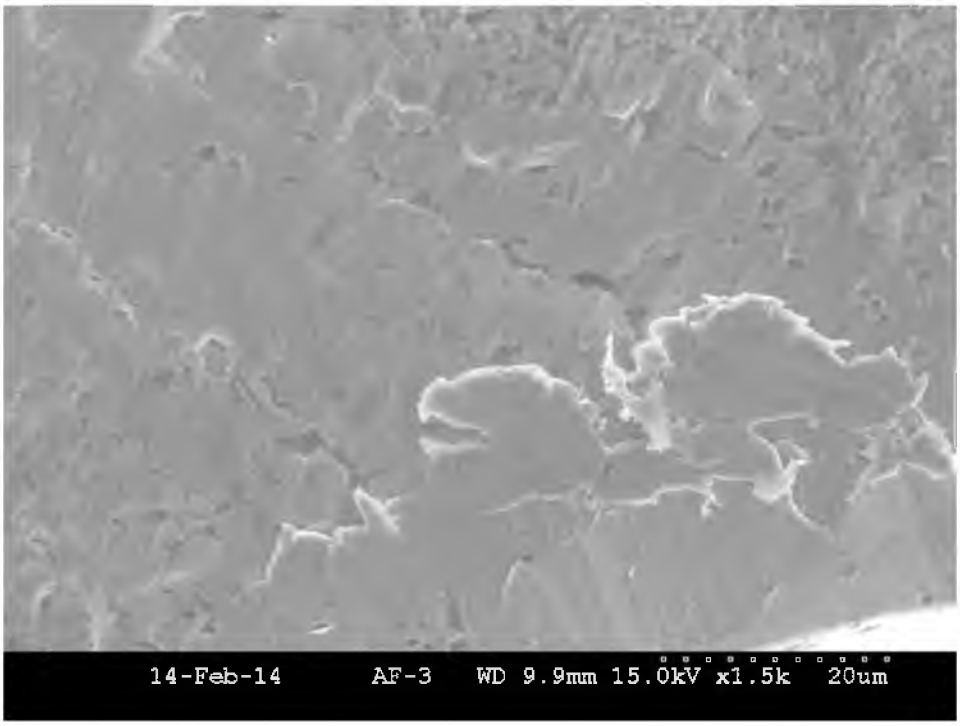

Figure 89 GT270-14 1,500x Image of Spectrum B Striations.

REFERENCES

[1] Boeing, "Commercial Airplanes Jet Prices," Boeing, 2014. [Online]. Available: http://www.boeing.com/boeing/commercial/prices. [Accessed 22 February 2014].

[2] United States Air Force, "F-16 Fighting Falcon Fact Sheet," United States Air Force, 15 October 2007. [Online]. Available: http://www.af.mil/AboutUs/FactSheets/Display/tabid/224/Article/104505/f-16-fighting-falcon.aspx. [Accessed 22 February 2014].

[3] Federation of American Scientists, "A-10/OA-10 Thunderbolt II," Federation of American Scientists, 2013. [Online]. Available: http://www.fas.org/programs/ssp/man/uswpns/air/attack/a10.html. [Accessed 11 November 2013].

[4] United States Air Force, "B-52 Stratofortress FactSheet," United States Air Force, 20 September 2005. [Online]. Available: http://www.af.mil/AboutUs/FactSheets/Display/tabid/224/Article/104465/b-52-stratofortress.aspx. [Accessed 11 November 2013].

[5] American Society for Testing Materials, "ASTM E1823 Standard Terminology Relating to Fatigue and Fracture Testing," 1 February 2013. [Online]. Available: http://specs4.ihserc.com/Document/Document/ViewDoc?docid=ZFRBDFAAAAAAAAAA. [Accessed 20 March 2014].

[6] H. A. Wood and R. M. Engle, USAF Damage Tolerant Design Handbook: Guidelines for the Analysis and Design of Damage Tolerant Aircraft, Wright-Patterson Air Force Base, OH: United States Air Force, 1979.

[7] Department of Defense, "MIL-STD-1530 Standard Practice Aircraft Structural Integrity Program (ASIP)," 1 November 2005. [Online]. Available: http://specs4.ihserc.com/Document/Document/ViewDoc?docid=ZLQOIBAAAAAAAAAA. [Accessed 20 March 2014].

[8] M. Levy, "Test Plan - Fatigue Crack Evaluation of Training vs. Non Training Missions," Northrop Grumman Aerospace Systems, Bethpage, NY, 2013.

[9] J. Mackerelle, *Fatigue Crack Evaluation of Training versus Non-Training Missions Development of Non-Training Mission Maneuver Spectrum,* 2012.

[10] R. Beal, "Spectrum Comparison of an Extended Service Life System using 2024-T351 Aluminum," University of Utah, Salt Lake City, UT, 2014.

[11] J. Kokoris, "Spectrum Usage and Development," Northrop Grumman Aerospace Systems, Bethpage, NY, 2006.

[12] M. Janssen, J. Zuidema and R. Wanhill, Fracture Mechanics 2nd Edition, Delft, The Netherlands: VSSD, 2006.

[13] J. Schijve, "Observations on the Prediction of Gatigue Crack Growth Propagation Under Variable-Amplitude Loading," in *Fatigue Crack Growth Under Spectrum Loads*, Philidelphia, PA, American Society for Testing and Materials, 1976, pp. 3-23.

[14] P. J. Bernard, T. C. Lindley and C. E. Richards, "Mechanisms of Overload Retardation During Fatigue Crack Propagation," in *Fatigue Crack Growth Under Spectrum Loads*, Philidelphia, PA, American Society for Testing and Materials, 1976, pp. 78-97.

[15] W. X. Alzos, A. C. Skat and B. M. Hillberry, "Effect of Single Overload/Underload Cycles on Fatigue Crack Propagation," in *Fatigue Crack Growth Under Spectrum Loads*, Philidelphia, PA, American Society for Testing and Materials, 1976, pp. 27-40.

[16] R. I. Stephens, D. K. Chen and B. W. Hom, "Fatigue Crack Growth with Negative Stress Ratio Following Single Overloads in 2024-T3 and 7075-T6 Aluminum Alloys," in *Fatigue Crack Growth Under Spectrum Loads*, Philidelphia, PA, American Society for Testing and Materials, 1976, pp. 27-40.

[17] J. Reiman, M. Landy and M. Kaplan, "Effect of Spectrum Type on Fatigue Crack Growth Life," in *Fatigue Crack Growth Under Spectrum Loads*, Philadelphia, PA, American Society for Testing and Materials, 1976, pp. 187-202.

[18] W. Zhuang, S. Barter and L. Molent, "Flight-by-flight fatigue crack growth life assessment," *International Journal of Fatigue,* vol. 29, no. 9, pp. 1647-1657, 2007.

[19] S. U. Khan, R. C. Alderliesten, J. Schijve and R. Benedictus, "On the fatigue crack growth prediction under variable amplitude loading," in *Computational and experimental analysis of damaged materials*, Delft, The Netherlands, Delft University of Technology, 2007, pp. 77-105.

[20] S. Kalnaus, F. Fan, Y. Jiang and A. Vasudevan, "An experimental investiation of fatigue crack growth of stainless steel 304L," *International Journal of Fatigue,* vol. 31, pp. 840-849, 2009.

[21] L. Smith, "The Generalized Willenborg Shutoff Overload Ratio and Its Sensitivity to Analytical Parameteres and Techniques," Southwest Research Institute, San Antonio, TX, 2006.

[22] J. Willenborg, H. A. Wood and R. M. Engle, "A crack growth retardation model using an effective stress concept," Air Force Flight Dynamics Laboratory, Wright Patterson Air Force Base, OH, 1971.

[23] ASM International, Metal Handbook Desk Edition, Russell Township, OH: ASM International, 1998.

[24] SAE International, "SAE AMS5528 Steel, Corrosions - Resistant, Sheet, Strip, and Plate 17Cr - 7.1 Ni - 1.1 Al Solution Heat treated, Precipitation Hardenable," October 2012. [Online]. Available: http://specs4.ihserc.com/Document/Document/ViewDoc?docid=WRRQAFAAAAAAAAAA. [Accessed 20 March 2014].

[25] Northrop Grumman Corporation, "Mechanical Properties of 17-7 PH Test Material," Northrop Grumman, Bethpage, New York, 2012.

[26] D. Andrew, "Investigation of Cold Expansion of Short Edge Margin Holes with Pre-existing Cracks in 2024-T351 aluminum Alloy," University of Utah, Salt Lake City, UT, 2011.

[27] Gaertner Scientific Corporation, *Packing List,* Chicago, IL: Gaertner, 2010.

[28] American Society for Testing and Materials, "ASTM E647 Standard Test Method for Measurement of Fatigue Crack Growth Rates," 15 October 2013. [Online]. Available: http://specs4.ihserc.com/Document/Document/ViewDoc?docid=ONKMHFAAAAAAAAAA. [Accessed 20 March 2014].

[29] G. C. Sih, Handbook of Stress-Intensity Factors, Bethlehem, PA: Institute of Fracture and Solid Mechanics at Lehigh University, 1973.

[30] J. Harter, AFGROW Users Guide and Technical Manual, Centerville, OH: LexTech, 2010.

[31] R. Pilarczyk and T. Allred, "Damage Tolerance Analysis Ground Rules," A-10 ASIP Group, Hill AFB, UT, 2010.

[32] SAE International, "AMS 2759/3E Heat Treatment Precipitation-Hardening Corrosion-Resistant and Maraging Steel part," 08 2008. [Online]. Available: http://sape4.ihserc.com/Document/Document/ViewDoc?docid=CTWAHCAAAAAAAAAA. [Accessed 18 04 2014].